10-29-2018

Elemental Analysis of Adhesive Tapes by Laser-Based Methods

Claudia Martinez Lopez
cmart327@fiu.edu

FLORIDA INTERNATIONAL UNIVERSITY

Miami, Florida

ELEMENTAL ANALYSIS OF ADHESIVE TAPES BY LASER-BASED METHODS

A dissertation submitted in partial fulfillment of

the requirements for the degree of

DOCTOR OF PHILOSOPHY

in

CHEMISTRY

by

Claudia Martinez Lopez

2018

To: Dean Michael R. Heithaus
College of Arts, Sciences and Education

This dissertation, written by Claudia Martinez Lopez, and entitled Elemental Analysis of Adhesive Tapes by Laser-Based Methods, having been approved in respect to style and intellectual content, is referred to you for judgment.

We have read this thesis and recommend that it be approved.

_____
Shekhar Bhansali

_____
Yong Cai

_____
Kevin O'Shea

_____
Kathleen Rein

_____
Jose R. Almirall, Major Professor

Date of Defense: October 29, 2018

The dissertation of Claudia Martinez Lopez is approved.

_____
Dean Michael R. Heithaus
College of Arts, Sciences and Education

_____
Andrés G. Gil
Vice President for Research and Economic Development
and Dean of the University Graduate School

Florida International University, 2018

DEDICATION

To my dad, for all his love and support.

ACKNOWLEDGMENTS

I wish to thank my committee for their support; Dr. Bhansali for his "out-of-the-box" thinking and advice, Dr. Cai for his scientific curiosity and really difficult questions that kept me thinking weeks after each meeting, Dr. O'Shea for reminding me of my personal and professional improvement throughout the PhD path, and Dr. Rein who was always concerned with my progress and the timeline to my graduation. I would especially like to thank my major professor, Dr. Almirall, for accepting me into his research group, for providing me with all the means needed to conduct my research, and for always encouraging me to aim higher.

I am very grateful for the support from Dr. Tatiana Trejos and Dr. Sarah Jantzi; they mentored me through the toughest parts of these years with their professional and personal advice. I also want to thank my lab mates and friends Brandy, Tricia, and Ruthie for sharing their feedback and support when I needed it, and for all the brainstorming and insightful conversations we shared inside the laser lab. I am thankful to the "A-team" and the visiting undergraduate students and scientists who collaborated with me in different parts of my project. Special thanks to Antoinette Lyndor, Ivy Cheung, Tatiana Jaramillo, and Saeed Almaheiri.

I would like to acknowledge Maggie and Dr. Lees for their help and guidance through the PhD path.

I was fortunate to receive the Bridge to Doctorate fellowship during the first two years of the PhD program (NSF FGLSAMP FIU Bridge to the Doctorate award HRD #1301998). The fellowship supported me financially, gave me the opportunity and the

means to travel to professional development conferences, and allowed me to network and socialize with very successful collogues in different higher education careers.

In the last year of the PhD, I received the FIU Graduate School Dissertation Year Fellowship (DYF). This fellowship allowed me to complete my research and ultimately write my dissertation thesis.

My research project was made possible thanks to the NIJ tape grant (NIJ Award 2015-DN-BX-K050) which provided me with the means to conduct my experiments, present the results at prestigious scientific conferences, and design and perform interlaboratory exercises with well-known scientists and practitioners in the field of forensic science.

Last, but not least I want to thank my family: my father Juan, my mother Laura, my brother José Carlos, and my husband Matthew. Without their love and encouragement, these past years would have been extremely difficult to endure.

ABSTRACT OF THE DISSERTATION

ELEMENTAL ANALYSIS OF ADHESIVE TAPES BY LASER-BASED METHODS

by

Claudia Martinez Lopez

Florida International University, 2018

Miami, Florida

Professor Jose R. Almirall, Major Professor

Adhesive tapes are a common type of evidence involved in violent crimes and national security threats. This research evaluated the utility of LA-ICP-MS and LIBS for the characterization of the trace elemental signature in adhesive tapes for forensic comparisons. LA-ICP-MS and LIBS methods were developed, for the first time, for the qualitative and quantitative analysis of adhesive tapes.

The backings of 90 black electrical tapes, previously characterized by conventional techniques (physical examination, IR, Py-GC-MS, and SEM-EDS), were analyzed by LA-ICP-MS to evaluate the ability of the technique to discriminate samples originating from different sources and to associate pieces of tapes originating from the same roll. The discrimination for the LA-ICP-MS analysis of the 90 samples was found to be 93.9%, greater than the discrimination found using SEM-EDS (87.3%). Moreover, 100% correct association resulted for the control samples evaluated in this study.

The analysis of tapes by LIBS allowed to separate pairs of tapes that were not previously distinguished by LA-ICP-MS by detecting differences in lithium, calcium, and potassium.

The potential of normalization strategies was evaluated for LIBS spectral and statistical comparisons.

Two quantitative analysis methods were developed for the analysis of tapes and other polymers. These quantitative methods can help in creating and populating databases that can lead to the use of likelihood ratios and the development of standard methods of analysis and interpretation for tape evidence.

Two interlaboratory trials including 7 operational and research laboratories were completed as part of this study. SEM-EDS resulted in 16.7% and 12.5% false positive rates for interlaboratory tests #1 and #2, respectively. Up to 7 and 8 elements were detected by SEM-EDS for interlaboratory test #1 and #2, respectively. LIBS and LA-ICP-MS resulted in no false positives or false negatives. In addition, increased characterization of the samples was obtained by detecting up to 17 elements by LIBS and 32 elements by LA-ICP-MS. The increased sensitivity and selectivity of LIBS and LA-ICP-MS methods has been shown to distinguish tapes originating from different sources, and to correctly associate tapes belonging to the same rolls in different laboratories and by different analysts.

TABLE OF CONTENTS

LIST OF TABLES

TABLE PAGE

LIST OF FIGURES

FIGURE PAGE

ABREVIATIONS AND ACRONYMS

ANOVA	Analysis of Variance
CCD	Charge Coupled Device
FBI	Federal Bureau of Investigation
FIACS	Forensic Ink Analysis and Comparison System
FIU	Florida International University
FTIR	Fourier Transform Infrared Spectroscopy
LA-ICP-MS	Laser Ablation-Inductively Coupled Plasma-Mass Spectrometry
LIBS	Laser Induced Breakdown Spectroscopy
LOD	Limit of Detection
NA	Not Applicable
Nd:YAG	Neodymium: Yttrium Aluminum Garnet
NIST	National Institute of Standards and Technology
PCA	Principal Component Analysis
PE	Polyethylene
PLSDA	Partial Least Squares Discriminant Analysis
PMT	Photomultiplier Tube
PPB	Parts per Billion
PPM	Parts per Million

PVA	Polyvinyl Acetate
PVC	Polyvinyl Chloride
Py-GC-MS	Pyrolysis-Gas Chromatography-Mass Spectrometry
RF	Radio Frequency
RPM	Revolutions per Minute
RSD	Relative Standard Deviation
SD	Standard Deviation
SEM-EDS	Scanning Electron Microscopy-Energy Dispersive Spectroscopy
SNR	Signal to Noise Ratio
SRM	Standard Reference Material
XRF	X-Ray Fluorescence Spectroscopy

1 INTRODUCTION

1.1 Research motivation

Kidnappings, murders, illicit drug packaging, and improvised explosive devices (IEDs) are some of the many criminal activities involving adhesive tapes. In the case of IEDs, electrical tapes can be recovered as part of the post-blast evidence, as tapes are, for the most part, resistant to high temperature and impact. Numerous different types of evidence can be attached to the tapes such as fibers, fingerprints, and DNA; however, the tapes themselves represent a very important type of evidence that can be used to assist a criminal investigation. In addition to the evidence attached to the tape, a tape roll found in possession of a suspect can be potentially linked to the one found in the crime scene.

The analysis of adhesive tapes typically involves the comparison of two or more pieces of tape using physical and microscopical examinations, and chemical identification of organic and inorganic constituents. Typically, a questioned piece of tape is compared to a tape of known source. Alternatively, the lab might be asked to identify a possible source of questioned tape and trace it back to a possible manufacturer and/or distributor.[1] Although a physical match between ends of tape samples represents a strong evidence of association, this can be challenged because of the elasticity and deformation of tape.

1.2 Significance of the study

The most common methods used for the organic analysis of electrical tapes are Fourier-Transform Infrared spectroscopy (FTIR) and Pyrolysis-Gas Chromatography-Mass Spectrometry (Py-GC-MS).[2-4] Infrared spectroscopy is a quick and well-known

technique that provides identification of organic compounds without the need for sample preparation. However, in some instances, FTIR presents some limitations for the analysis of electrical tape backings because primary components of the plasticizer may mask the detection of other components.[1] Pyrolysis gas chromatography mass spectrometry is capable of providing chemical information on a wide range of organic materials difficult to be analyzed by IR. Pyrolysis GC-MS is therefore complementary to infrared spectroscopy, and it provides separation (retention time) and identification (mass spectrometry) of organic compounds.[4] However, Py-GC-MS is destructive and time consuming and therefore is recommended as the last analytical step in tape examinations.

The elemental composition of adhesive tapes has been previously analyzed by Scanning Electron Microscopy-Energy Dispersive Spectroscopy (SEM-EDS) and Micro-X-Ray Fluorescence (μ-XRF).[2-5] As reported by Mehltretter et al.,[4] the elemental characterization by SEM-EDS allowed for 87% discrimination by pairwise comparison; SEM-EDS showed to be the most discriminating tool for electrical tape backings. Although SEM-EDS and μ-XRF proved useful for the inorganic characterization of tapes, these techniques present some limitations such as low sensitivity and selectivity. In addition, the penetration depth of the μ-XRF beam into the sample may cause contamination issues between the backing and adhesive layers, requiring additional sample preparation steps.

In order to better identify and characterize the evidence, state-of-the-art instrumentation needs to be adopted by forensic laboratories. My project includes the method development and optimization of Laser Ablation-Inductively Coupled Plasma-Mass Spectrometry (LA-ICP-MS) and Laser Induced Breakdown Spectroscopy (LIBS) for

the analysis of tape backings, as well as the design of interlaboratory exercises involving the practitioner community.

Laser ablation ICP-MS and LIBS are proposed as valuable complementary tools in tape examinations because of their superior sensitivity and selectivity, minimal sample destruction, short analysis time, and little to no sample preparation. The chemical signature of tape backings was investigated to be used beyond comparative purposes to provide useful intelligence information about sources of origin. Moreover, the current project included pattern recognition and chemometric tools to characterize and identify tape groups.

Quantitative methods of analysis have been developed and tested for the analysis of tape samples. A quantitative method for the analysis of tapes by LA-ICP-MS allows the validation of methods of analysis between different laboratories using various instrumentation, and therefore create standard documents for the analysis of tape evidence for laboratories across the world. Reporting absolute concentrations for tape samples allows the creation of a comprehensive tape database for the future. A database enables the use of likelihood ratios and the establishment of interpretation standard documents that will allow the forensic community to report the results of tape evidence comparisons.

A series of interlaboratory tests were conducted to assess and improve the current analytical methodology for the forensic analysis of tape evidence. The conventional methods for the comparison of tapes (physical and microscopic examination, IR, Py-GC-MS, and SEM-EDS) were compared to the newly developed LIBS and LA-ICP-MS

methods for the analysis of the same tape samples by several laboratories in the US and different parts of Europe.

A set of packaging tapes originating in Asia were analyzed by LA-ICP-MS and LIBS. The purpose of this part of the project was to assess the capabilities of LIBS, compared to LA-ICP-MS, for the analysis of this type of tape. In addition, a normalization strategy and different match criteria were investigated for the set of eight packaging tapes.

1.3 Chemical composition and manufacturing of adhesive tapes

Although adhesive tapes as we know them seem a recent concept, the technology that makes them possible dates back to the 1800s.[6] The first patent relating to adhesive tapes was awarded in 1845 for a surgical pressure sensitive adhesive.[7] In 1971, a patent was granted[8] to what it would fall in today's definition of a satisfactory adhesive tape.[6] The 1971 patent stated that the tape would adhere to the skin without leaving adhesive residues.[6] In the late 1800s and early 1900s, with the development first of the bicycle and then the automotive and their need for tires, the rubber industry flourished,[6] allowing for a greater demand of rubber products, hence and improvement in the technology for the adhesive tape industry.

Patents for the process and product development of tapes continue to be granted, even today. Current environmental concerns force the industry to develop new and improved ways to manufacture adhesive tapes. Similarly, the number of applications for adhesive tapes continues to grow, and the capabilities of the old designs continue to improve.

The definition of an adhesive is any material that will usefully hold two objects together solely by surface contact.[6] The molecular attractions between two bodies, Van der Waal's forces, are what hold parts together in adhesion.[6] In order to reshape to the characteristics of the substrates, adhesives must initially be in liquid form. While in use, however, the adhesive must resist the separation of the parts in contact. This is achieved by returning the adhesive to a solid form. The change between liquid and solid states is easily accomplished by the use of a solvent that can be evaporated after adhesion. Typical components present in adhesives are: the elastomer (elastic natural or synthetic polymer), and modifiers (stabilizers, elastomer modifiers, tackifying agents, plasticizers, fillers, among others).

The backing of the tapes consists basically of a thin substrate for the adhesive. The backing is cut into the desired dimensions and wound up into a roll. Backing thickness is typically between 0.025 to 0.25 mm.[6] The main quality of the backing layer is to be able to securely attach to the adhesive. Adhesion between the surface and the adhesive must be moderate in order to be able to detach the tape by hand. However, the adhesion between the adhesive and the backing layer must be strong in order to prevent the separation from the adhesive and the tape backing. Coating of the adhesive-side of the backing layer with a prime coat that allows stronger adhesion, while maintaining moderate adhesion to the other side of the tape backing, is normally accomplished. Typical components present in tape backings are: plastic film (PVC, polypropylene, polyethylene), fabric (in the case of duct tape), and release and prime coats.

The following sections describe the raw materials added to the adhesive and backing and the manufacturing process of adhesive tapes.

1.3.1 Raw materials and chemical formulation of adhesive tapes

Adhesive components

The main component of the adhesive is the elastomer, which consists of an elastic rubber-like polymer. Combination of elastomers allows for more ideal properties in the adhesive than using the single component elastomers.

The most useful elastomer used, alone and in combination with other elastomers, for pressure sensitive adhesive is natural rubber.[6] Natural rubber consists mainly of polyisoprene (Figure 1, A) and is very compatible with other raw materials added to the adhesive formulation. Natural rubber is obtained from the latex of the tree *Hevea Braziliensis*, and is found to be soluble in many hydrocarbons, but insoluble in alcohols and ketones.[6] Natural rubber is immediately available, but the price can be high.

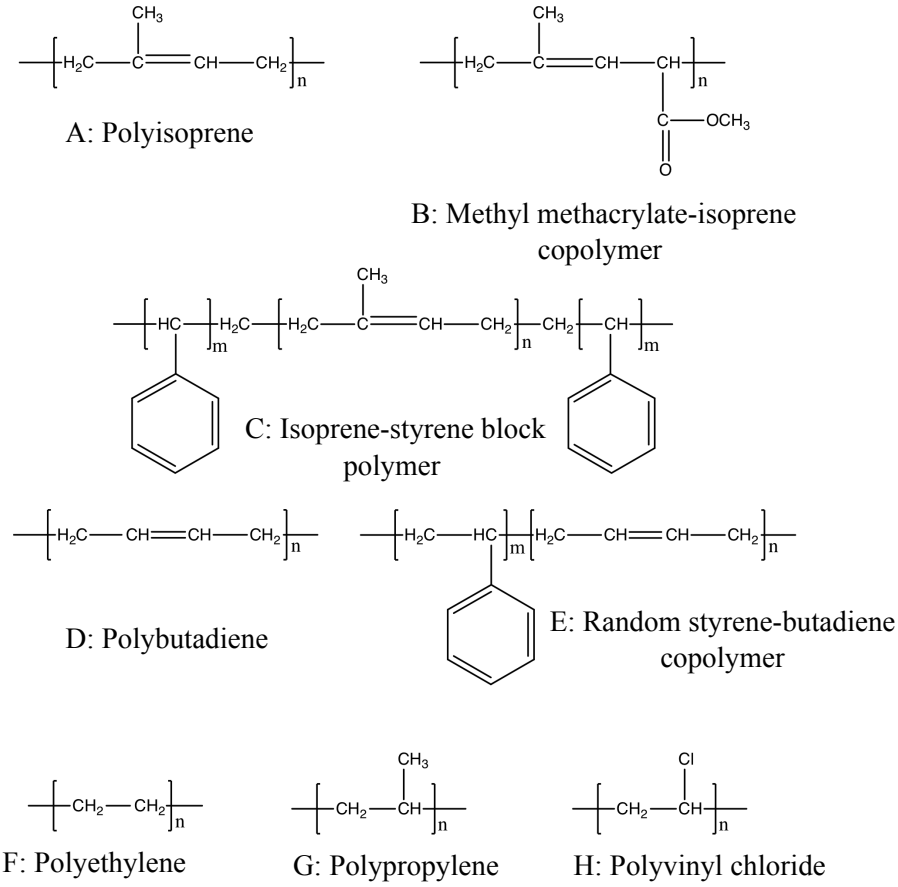

Figure 1 – Chemical structures for the different polymers used in the production of the backing and adhesive of tapes.

Another elastomer commonly used is synthetic polyisoprene (Figure 1, A). The original purpose of the synthetic form was to duplicate natural rubber, but to give it similar properties to the natural form, a different processing was required. Therefore, polyisoprene as a polymer is a completely different product because of its production process. Synthetic polyisoprene is much better in color and it lacks proteins and other chemicals present in natural rubber, therefore making it less prone to cause allergic reaction to the skin.[6] Unlike natural rubber, synthetic polyisoprene is essentially 100% polyisoprene.

The insertion of methyl methacrylate into natural rubber polyisoprene chain is another type of elastomer used for adhesive manufacturing. The amount of grafted methyl methacrylate (Figure 1, B) usually ranges from 30% to 40%.[6] The methyl methacrylate elastomer combination is too tough to be used alone, but it is very useful in the creation of prime coats for natural rubber and other elastomers because of its polarity and composition.

Another elastomer commonly used is isoprene styrene block copolymer (Figure 1, C). The isoprene styrene copolymer consists of styrene monomers attached to the isoprene chain. The number of isoprene monomers between two styrene blocks can be adjusted. Different combinations of molecular weight for the isoprene middle block allow to create a family of styrene-isoprene-styrene copolymer ranging from soft to firm.[6] The combination to use depends of the desired adhesive product.

A rather soft elastomer also used in adhesive formulations is polybutadiene (Figure 1, D). The presence of the double bonds allows it to be cross-linked.[6] These double bonds also indicate that it is prone to oxidation and degradation by heat and ultraviolet light.[6] Polybutadiene can be used alone, but copolymers are also common.

Random styrene butadiene copolymer (Figure 1, E) is a butadiene copolymer with a typical butadiene to styrene ratio from 70% - 77%.[6] The copolymer breaks down faster and more easily than natural rubber styrene copolymers. Oxidation causes polybutadiene to become firm as a result of cross-linking, in contrast with natural rubber. Therefore, a blend of random styrene butadiene and natural rubber compensates for this hardening effect and extends the service life of the adhesive.[6]

A very important part of the production of the adhesives is the addition of elastomer modifiers. Once the appropriate elastomer has been selected, stabilizers, tackifying resins, reinforcing resins, liquid tackifiers, plasticizers, depolymerizers, crosslinking agents and accelerators, and fillers are added to the composition for different purposes.

Stabilizers can be anti-oxidants, ultraviolet stabilizers, heat stabilizers, or combinations of stabilizers. It is important to protect the adhesive from the harsh manufacturing process. An adhesive is much more affected by the manufacturing process than by the customer use.[6] To determine the best stabilizers to use, the elastomer's characteristics and the type of manufacturing process need to be considered. Phenolic-based antioxidants have proven to be the most popular for pressure sensitive adhesives.[6] Dithiocarbamates are used as antioxidants and for heat stability.[6] Fillers, such as zinc oxide, titanium dioxide, and carbon black, can be used to improve ultraviolet stability.[6]

Tackifying resins are added to the elastomer to impart tack, and to provide the elastomer with much greater mobility. These resins are divided in those derived from pine tree rosin (mainly abietic acid), polyterpenes (mainly from turpentine), and hydrocarbon resins (derived from petrochemicals).[6]

Reinforcing resins should not contribute to the tack, but an increase of adhesion can be observed. By adding a component to the elastomer with higher glass transition temperature (transition between hard and brittle state to viscous and rubber-like state upon temperature increase), an adhesive system with higher cohesion and higher shear adhesion failure temperature is developed without the need of a cross-linking agent.[6]

Liquid tackifiers are added to temporarily increase tack of an adhesive. They not only improve the tack or wettability, but they also have a heavy effect on the deformability. Liquid tackifiers include liquid polybutenes and liquid glucose.[6]

Plasticizers are added to adhesives to improve malleability. Plasticizers should not affect the glass transition temperature of the elastomer. They have a special dramatic effect on deformability, shear resistance, and stress relaxation.[6] Plasticizers include polyolefins, depolymerized polyisoprene, and waxes. The main challenge with plasticizers is their migration to the backing layer because of their high mobility. One solution is to add the same concentration of plasticizers to both mediums, therefore allowing equilibrium and alleviating the migration from one medium to the other.

Depolymerizers are used to reduce the molecular weight of the rubber. They are usually captans and sulfonic acid derived. Depolymerizers are extremely temperature dependent and very little amount is needed in the production process.[6]

Cross-linking agents and accelerators improve three basic properties: provide high temperature, shear, and solvent resistance. Cross-linking implies loss of tack and low temperature performance; therefore, caution must be taken. Adding cross-linking agents improves oxidation resistance, giving a long life to the adhesive. The most popular accelerator is zinc resinate.[6]

Fillers are added to improve the bulk without altering the properties of the material. The main purposes of the fillers are: to reduce the cost of the adhesive, to create an opaque adhesive, to give color, to reinforce and improve the holding power and adhesion, to dry a too-tacky adhesive, to provide flame retardance, and to provide electrical conductivity.

Backing components

The backing is a thin film that can be coated with the pressure sensitive adhesive. For many years the main backing material was cotton fiber, followed by paper and cellophane.[6] Nowadays the possibilities for tape backing materials are nearly endless. Backing materials now include plastics, metal foils, fabrics, paper, etc.

Backings components include saturants, prime and release coats, and the backing film (polyester, polypropylene, polyethylene, polyvinyl chloride, paper, fabrics, metal foil, among others).

When paper is used as the backing, a saturant is needed to improve the internal strength of paper. The paper is impregnated with a suitable elastomer, known as saturant.[6] Saturants also improve the tensile strength, reduce porosity, and improve water resistance.[6] A saturant has no inter-reaction with the other tape components for prolonged periods of time. A test is performed after saturation to check for the delamination resistance of the saturated paper.

A prime coat is often needed to improve the adhesion of the elastomer adhesive and the backing. The prime coat is an adhesive itself, which is very compatible with both the backing and the adhesive layer. Polar materials, such as butadiene acrylonitrile, Neoprene, and natural rubber/methyl methacrylate copolymer have been used for prime coats.[6]

The release coat is applied to the tape backing so that it does not react with the adhesive when adhesive and backing come in contact.

The main objective is that tape is easy to peel off the roll. Release coat are usually proprietary and bought commercially.[6] They include materials such as stearates,

carbamates, polyvinyl acetate, polyethylene emulsion, chromium complexes, fluorocarbons, silicones, among others.[6]

Different materials are used for the backing film, such as polyester, polyethylene, polypropylene, polyvinyl chloride, paper, fabrics, metal foil, among others.

Polyester film provides excellent clarity, high abrasion, tear and solvent resistance, and good physical characteristics.[6] Polyester films are available in many grades, including matte, white, pearl, etc. It is also available in different thicknesses, and colors. The colored tapes are usually marked-up because of the dying process.

Polyethylene (PE) (Figure 1, F) has the highest stretch available for a plastic film, being approached only by Teflon. Polyethylene backings are especially common in the production of duct tapes.

Polypropylene (PP) (Figure 1, G) backing is one of the most common types because of the very good physical characteristics and low price.[6] It is more flexible than polyester tapes. For both polyester and polypropylene, a clean-cut film is hard to tear, however, once nicked it tears very easily. Polypropylene backings are commonly used for general purpose packaging tapes.

Polyvinyl chloride (PVC) (Figure 1, H) is a common type of polymer used in tape backings; specifically, for electrical tapes. Polyvinyl chloride is typically rigid at room temperature; therefore, plasticizers are added to the polymer to improve malleability. Like PE, plasticized PVC provides high elongation. Plasticized PVC requires a prime coat and sometimes a release coat.[6] The type of plasticizer plays an important role in the finish product. The main problem of plasticized PVC is the migration of the plasticized into the

adhesive layer. The migration can be avoided by using the same kind of plasticizer and in similar quantities for both backing and adhesive.

Just like in the case of the adhesives, fillers are added to the backing material for different purposes: cost reduction, to give color, to provide flame retardance, etc.

A review of several electrical tape and pressure sensitive adhesives patents[9-14] confirmed the use of several elements as raw materials in tape formulations. For instance, inorganic additives include fillers (aluminum oxide and aluminum silicate, barium sulfate, cadmium oxides and silicates, calcium carbonate and calcium sulfate, iron oxide, lead oxides and silicates, magnesium oxide, silica, titanium oxides and silicates, zinc oxides and silicates), flame retardants (antimony oxide and molybdenum oxide), heat resistant components (aluminum, barium, calcium, chromium, iron, magnesium, niobium, sodium, strontium, tin, titanium, and zirconium oxides), pigments, catalysts and others (aluminum phosphate, calcium silicate, calcium stearate, iron salts, lead silicate, lithium catalysts, titanium dioxide, and zinc oxide). These inorganic components and their concentration were found to vary per brand and product; this variability is of great importance to forensic science.

1.3.2 Manufacturing and distribution of adhesive tapes

The manufacturing process of tapes can be summarized in the flow chart shown in Figure 2.

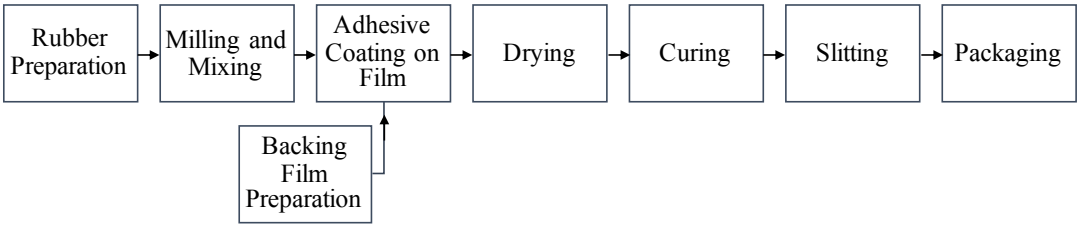

Figure 2 – Flow chart of an example of the manufacturing process of tapes.

Once the rubber has been acquired, it must be used quickly or else it recrystallizes, making it very hard to handle. Using an old, frozen, or crystallized rubber might end up making the process more expensive than getting a new batch of rubber.

After the rubber is acquired, a milling process is necessary to impart plasticity, and to mix the filler and processing aids with the rubber. A common type of milling method is the Banbury mixer, which basically masticates the rubber while mixing it with other ingredients. The Banbury method consists of a super two-roll mill with shaped intermeshed rotors in a water jacketed housing for cooling.[6] A hydraulic ram holds the mix firmly between the rotors during the mixing cycle and the raw materials are fed through a hopper door at the top of the machine.[6] The Banbury mixer facilitates both mixing and rubber breakdown. The temperature of the machine, and rubber, are carefully controlled to prevent excessive rubber breakdown.

After processing the rubber at the milling base, it needs to be in a form suitable for addition to a solvent mixer.[6] The mixing process is usually slow, therefore small batched are performed at a time to reduce the surface area of the material being mixed. The tackifying resin is mixed with the Banbury rubber by a process of kneading.

In the case of the film, the backing material (e.g., PVC) is mixed with the plasticizers and additives to produce what is referred as the “rope”. The “rope” can then be

squeezed to the desired thickness using large rollers and put into rolls using carrier paper. The film rolls are then transported to the facilities where they are coated with the prime and adhesive layer, if they are not processed in the same factory where they are produced.

There are different ways of producing the backing films and they vary among manufacturers. One way is referred as “blown” film, which results in very smooth sides of the backing. There are other ways such as one- and two-pass manufacture of films using rollers; these leave dimples on the backing material. By examining the texture of the backing material, the manufacture process can be predicted.

The coating of the adhesive on the backing material is achieved in different ways, also depending on the manufacturer. A typical way to deposit the adhesive on the backing film is by passing the film through a roll while the adhesive is delivered. These rolls are temperature controlled. There are manufacturers that produce the film in the same facility as the adhesive coating. In the case of duct tape, when polyethylene is produced and mixed with the fibers and adhesive, the fibers appear to be embedded in the backing, and not just in the adhesive. In the case of electrical tapes, a prime coat is used to increase the adhesion between adhesive and backing. A prime coat is sometimes not necessary for polyethylene backings as this material is less likely to resist the adhesion of the adhesive layer.

After the adhesive has been coated onto the backing, a drying process follows. There are different types of dryer ovens, but they are mainly divided in two categories: hot air circulation and inert gas circulation. The inert system reduces the chances of fire.[6] The ability to dry the adhesive depends on the type and thickness of the adhesive, the technology used, and also the backing material.

After drying is properly accomplished (improper drying can affect the curing process), the adhesive tapes proceed to chemical curing. The main purpose of curing is reduction of the mobility of the adhesive polymer. The mobility reduction is tricky as it also reduces tack and temperature resistance.

Curing also helps in reducing oxidation and degradation by the addition of cross-linking reagents.

After the tapes are rolled up into large jumbo rolls, slitting and packaging is needed to transport them to their destinations. The slitting can be done by unwinding the jumbo roll, cutting to the desired thickness and rewinding it; or by directly splitting the jumbo roll to the desired thickness. Tape rolls can be slit by the manufacturer or by slitting facilities out of the manufacturing site.

Packaging of tapes is a very important step in the manufacture process. Jumbo rolls should be kept at cool temperatures before slitting, the manufacturing date should always be stated as tapes can deteriorate over time.

It is especially important for provenance studies to understand that a manufacturer of tapes can sell the product in jumbo rolls to distributors, using a completely different label on the core of the rolls. For example, 3M is the main US manufacturer, they make tapes but also buy tapes from other US manufacturers or import them from Asia. A tape roll with a core labeled “3M” might have been made in the US or imported from China or Taiwan. Another example constitutes the manufacturer Shurtape, which produces the duct tapes of Duck brand popularly found in hardware stores. Tracking the manufacturing country can sometimes be accomplished by noting the UL (Under Laboratories) code

written on the label. However, as previously stated, a brand (e.g., 3M) can report their labels in the core or center of the tape roll, but the product was actually bought from a different manufacturer.

1.4 Forensic analysis of tapes

The analysis of tapes typically involves the comparison of pieces of tape using physical and microscopical examinations, usually followed by chemical identification of the organic and inorganic constituents of the tape samples. The most common methods used for the organic analysis of electrical tapes are FTIR and Py-GC-MS. The elemental composition of adhesive tapes has been previously analyzed by SEM-EDS and Micro-X-ray Fluorescence (μ-XRF), and more recently, the methods of analysis for LA-ICP-MS and LIBS have been developed.

1.4.1 Physical and microscopic examination

In 1984, J. D. Benson[15] reported the comparison of twelve (12) duct tape samples by examining the weave pattern of the reinforcing fibers, counting the number of threads per inch of cloth, and by determining the type of twist of the fibers. Most of the twelve samples were distinguished on the basis of the thread count and weave pattern. In the same year, T. G. Kee[16] and R. O. Keto[17] reported the comparison of PVC electrical tapes by microscopic and visual examination. The authors reported that the color and gloss of electrical tape backings, as well as their width and thickness, can be used for comparison purposes. Features such as ridges, irregular grooves, and oval pits were used to describe differences between tape samples.

The comparison of backings was performed after the tapes were immersed in hexane; after adhesive removal, ridges and marks left by the rollers used in the manufacturing of tapes could be visible. The comparison of six electrical tapes from different brands was performed by the use of a stereomicroscope. Surface features such as the differences in texture that result from stippling, striation, and cratering allowed investigators to differentiate some of the tape samples.

In 1987, R. D. Blackledge[18] published an article on the forensic comparison of adhesive backings using physical match ("jigsaw" fit) criterion. If a physical match was not found, additional tests should be performed to the samples such as elemental analysis and infrared spectroscopy.

In 1991, H. Snodgrass[19] published a review article on the construction, components, and distinguishing characteristics of duct tapes. In this article, thickness ranges, backing and adhesive colors, fabric penetration into the backing, type of fiber, and yarn count were discussed.

In 1998, J. Smith[20] reported the first "database" of tapes which included a table with the main characteristics (scrim count, yarn type, thickness, width, and adhesive color) for 51 duct tapes of different brands. The work by J. Smith showed the variability of physical characteristics in duct tapes among manufacturers.

In 2001, P. Maynard et al.[21] published an article on the analysis of 58 clear sticky and brown packaging tapes. The research group utilized a stereomicroscope for the determination of the width and thickness of the tapes and for the examination of the backing texture. The tapes were described on the basis of their texture pattern, striations,

perforations, or the absence of features. Both the packaging and clear sticky tapes were grouped in 4 individual groups depending on these physical characteristics. To measure the backing thickness, the adhesive was removed. Thickness measurements only differentiated two of the packaging tape samples.

In 2004, A. S. Teetsov and M. L. Stellmack[22] reported a method for preparing and comparing cross-sections of tapes. The method involved immersing the samples in liquid nitrogen prior to cutting using an in-house built X-Acto knife. The method was mainly oriented to further chemical analysis such as IR. However, it is a still useful guideline to obtain reliable cross-sections for physical comparisons of thickness between samples and for visualization of the layers and fibers present in tapes.

In 2006, M. J. Bradley et al.[23] published an article on the validation for duct tape end matches. Three duct tape rolls were used in the study. The research group found that 92% of the end matches that existed were identified and that the end matches not identified were reported as inconclusive. In the inconclusive cases, the analyst would proceed to more confirmatory techniques or a more in-depth comparison of the tapes using the yarn count and the weave pattern. The comparison of end matches for samples cut with scissors resulted in more errors than the torn pieces, which was probably the result of the lack of comparison points in the clean scissors cut.

In 2007, Goodpaster et al.[5] published a study on the microscopic examination of 67 electrical tapes. The surface texture of the tapes was described using the defects produced from the manufacturing process. Some tapes were found to be smooth as a result of the fine, uniform filler particle sizes used; other tapes had noticeable dimples or craters on the

surface. These distinctions were associated with the type or brand and quality of the products.

In 2011, A. Mehltretter et al.[3-4] reported the analysis of 90 electrical tapes by physical and microscopic examination of both the adhesive and backing. In the first publication the color of the adhesives of the 90 tapes was compared using a stereomicroscope following the manual separation of the adhesive from the backing.[3] Three main color adhesives were observed: clear, colorless adhesive; clear adhesive with a brown hint; and black adhesives. Interestingly, most of the black adhesives corresponded to 3M and 3M Scotch tapes. The second study consisted of the comparison of the backings of the 90 electrical tapes.[4] Physical characteristics of the tapes were recorded using visual and stereomicroscopical evaluation. The width of the tapes was measured to the nearest 0.5 mm using a ruler and the thickness was measured to the nearest 0.05 mil using a digital micrometer. On the basis of manufacturer tolerances, considerably differences in thickness consist of a thickness difference of 0.2 mil. The physical characteristics of the tape were described using the backing appearance, sheen, width and thickness. Physical examination and microscopy resulted on 64% discrimination, which represented 24 distinguished groups.

Also in 2011, M. J. Bradley et al.[24] published a paper on the validation of vinyl electrical tape end matches. A total of seven tape rolls were used in the study. Unlike duct tapes, the end matches for torn electrical tapes were not studied; electrical tape does not tear but gets deformed. From a total of 106 end matches, 98 were identified while the other eight were reported inconclusive. Bradley's work also concluded that, unlike rigid

materials, elastic electrical tapes can lead to a higher false inclusion rate. In addition, more confirmatory methods of comparison are recommended, even after a match was found.

In 2012 and 2015, A. Mehltretter et al.[25-26] reported the comparison of duct tapes by physical and microscopical examination. The first study consisted of the analysis of 82 duct tapes by monitoring the backing and adhesive color, backing texture and layers structure, and width and backing thickness. The fabric characteristics observed were weave/knit pattern, yarn description, yarn composition, fluorescence, and scrim count. The first study reported a 99.8% discrimination only by physical and microscopic examination for the set of duct tapes under study. The second study consisted of an intra-roll and intra-jumbo roll study for a set of duct tapes. It was concluded that scrim count and width do not vary significantly within single rolls. Width, however, may vary between different rolls from the same jumbo roll.

In addition to these publications, guidelines exist for the microscopic and physical examination of tapes.[27-29] These guidelines explain the handling of tapes, as well as the different terminology used in tape analysis. In addition, the guidelines help describe the different characteristics observed in tape samples and determine the individualizing features to better distinguish the tapes.

1.4.2 IR spectroscopy

Infrared (IR) spectroscopy has been widely used for the organic characterization of the components present in tapes.

In 1984 J. D. Benson[15] reported the analysis of twelve duct tapes by IR spectroscopy. The adhesive material of the 12 tapes was found to be polypropylene-based

and the backings made of polyethylene. Infrared spectroscopy also reported carbonate and small amounts of silicate fillers in some of the tapes.

In 1984, T. G. Kee[16] reported that IR spectroscopy of either backing or adhesive allowed to detect the phthalate in the tapes; for example, di(2-ethyl-hexyl) phthalate. He also concluded that small contributions were made by PVC and that infrared spectroscopy was typically only performed for the top surface.

In the same year, R. O. Keto[17] analyzed six (6) PVC electrical tapes of different brands by IR spectroscopy. He found that the adhesives differed from each other. All of the spectra contained aliphatic C-H stretching and CH_2 and CH_3 bending absorptions, indicating long aliphatic hydrocarbons. All spectra showed the presence of aromatic ester type plasticizers. Different brands were separated on the basis of the rubber used (polybutadiene or styrene/butadiene copolymer).

J. Smith,[20] in 1998, published the analysis of 51 duct tapes by IR spectroscopy. Smith identified the bands corresponding to tackifiers (polyterpene resin), rubber (isoprene), synthetic resin (synthetic polyterpene), clay (aluminum silicate), titanium dioxide, calcium sulfate, and zinc oxide. From the 51 tapes, six different IR spectra were developed.

R. A. Merrill and E.G. Bartick[30] published an article in 2000 where four duct tapes, six electrical tapes, one packaging tape, and two office tapes were analyzed by different types of IR spectroscopy instrumentation. A within-compartment ATR with a single reflection diamond was found to provide the best results. The authors concluded that at least 0.75 mm (crystal diameter) of the sample should be cleaned and free from dust prior

analysis. Severe sloping baselines were obtained in electrical tapes due to carbon black interferences.

In 2001, P. Maynard et al.[21] reported the analysis of 58 tapes (31 packaging and 27 clear sticky) by IR spectroscopy. All the packaging tape backings were identified as polypropylene while the clear sticky tape backings were found to be polypropylene, cellulose acetate, cellophane, and polypropylene/acrylate. One of the sticky tapes had an unidentified backing material. The adhesives for the packaging tapes were classified in eight groups while the ones for sticky tapes were classified in six groups. Adhesives were classified on the basis of acrylic or block copolymers.

In 2002, A. M. Dobney et al.[31] reported the comparison of packaging tapes by IR spectroscopy. Natural rubber and acrylic glue were discriminated as the adhesives in the samples. Infrared spectroscopy was found to be insufficient to discriminate several samples of tapes from the same brand but that belonged to different rolls.

In 2003, S. Masataka et al.[32] utilized IR spectroscopy to analyzed a set of twenty (20) colorless packaging tapes. All backing materials were confirmed to be polypropylene. The samples were not discriminated from each other using only IR spectroscopy.

In 2006, Y. Kumooka[33] reported the analysis of three deteriorated rubber-based adhesive tapes by IR spectroscopy. The samples were exposed to sunlight for six months and the adhesives were removed and pulverized after exposure. The IR spectra changed drastically after exposure, preventing the visibility of sharp peaks. Infrared spectroscopy did not prove suitable for analyzing deteriorated tapes.

In 2009, J. Goodpaster et al.[2] published an article of the analysis of nine (9) electrical tapes by IR spectroscopy. The plasticizer (typically an aromatic and/or aliphatic ester) dominated the spectrum with a large carbonyl absorption at 1730 cm and C–O stretching evident in the fingerprint region. Differences in plasticizer type and content, as well as additional components of the tape backing and adhesive, allowed for differentiation. It was found that older rolls grouped separately form new rolls for the 3M brand. Infrared spectroscopy analysis of the tape backings did not offer significant advantage. Infrared spectroscopy analysis of the adhesives was significantly more accurate. The accuracy for IR for clear adhesive proved better than the accuracy of energy dispersive spectroscopy analyses for the same samples.

In 2011, A. Mehltretter et al.[3-4] reported the analysis of 90 electrical tapes by IR spectroscopy. In the first study,[3] the adhesives of the samples were compared. The adhesives were divided by color: clear and black adhesives. The clear adhesives grouped in six distinctive groups while the black adhesives grouped in two distinctive groups. A 67% discrimination was found for the adhesive analysis. The components of the adhesives responsible for the grouping consisted of butadiene, isoprene, acrylic, and an unidentified constituent. In the second paper[4], the backings were analyzed by IR spectroscopy. A total of 14 distinctive groups were found by IR spectroscopy of the backings. Notable components reported which accounted for the differentiation between the samples included PVC, adipates, phthalates, calcium carbonate, aluminum oxide, PE (polyethylene), and BR (butyl rubber). Additional differences in absorption peaks were observed and unidentified. An 83% discrimination was found for the backing analysis by IR spectroscopy.

In 2011, J. Zięba-Palus and A. Augustynek[34] analyzed the adhesives and backings of 48 tapes (packaging, electrical and office tapes) by IR spectroscopy. The adhesives were divided into four groups defined by the detection of polyhydrocarbons (polypropylene), isoprene, polyester (acrylics), and an unidentified group. The backings were divided in three groups: polyhydrocarbons (polyethylene and polypropylene), cellulose, and polyester.

Infrared spectroscopy was performed on 82 duct tapes by A. H. Mehltretter and M. J. Bradley[25] on 2012. The backings of the tapes were cleaned with hexane. Only the samples not distinguished by physical characterization and microscopy were further analyzed by IR spectroscopy. Physical and microscopic examination alone reported a 99.6% of discrimination resulting in 12 distinctive pairs. IR spectroscopy further differentiated three of these 12 pairs; the differences could be attributed to the presence of kaolin in the adhesive of one of the samples, and the presence of dolomite versus calcite in the adhesives of other samples.

In 2013, D. M. Wright and A. H. Mehltretter[35] published an article on a casework example consisting of the analysis of duct tapes by IR spectroscopy. The IR data obtained for the adhesive included the identification of peaks associated with talc, styrene, calcite and/or dolomite, isoprene, and butadiene. The tackifying resin was also indicated. Polyethylene was reported for both sides of the backing. Additional tests were conducted to this casework samples in order to arrive to the final conclusions.

In addition to these publications, a guideline exists for the analysis of adhesive tapes by IR spectroscopy.[36] The guideline provides basic recommendations and information

about IR spectrometer components and accessories, with an emphasis on sampling techniques specific to tape components.

In 2015, A. Mehltretter et al.[26] conducted an intra-roll and intra-jumbo rolls study by IR spectroscopy. Differences within rolls were found to be much smaller than differences between rolls by IR spectroscopy. Two of 15 individual rolls of duct tape showed statistically significant variation in their FTIR spectra along the roll length. Visual inspection by spectral overlay of the statistically identified outlier samples showed differences that would not lead to an exclusion in a forensic examination.[26]

1.4.3 Py-GC-MS

In 1988, E. Williams and T. Munson[37] published an article on the analysis of 30 black electrical tapes by Py-GC-MS. From the 30 tapes, 26 had unique pyrograms. The tape samples with different pyrograms almost always originated from different sources.

A set of 58 tapes was analyzed by P. Maynard et al.[21] by Py-GC-MS in 2001. A set of six samples undistinguished by IR were further analyzed by Py-GC-MS. Two more groups were found by pyrolysis, one containing two tapes and another containing the other four. Pyrolysis GC-MS was the last step in the analytical scheme, therefore not a lot of samples were analyzed, and limited information was provided for those six samples.

In 2003, S. Masataka et al.[32] analyzed 20 packaging tapes by Py-GC-MS. A total of 12 groups were found using pyrolysis; Py-GC-MC further discriminated samples not differentiated by IR. By combining both techniques, the 20 samples were distinguished from each other.

In 2006, Y. Kumooka[33] reported the analysis of three deteriorated rubber-based adhesive tapes by Py-GC-MS. Pyrolysis proved more suitable than IR spectroscopy for these weathered tapes. The compounds identified from the pyrograms and MS analysis included isoprene, limonene, styrene, indene, methyl abietate, methyl benzoate, dimethyl phthalate, 1,2,3-trimethoxypropane, among many others. Natural rubber and aliphatic petroleum resins decomposed after exposure to sunlight for six months. Other compounds such as aromatic resins were more resistant.

In addition to these publications, a guideline exists for the analysis of adhesive tapes by Py-GC-MS.[38] The guideline provides direction on sample preparation techniques, parameters to consider when optimizing and validating a method, and what information the data provides for pyrolysis analyses.

In 2011, A. Mehltretter et al.[3-4] reported the analysis of 90 electrical tapes by Py-GC-MS spectroscopy. In the first study[3] the adhesives were analyzed. Out of the 90 tapes, 16 distinctive groups were found by Py-GC-MS on the adhesive analysis. The chemical components detected that accounted for the differences between the samples included butadiene, styrene, phthalate mixtures, fatty acids, adipates, benzenamine, acrylic, single phthalate, trimellitate, methyl methacrylate, and sebacate. The adhesive comparison resulted in 83% discrimination.

In the second study,[4] the backings were compared by pyrolysis. A total of 12 groups (81% discrimination) were found by Py-GC-MS of the backings. The main components detected were PVC, phthalates and mixtures, trimellitate, adipate, sebacate, azelaic acid plasticizer, and possible glutarate.

1.4.4 SEM-EDS and XRF

In 1984, T. L. Jenkins[39] reported the use of energy dispersive X-ray spectrometry for the analysis of silver duct tape. Seven elements were identified using this method: titanium, calcium, zinc, iron, copper, lead and chlorine. The elemental composition varied from three to a maximum of five elements for the sample set under study (over 65 tapes).

In 1984, J. D. Benson[15] reported the elemental analysis of tapes my emission spectroscopy. A total of seven elements (Ca, Al, Si, Fe, Ti, Zn, and Mg) were detected at high, medium and low concentrations. Out of the 12 samples, 11 samples were distinguished by the elemental method. The sample pair not distinguished belonged to the same brand. Brenson's research showed that calcium and zinc were not present in all samples, therefore these elements were discriminating between tape brands.

In 1984, T. G. Kee[16] analyzed black electrical PVC tapes by XRF. On the baiss of the absence and presence of calcium and lead, the samples were classified in four groups. Lead and calcium were used because lead carbonate was known to be used as stabilizer while calcium carbonate was commonly used as filler. Furthermore, the samples not distinguished by lead and calcium were eventually distinguished using antimony, phosphorous, and silicon. These elements were attributed to antimony oxide, phosphorous plasticizers, and possibly to a silicon filler.

In 1984 R. O. Keto[17] analyzed six PVC electrical tapes by XRF detecting up to 10 elements in the samples (Al, Si, S, Cl, Sb, Ca, Ti, Fe, Zn, Pb). These elements were associated with PVC (chlorine), titanium oxide, calcium carbonate, barium sulfate, kaolin (aluminum and silicon), talc, lead carbonate, lead sulfate, among others. The XRF method

showed that the six samples presented different elemental profiles, while two rolls from a same brand were indistinguishable.

In 1998, J. M. Smith[20] reported the use of energy dispersive X-ray spectroscopy for the analysis of 51 duct tapes. A total of 10 distinctive groups were found using the elemental technique. Elements detected included titanium, aluminum, silicon, calcium, titanium, iron, and zinc.

In 2000, A. M. Dobney et al.[40] reported the use of XRF for the analysis of three packaging tapes. The technique was not able to distinguish the three samples using the sulfur-to-phosphorous and titanium-to-iron ratios. The same research group[41] reported the comparison of 16 rolls of packaging tapes by XRF. Similarly, they concluded that XRF did not always differentiate the different brands by the above-mentioned ratios.

In 2007, J. V. Goodpaster et al.[5] published an article on the analysis of 67 electrical tapes by SEM-EDS. The samples were divided into black and clear adhesives. The element menu for the clear adhesive samples consisted of magnesium, aluminum, silicon, sulfur and lead, chlorine, antimony, calcium, titanium, and zinc. The element menu for the black adhesive samples consisted of magnesium, aluminum, sulfur and lead, chlorine, antimony, and calcium.

In addition to these publications, a guideline exists for the analysis of adhesive tapes by SEM-EDS.[42] The guideline explains the terminology, sampling and handling, and the analytical procedures for the analysis of tape samples for SEM-EDS analysis.

In 2011, A. Mehltretter et al.[3-4] reported the analysis of 90 electrical tapes by SEM-EDS. The first study[3] consisted of the analysis of the adhesives while the second study[4]

consisted of the analysis of the backings. In the case of the adhesives, five distinctive groups were found. The five groups were separated on the basis of the amount (and absence or presence) of zinc, chlorine, sulfur/lead, calcium, chlorine/lead, and zinc. Most adhesive samples fell under the first group which lacked most of the aforementioned elements. The adhesive analysis by SEM-EDS represented a 53% discrimination.

In the case of the backing comparisons,[4] the samples were divided into 15 distinctive groups which represented an 87.3% discrimination rate. The main differences between the 15 groups by SEM-EDS consisted of intense chlorine with aluminum and silicon both present in significant amounts, intense chlorine with calcium and⁄or antimony present in significant amounts, chlorine only, and minimal, if any, chlorine.[4]

1.5 Fundamentals of the laser-based analytical methods

Recently, the methods for the analysis of tapes by LA-ICP-MS and LIBS have been developed by our group.[43-44] These methods have proven extremely useful in the characterization and comparison of tape samples because of their high sensitivity and selectivity compared to the traditional methods used for the forensic analysis of tapes (physical and microscopic examination, SEM-EDS, IR, Py-GC-MS, SEM-EDS and μXRF). The instrumental principles of LA-ICP-MS and LIBS are described below.

1.5.1 Instrumental principles of LA-ICP-MS

Inductively Coupled Plasma-Mass Spectrometry (ICP-MS) is a technique for the elemental characterization of virtually any material. It evolved during the late 1990s into the well-established analytical procedure currently used in numerous fields such as geology, environmental chemistry, and forensic science. The main advantages of ICP-MS

consist in the ability of the method to perform multi-elemental analysis, its capability to provide comprehensive qualitative and quantitative information, and the ability to detect concentrations at very low levels.

A wide range of state-of-the-art ICP-MS instrumentation is commercially available. The instrumentation technology varies and continuously improves to meet the needs of chemists in different fields.

Before explaining is detail each aspect of the instrumentation, it is worth describing some of the basic concepts typically used in ICP-MS, such as the definition of an isotope and of ionization energy.

Different atoms of a same chemical element can have different masses; these are called isotopes. For example, ^{35}Cl and ^{37}Cl are two different isotopes of chorine: ^{35}Cl has 17 protons and 18 neutrons for a total mass of 35 amu, ^{37}Cl has 17 protons and 20 neutrons for a total mass of 37 amu. Some elements have only one stable isotope; these are referred as monoisotopic elements. Examples of monoisotopic elements are arsenic, aluminum, and sodium (^{75}As, ^{27}Al, and ^{23}Na). Other elements that have more than one stable isotope usually have constant isotopic abundances. In the case of chlorine isotopes, the relative abundance is 75.8% for ^{35}Cl and 24.2% for ^{37}Cl. An exception to this rule is lead, which is the decay product of other elements that are radioactive. The isotopic abundances of lead isotopes vary depending on the concentration and history of the precursor radioactive element.

By adding external energy, an electron can be removed from a neutral atom, thus creating an ion with a net positive charge. The electron's mass is negligible; therefore, the

ion's mass is approximately the same as the mass of the neutral atom. By application of more energy, a second electron can be removed, resulting in doubly charged species. The energy required to remove the electron (and produce the ion) is referred as ionization energy. Energies for ionization can be applied by thermal radiation, collision with other ions or electrons, or by exposure to high-energy photons.[45]

A schematic of the LA-ICP-MS instrumentation is shown in Figure 3. In LA-ICP-MS, a pulsed high-power laser is focused onto the surface of the sample. The laser beam removes a fixed volume of material and these particles are transported to the plasma torch where they are vaporized, atomized, and ionized. The torch consists of three concentric quartz tubes for the sample introduction, plasma formation gas, and cooling. The plasma is initiated by the addition of a few "seed" electrons generated from a spark. As the seed electrons are accelerated by a RF field, collisions with the neutral argon atoms create the ionized medium of the plasma.[45] Once the gas is ionized, the plasma is self-sustained by the RF field and a constant flow of argon gas. The ions produced in the plasma are transported to the interface where the pressure is reduced to the vacuum pressure needed for the spectrometer. The ions are guided to the quadrupole mass filter by the use of electrostatic ion lenses.[45] Once the ions reach the quadrupole mass analyzer, they are sorted by their mass to charge ratio (m/z). The spectra resulting from LA-ICP-MS is reported as intensity vs. m/z, although transient analysis (intensity vs. time) is also commonly used. The intensity counts are proportional to the concentration of each ion in the sample.

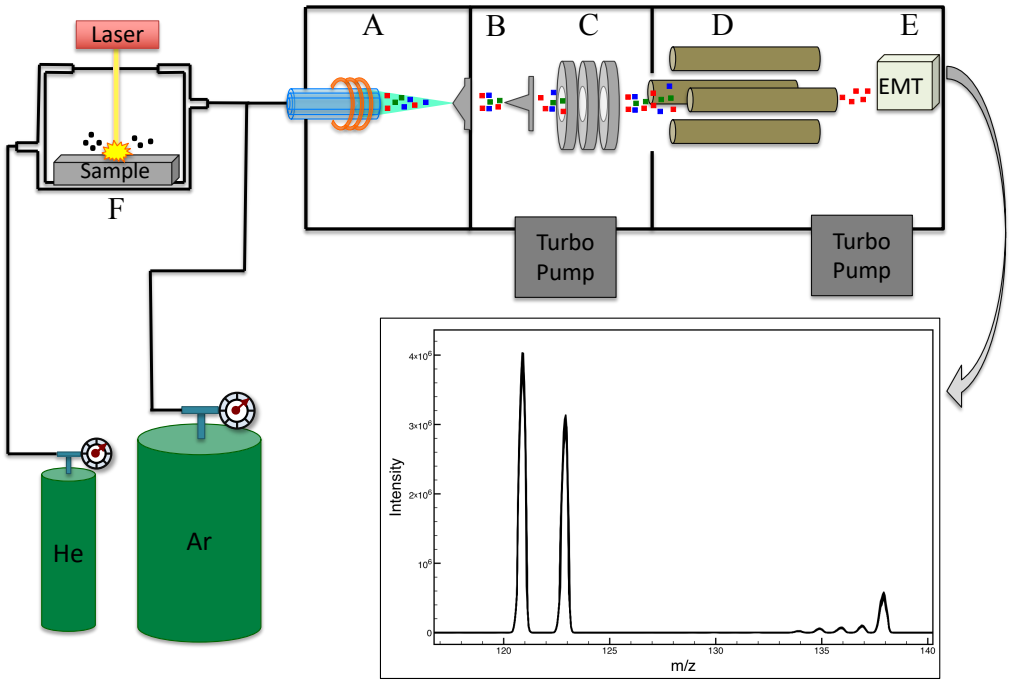

Figure 3 – Schematic of LA-ICP-MS showing the plasma (A), interface (B), ion lenses (C), quadrupole mass analyzer (D), detector (E), and laser ablation system (F), and the typical spectra obtained by LA-ICP-MS analysis (intensity vs. m/z).

In order to properly explain the different parts of the instrumentation, the components of the LA-ICP-MS system will be divided in different sections: plasma (Figure 3, A), interface (Figure 3, B), ion lenses (Figure 3, C), mass spectrometer (Figure 3, D), detector (Figure 3, E), and sample introduction: laser ablation (Figure 3, F) and solution nebulization.

Plasma

The definition of a plasma is an electrically neutral gas made up of positive ions and free electrons.[45] Plasmas have enough energy to atomize and ionize virtually all the elements in the periodic table. There are different types of plasmas, such as direct current

and microwave induced plasmas; however, inductively coupled plasma has demonstrated the most useful as an ion source for analytical spectrometry.[45] The gases typically used for producing the plasma are the inert gases helium and argon; however, plasmas can also be sustained in air and nitrogen. Inert gases offer the advantage of minimum chemical reactivity with the elements in the sample matrix.

Inductively coupled plasmas are formed by coupling energy produced by a RF generator to the plasma support gas (i.e., argon) with an electromagnetic field. The field is produced by applying a RF power (typically 700 to 1500 W) to a load coil made of copper positioned around the quartz torch assembly designed to configure and confine the plasma.[45] Figure 4 shows a schematic of the plasma torch and the load coil.

The plasma is initiated by the addition of a few seed electrons generated from a spark of piezoelectric starter to the flowing gas close to the load coil. After the plasma is initiated, it is sustained by a process called inductive coupling. As these seed electrons are accelerated by the electromagnetic RF field, they collide with the neutral gas atoms creating the ionized medium of the plasma, and these collisions create additional electrons. The plasma is sustained as an outcome of the cascading effect. Once the gas is ionized, it is sustained as long as the RF power is supplied to the load coil. The ICP has the appearance of an intensely bright fire-ball shape discharge (Figure 4).[45]

There are two basic types of generators used to produce the RF energy required for the ICP: the fixed frequency crystal-controlled oscillator and the free-running variable frequency oscillator.[45] The crystal controlled oscillator uses a piezoelectric crystal in the feedback circuit of the oscillator.[45] The oscillator has a frequency doubler as part of the

circuit which provides a typical operating frequency of 27.12 MHz. The free-running oscillator does not have a crystal. The frequency of these oscillator is determined by the combination of values of the components in the circuit.[45] An advantage of the free-running oscillator is the ease with which the plasma is initiated, making it easier to operate without too many moving parts or controls.

The load coil usually consists of a 3 mm inner diameter copper tubing wound into a 3 cm diameter spiral.[45] Cooling gas is passed through the coil to dissipate thermal energy (Figure 4). The coil serves as an antenna to produce an electromagnetic field to sustain the plasma. The coil is grounded to earth potential.

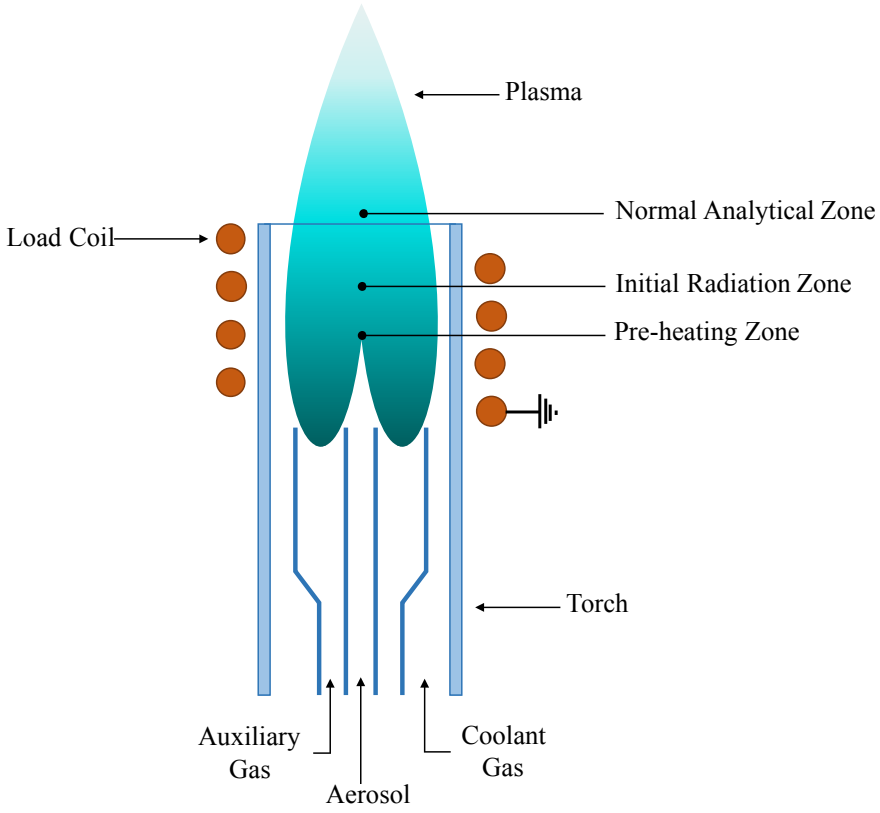

Figure 4 – Schematic of the inductively coupled plasma showing the torch, the different gases, and the various energy zones.

The torch is made of quartz and it contains and assists the configuration of the plasma. Quartz can tolerate the high temperature produced by the plasma before melting. A main quality of the torch is its RF transparency; the torch does not attenuate the frequency produced by the RF field. The quartz tube used as the torch has three concentric cylinders. A coolant gas (argon typically) is introduced between the outer and center tubes. The purpose of this gas is to prevent melting of the torch and to promote the annular shape of the plasma (Figure 4). The center tube is for the injection of the sample aerosol into the plasma. An auxiliary flow is supplied between the aerosol tube and the coolant gas tube to assist in the formation of the plasma, and to ensure the plasma is forced away from the tip of the injector (i.e., the end of the aerosol tube) (Figure 4). The different gas flows are typically 15 L/min for the coolant, 0 to 2 L/min for the auxiliary flow, and 1 L/min to the nebulizer flow. These flows vary between configurations and differences in experimental set-up.

The RF power couples mainly with the outer parts of the plasma, giving it its "doughnut" shape.[45] That region can reach a temperature of up to 10,000 K. The center region where the sample is introduced reaches a lower temperature (~5000 - 7000 K).[45] The intensity of the Ar^+ ions are minimum in the center of the annular region and maximum in the outer regions. For the sample ions, the maximum intensity happens in the center region which is another advantage of the plasma annular shape. Figure 4 shows the different plasma energy zones. Solvent evaporation and aerosol decomposition occur in the pre-heating zone before the sample enters the plasma. Atomization or decomposition of crystalline materials and dissociation of molecules occurs in the initial radiation zone.[45] Ionization of atomic species finally happens in the normal analytical zone.

Interface

The interface has three main functions: sample ions produced in the plasma, export them from the high temperature atmospheric pressure plasma, and facilitate their transport into the mass spectrometer.[45] The interface consists of two concentric cones made of nickel or platinum. Figure 5 shows a drawing schematic of the interface showing the two different cones: sampler and skimmer. The sampler cone orifice is located in the normal analytical zone of the plasma.[45] The diameter of the orifice of the sampler cone is approximately 1 mm. The skimmer cone is position right after the sampler cone. The diameter of the orifice of the skimmer cone is approximately 0.5 mm. The skimmer cone orifice samples the supersonic gas jet expanding through the sampler cone orifice, directing ions into the mass spectrometer.[45]

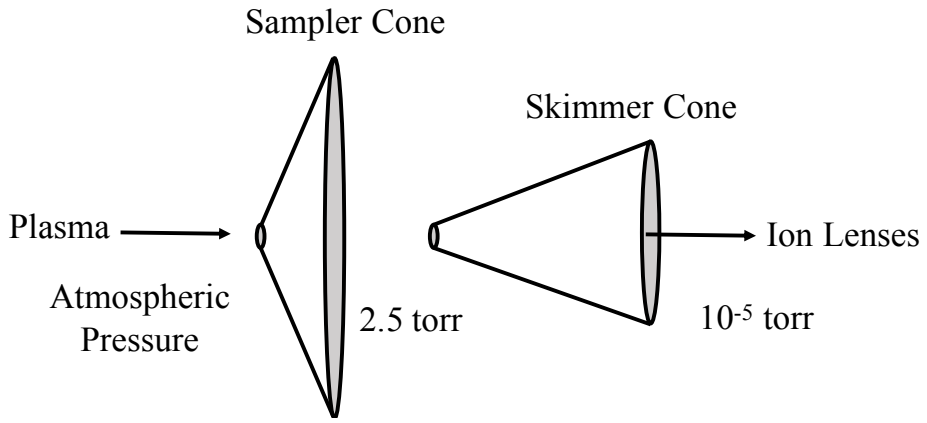

Figure 5 – Schematic of the interface sample and skimmer cones showing the different pressure regions.

A pump system consisting of two pumps is used to reduce the pressure from atmospheric pressure to 2.5 torr by a mechanical vacuum pump, further reduced to 10^{-5} torr with a turbomolecular pump.

Ion lenses

The ion beam passes through the ion lenses, which consist of one or two cylindrical electrodes. The first part of the ion lens in the photon stop (Figure 6). The purpose of the stop is to intercept photons and energetic neutral species produced in the ICP.[45] When photons reach the mass analyzer, they produce an increase in the background signal obtained from the spectrometer.

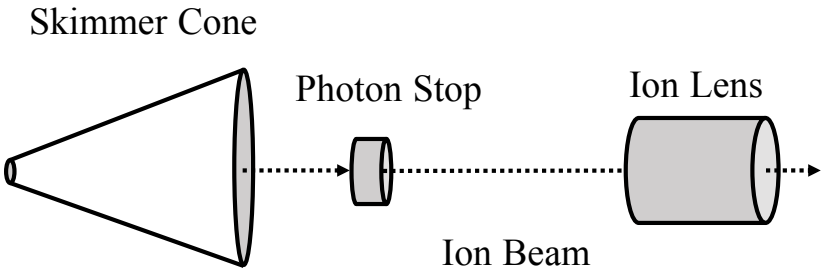

Figure 6 – Schematic of the ion lens showing the photon stop after the skimmer cone.

Mass spectrometer

The ions produced in the plasma can be measured by the use of a mass spectrometer. The mass spectrometer is essentially a mass filter designed to isolate a specific mass-to-charge ratio (m/z) ion from the multi-ion beam.[45] After separation of the individual ion beams, they are sequentially transported to the detector where each ion current is measured. The ion currents are proportional to the concentration of the analytes in the ion beam. Measuring the m/z ratio of an ion allows for the qualitative identification of the isotope being measured. The magnitude of the ion current allows the quantitation of the amount of analyte in the sample.

There are several different types of spectrometers currently used for ICP-MS instrumentation. The quadrupole mass spectrometer is one of the simplest designs which provides great stability, ease of operation, and relatively low cost.

A quadrupole mass spectrometer consists of four parallel rods as shown in Figure 7. The quadrupole rods are made of polished metal or metal-plated (gold) ceramic.[45] The ion beam passes through the center of the four rods. Only a single m/z value is allowed to travel through the rods and exit at the end. The rest of the m/z ions are rejected by the quadrupole. Both a direct current potential and a RF alternating current potential are applied to the rods (Figure 7). A positive potential is applied to a pair or rods, while a negative potential is applied to the opposite rods.

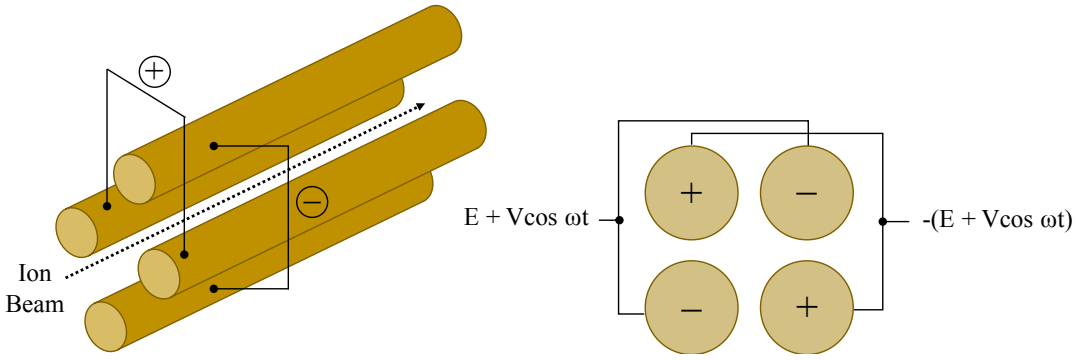

Figure 7 – Schematic of the quadrupole mass spectrometer showing the voltage applied to the rods.

As the voltages are varied, an electromagnetic field is created; this field then interacts with the ion beam. All ions deflect in a spiral shape as the interact with the field. The magnitude of the spiral path depends on the potential applied. Those ions with a unique m/z value will follow a stable trajectory and will be transported through the quadrupole rods.

Detector

There are several types of detectors used in ICP-MS. The most common detectors are the continuous dynode electron multiplier, discrete dynode electron multiplier, and the Faraday cup.

The continuous dynode electron multiplier (Figure 8, top) converts the ions exiting the mass spectrometer into a measurable electrical current. The wall of the horn-shaped detector is coated with a metal oxide (typically PbO) and when the ions impact these walls, one or more electrons are ejected. The ejected electrons are accelerated down the curved tube and as they further impact the wall, more electrons are produced; this results in the multiplication of secondary electrons. The front end of the detector is negatively charged to attract the ions that exit the spectrometer. An increasing positive potential is applied through the detector to further accelerate the secondary electrons produced. Once the electrons reach the collector, a direct current is measured.

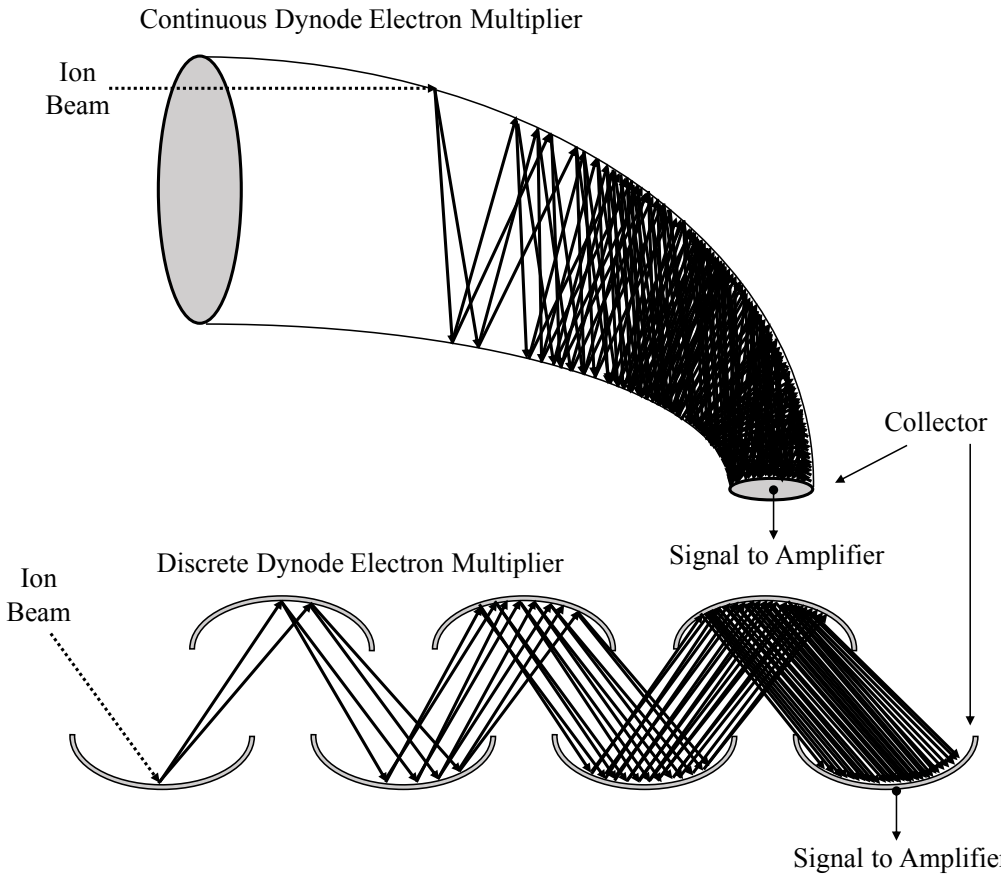

Figure 8 – Continuous dynode electron multiplier (top) and discrete dynode electron multiplier (bottom) schematics.

The continuous dynode electron multiplier has two modes: pulse-counting and analog. In pulse-counting mode, a high voltage is applied to the detector so that each ion causes significantly high amplification; this results in a gain of about 10^8. In analog mode, a lower voltage is applied to the detector resulting in an amplification of about 10^3 or less.

The current resulting from this detector is amplified, digitized, and eventually related to the analyte concentration. A drawback of this detector is its short life before replacement is required.[45]

Another type of detector used for ICP-MS is the discrete dynode electron multiplier (Figure 8, bottom). This detector is made of a series of individual dynodes. Similar to the continuous dynode electron multiplier, the dynodes are coated with a metal oxide. When an ion impacts the first dynode, two electrons are emitted. These electrons are accelerated by the increased positive potential across the dynodes' path, impacting with the following dynode and creating additional secondary electrons. The cascade process will continue for 15 or 16 stages with the final multiplied electron beam impacting a collector.[45] The multiplied electrons reach the collector and produce an electrical current proportional to the concentration of the ions in the sample. The amplification of this detector is of about 10^6.

Laser ablation sample introduction

In laser ablation, a short-pulsed high-power laser beam is focused onto a sample surface; the beam converts a finite volume of the solid sample instantaneously into its vapor phase constituents.[46] The ablated mass is a plume of hot atoms, ions, molecules, and particles.[47] The vapor is then transported to different detection systems for analysis (e.g., ICP-MS and LIBS).

Some of the mechanisms involved in the ablation process include thermal vaporization, shockwave propagation, plasma expansion, and solid exfoliation.[47] The occurrence of these mechanisms is related to the laser system used and the nature of the sample.

The laser ablation device (Figure 9) typically consists of an adjustable stage where the sample is located, a camera, a computer monitor, and a ns or fs laser. The sample is

placed in the ablation stage; the stage is controlled using the computer software which allows to move it in the x, y and z positions. A camera is used to visualize the sample in the computer monitor and properly focus the beam on the surface on the sample. The laser beam is focused on the surface of the sample though a transparent window. A pulse of energy from the laser strikes a specific region of the sample, removing a fixed amount of material depending of the duration and energy of the pulse.[45] The plume of particles ablated is moved to the plasma with the use of a carrier gas such as helium and argon. As the vapor reaches the plasma, it is atomized and ionized, and eventually moved towards the mass spectrometer and detector.

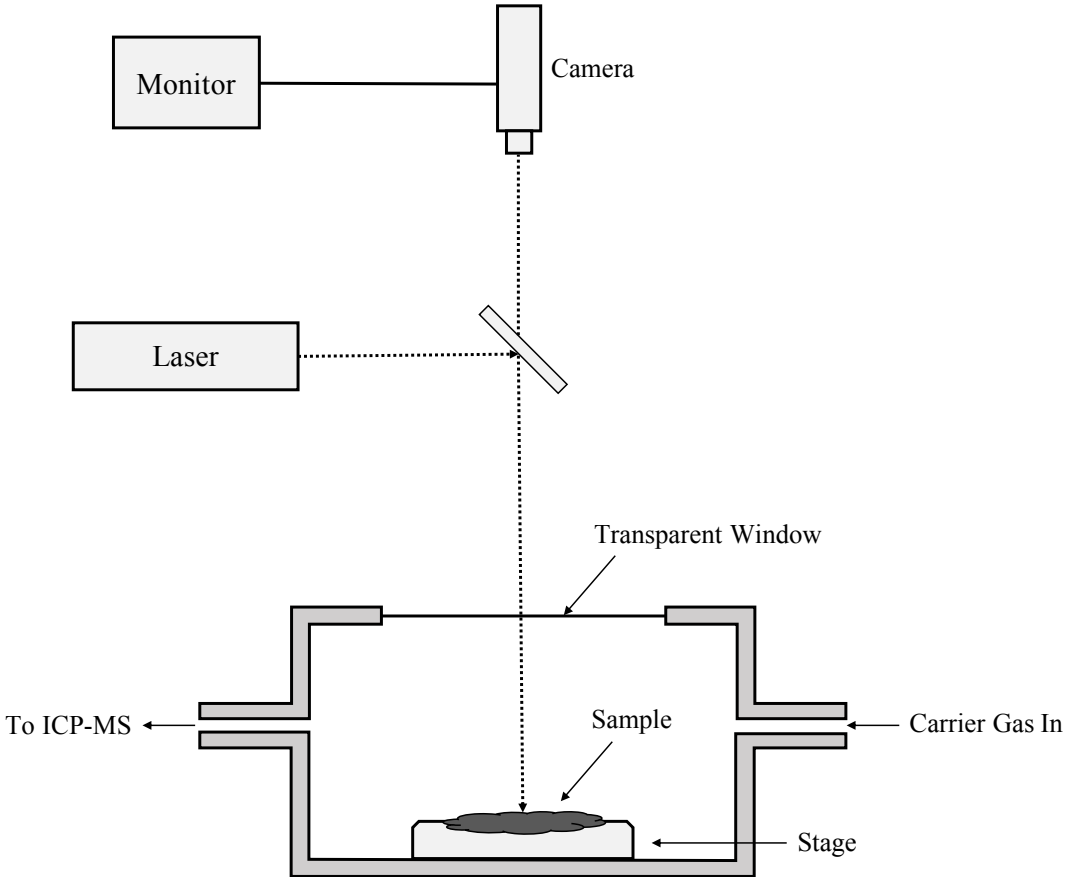

Figure 9 – Laser ablation sample introduction schematic showing the camera, laser, and sample chamber.

Different types of lasers are used for this technique. One of the most common lasers used is the neodymium-yttrium aluminum garnet (Nd:YAG) nanosecond laser.

The schematic of this laser is shown in Figure 10. The Nd:YAG laser is a solid-state laser consisting of three main components: the pumping source, the medium, and the optical resonator. Typically, flashtubes or laser diodes are used as the pumping sources. The Nd:YAG crystal is used as the laser medium. The medium is made of a crystalline material (YAG) which has been modified using neodymium. When the medium absorbs the pump energy, the low state energy electrons of Nd atoms are excited to high energy states. In other words, the medium is put into an excited state by the use of an external energy source (light source). The electrons do not stay in the highest energy state long, instead they decay to a decreased energy level, commonly referred as metastable level, emitting none-radiative energy (no photons) in the process. After some time in the metastable stage, the electrons decay down to the next state, this time emitting a photon in the process; this is called spontaneous emission. The photon released by spontaneous emission interacts with the electrons in the metastable stage, lowering them to the next energy stage while releasing two photons; this process is known as stimulated emission. When the two photons interact with the metastable electrons, four photons are released, and so on. Spontaneous emission occurs naturally, but stimulated emission requires a light source. The photons generated in the Nd:YAG medium bounce back and forth between the two mirrors (Figure 10) releasing more and more photons in the process, hence the light amplification. Eventually, the amplified light is allowed to exit the output mirror.

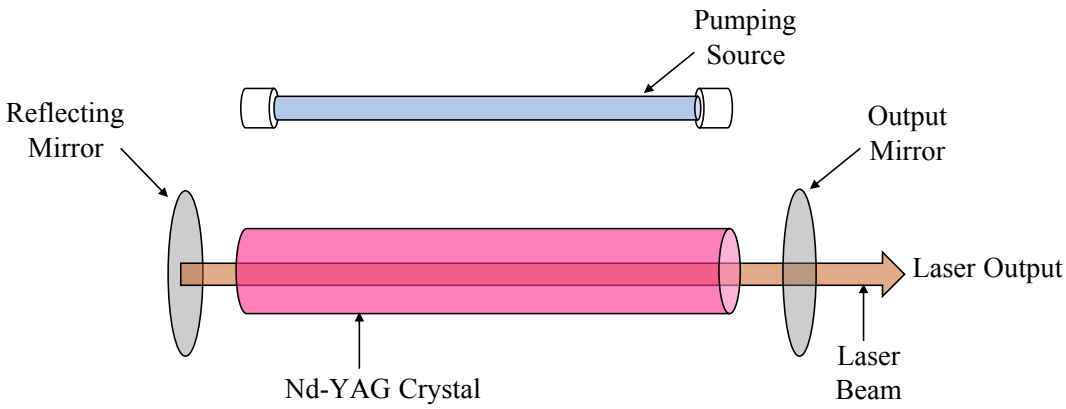

Figure 10 – Nd:YAG laser schematic showing the pumping source (lamp), the reflective and output mirrors, the Nd:YAG crystal, and the laser beam.

For stimulated emission to successfully work, more electrons should be in the excited state than in ground state; therefore, population inversion is needed. To induce population inversion, a process called pumping y performed. Pumping can be accomplished by light absorption, electrical discharge, or chemical reactions.

The typical output wavelength of the Nd:YAG lasers is 1064 nm. By using a series of crystals, the output frequency of the laser can be multiplied. For example, a resulting wavelength of 213 nm is obtained after multiplication of the output frequency by 5; this is referred as the fifth harmonic output of the laser. Fundamental wavelength (1064 nm), fourth (266 nm), and fifth (213 nm) harmonics are commonly used for Nd:YAG lasers. The output of 1064 nm has found to be useful for bulk analysis of samples; the fourth harmonic 266 nm has found to be a good compromise between ease of use, durability, and cost; the fifth harmonic 213 nm is a good compromise but it is more expensive than the 266 nm lasers and requires more maintenance.[48]

Solution nebulization sample introduction

Liquid samples are delivered to the plasma by the use of a nebulizer. Nebulizers convert the liquid sample to an aerosol. These small droplets are suspended in the plasma carrier gas. The liquid samples are first converted into a wet aerosol and then into a dry aerosol as soon as the reach the base of the plasma. The dry aerosol is then converted to molecules, atoms, and ions.

The process of nebulization can be achieved by the use of a pneumatic nebulizer. The principle of this nebulizer consists in using the force of a flowing gas, passed through an orifice or capillary tube, to create microdroplets from the liquid sample.[45] These microdroplets are transported with a stream of gas towards the plasma for vaporization, atomization and ionization. A common type of nebulizer is the concentric nebulizer, also known as Meinhard nebulizer (Figure 11). The one-piece nebulizer, usually made of glass, has an internal capillary tube of 10 to 35 μm in diameter mounted in a concentric fashion axial to an external tube. Nebulizer gas is passed through the external tube at a flow rate of about 1 L/min, which results in sample being pumped through the internal capillary at a rate of 0.5 to 1 mL/min, with aerosol formation occurring at the tip.[45]

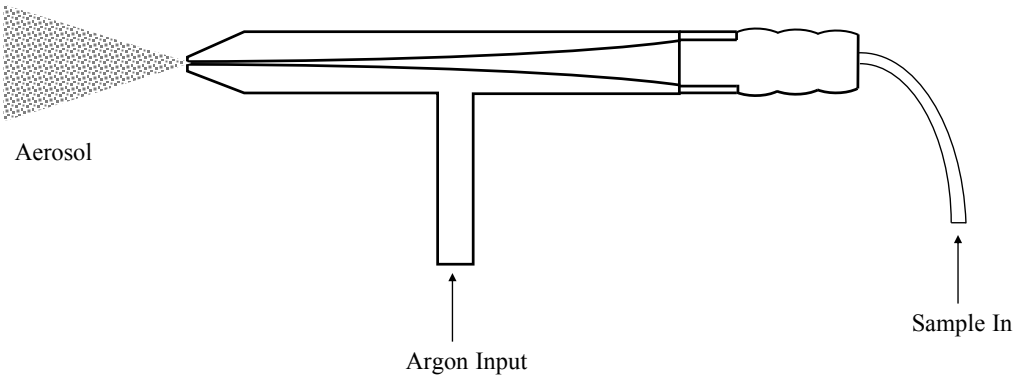

Figure 11 – Schematic of a concentric pneumatic nebulizer schematic.

The aerosol formed by the nebulization process creates a population of droplets that have a distribution of sizes ranging from 1 to 80 μm in diameter. Uniformity in the droplet size allows for precise results. The large droplets are harder to evaporate than the small droplets and eventually atomize and ionize, causing instability in the plasma. A spray chamber is used in order to reduce the larger droplets from entering the plasma.

The spray chamber provides an expansion space for the droplets to travel in a recurring trajectory. The larger droplets collide with the walls of the chamber where they are condensed. Only the small droplets are transported towards the plasma. A common spray chamber used consists of a cyclonic design. This device uses a tangential rotary flow path in a single circular compartment.[45] The centrifugal force of the aerosol results in the larger droplets being forced to the outside where they collide with the wall.[45] The small droplets are swept through the spray chamber and reach the exit towards the plasma.

With spray chambers, only a small percentage (less than 10%) of the original sample reaches the plasma. The bulk of the sample is delivered to waste.

1.5.2 Instrumental principles of LIBS

Laser Induced Breakdown Spectroscopy (LIBS) is a relatively new, and very powerful technique that can potentially be applied to all types of samples under ambient conditions. The instrumentation for LIBS is cheaper and relatively simpler than LA-ICP-MS, and it provides very good elemental information about the samples while causing minimum destruction of the material. The analysis by LIBS can be performed in seconds, and databases currently exist to assist in the interpretation of the data obtained from this spectroscopic technique.

Principles of LIBS

A schematic of LIBS principles of operation is shown in Figure 12. Laser Induced Breakdown Spectroscopy is a form of atomic emission spectroscopy in which a highly energetic laser pulse is focused onto the sample producing a micro plasma. The plasma is responsible for atomizing and exciting the sample. The formation of the plasma only begins when the focused laser achieves a certain threshold for optical breakdown, which generally depends on the environment and the target material.[49] After a short period of time, the excited species return to ground state energy levels emitting characteristic light in the process. It is important to mention that the plasma timeline depends greatly on the instrument parameters used. The times shown in Figure 12 might not be the same for different lasers, energy, frequency, and type of sample.

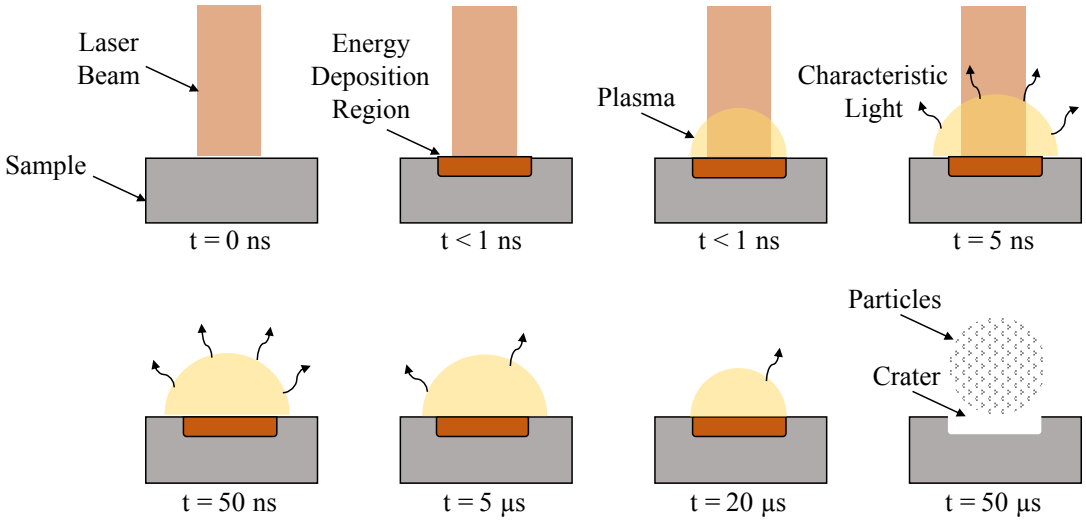

Figure 12 – LIBS principles schematic showing the timeline of the plasma and the interactions of the laser with the sample.

The element-characteristic light is collected by the fiber optic cable, separated by the spectrometer and detected by the time-gated detector. Since all elements are capable of

emitting light of characteristic wavelengths, virtually all elements can be analyzed by LIBS. The particles can be swept away using a carrier gas and/or transported to an ICP-MS for further analysis.

The instrumentation for LIBS commonly consists of the laser, the ablation chamber, a fiber optic cable, an optical spectrometer, and a time-gated detector (Figure 14).

The light collection and measuring time in LIBS is extremely important. If the light collection occurs too early, the spectrum results in a continuum because of molecular and neutral species (Figure 13). The continuum is primarily a consequence of bremsstrahlung (free-free) and recombination (free-bound) events. As electron-ion recombination proceeds, neutral atoms, and then molecules form.[50] The background continuum decays over time. However, if the collection of light occurs too late, the signal intensity is diminished, causing decreased sensitivity. The delay (or gate delay) is the length of time between the first laser interaction with the sample and the moment the detector starts reading. The observation window (or gate width) is the time the detector stays on.

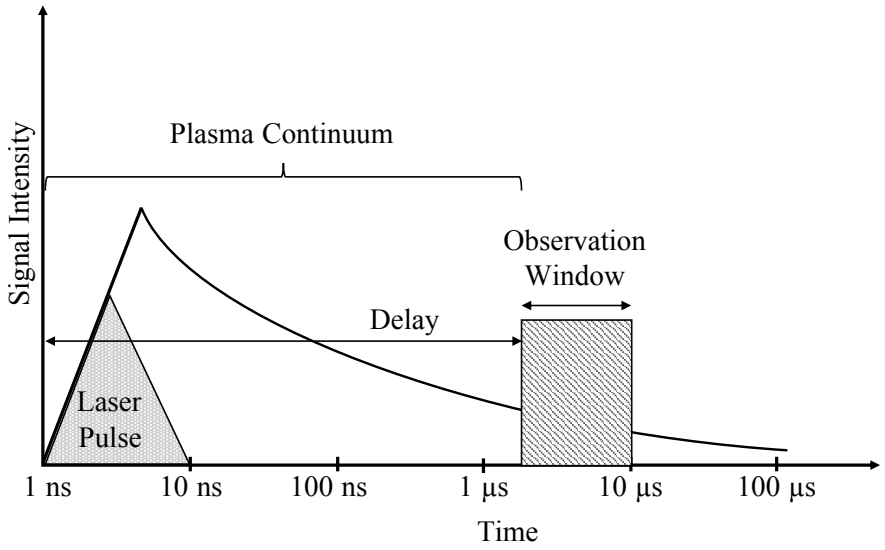

Figure 13 – Plasma timeline for LIBS after laser pulse interacts with the sample.

The laser system in LIBS is very similar to the laser used for LA-ICP-MS. The most widely spread are the flashlamp-pumped solid-state lasers with Nd:YAG as laser medium operated in the Q-switch mode to generate high-energy laser pulses with pulse durations in the nanosecond range.[51] Commercial instruments are available with the ability of performing LIBS analyses, as well as delivering the ablated material into the ICP-MS. Applied Spectra J200 Tandem System allows to capture and analyze the light emitted from the laser ablation plasma (LIBS), while transporting the ablated particles to the ICP-MS instrument. Short pulse lasers (ns and fs) are typically used for LA-ICP-MS and LIBS. The optical power of the laser appears in pulses of fixed duration at some frequency or repetition rate.

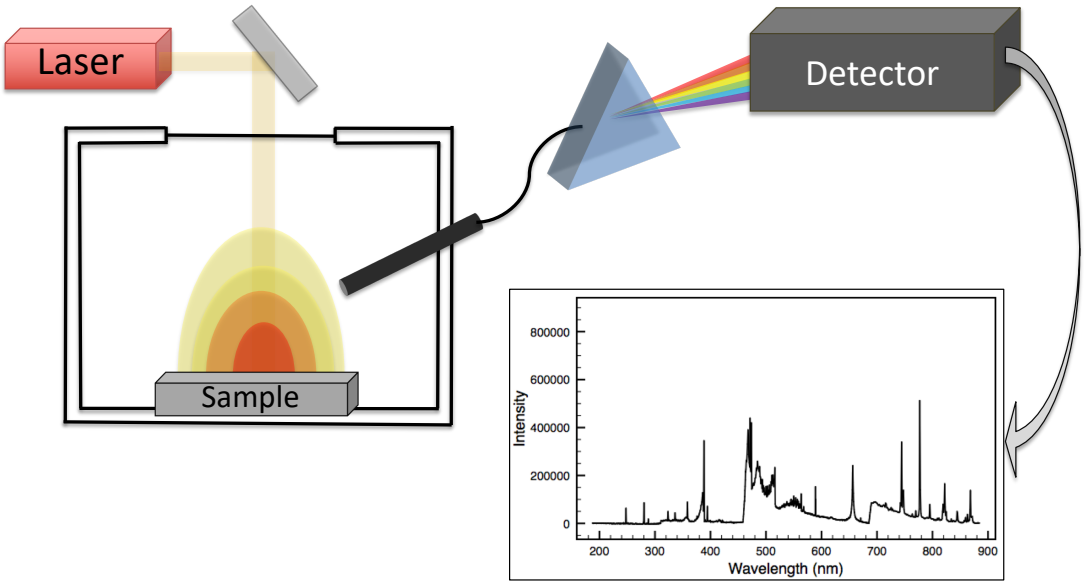

Figure 14 – Schematic for LIBS showing the laser, ablation chamber, fiber optic cable, spectrometer, detector, and typical signal obtained by LIBS analysis (intensity vs. wavelength).

The ablation chamber is where the sample is positioned. An adjustable stage allows to move the sample in the x, y and z directions to select the desired part of the sample to be ablated and to focus the beam on the sample surface. A camera is used for visualization of the sample morphology and to better focus the laser beam on the surface of the sample.

Once the laser interacts with the sample creating the plasma, excited species are formed. The excited species eventually return to ground energy state emitting light in the process. The light is collected by the fiber optic cable. The fiber transmits the light using total internal reflection and those light rays entering the fiber within the acceptance cone angle (numerical aperture) will be reflected down the fiber with high transport efficiency.[50] The acceptance angle of a fused silica fiber optic is ~26º so that light will be collected from all parts of the plasma if positioned a few centimeters distant.[50]

The light collected by the fiber optic cable is transmitted towards the spectrometer. The spectrometer disperses the emitted radiation of the laser-induced plasma to obtain a spectrum in terms of intensity as a function of the wavelength.[51] The main spectrometers used for LIBS are the Czerny-Turner and the echelle. In the Czerny-Turner, the light is directed to an entrance slit. The light passes the slit and reaches a curved mirror where the light is collimated (the light results in parallel beams). After reaching the reflecting mirror, the light undergoes diffracting grating and is eventually collected by another mirror which refocuses the light onto the exit slit. The exit slit is adjusted to let specific wavelengths pass. The Czerny-Turner is referred as a monochromator. The echelle is similar to the Czerny-Turner with the main difference being that the echelle has two dispersive elements instead of one (a grating and a prism). The echelle is therefore referred as a polychromator. The echelle offers higher resolution than the Czerny-Turner spectrometer and is typically expensive.

Once the light is dispersed with the help of the spectrometer, it is detected by the detector. The most common detectors used for LIBS are photomultiplier tubes (PMT), charge-coupled devices (CCD), and intensified charge-coupled devices (ICCD). In a PMT detectors, the light pulse striking the photocathode material results in the ejection of electrons that, through electrostatic focusing, travel through a set of dynodes coated with a secondary emissive material.[50] Similarly to the electron multiplier from ICP-MS, the electrons hitting the dynodes multiply and an amplification of up to 10^6 is obtained. The large number of electrons are collected at the anode and an electrical current is obtained. A CCD detector consists of a large number of light-sensing elements arranged in a two-dimensional array on a thin silicon substrate. In a CCD detector, photons strike the silicon

surface creating free electrons through the photoelectric effect. Electrodes covering the chip surface hold these electrons in place in an array of pixels, so that during exposure of the chip to light, a pattern of charge builds up that corresponds to the pattern of light.[52]

1.6 Statistical analysis and interpretation

Highly sensitive and selective techniques such as LA-ICP-MS and LIBS require suitable means of analysis and comparison of the recovered data. The qualitative data obtained by LA-ICP-MS can be in the form of intensity vs. m/z (mass scan) or intensity vs. time (transient mode). The abundance of the specific m/z values can be translated to concentrations and also used to confirm the presence of an element in the sample using its natural isotopic abundance. Both mass scan and transient mode can be used for further data analysis to report differences and similarities between samples, or to characterize the samples on the basis of their elemental profile. Typical comparison between samples by LA-ICP-MS using mass scan can be achieved by spectral overlay. In addition, the area under the curve for the selected m/z values (mass scan), and the area under the curve for a specific time range (transient mode) for the selected isotopes can be used for univariate and multivariate statistical analysis.

In the case of LIBS, the data are typically reported in intensity vs. wavelength. The intensity for all the emission lines can be related to the concentration of the element in the sample. Confirmation of the presence of an element in the sample can be achieved by monitoring similar emission lines for the same elements; this allows to rule out potential interferences.

Similarly to LA-ICP-MS, the area under the curve for the selected emission lines can be integrated and background-subtracted for further statistical analysis. Alternatively, the spectra resulting from LIBS for two different samples can also be qualitatively compared to report the main differences and similarities, and the characterization of the element menu obtained for each sample.

1.6.1 Spectral overlay comparison

The data resulting from LA-ICP-MS in the form of intensity vs. m/z were plotted and compared using the graphing software Plor2 (v2.0 for Mac). The data resulting from LIBS analyses in the form of intensity vs. wavelength was plotted and compared using the graphing software Plot2 (v2.0 for Mac) and Aurora (version 2.1, Applied Spectra, Freemont, CA). The first step in the spectral overlay comparison is the confirmation of the presence of the specific elements (ions or emission lines) above the detection threshold. Furthermore, the intensity for each element is compared using the presence or absence of the element, as well as the difference in intensity assuming the element is present in both samples. If the range in intensity of all the replicates overlapped with the range of all the replicates of the other sample for every element, the pair is said to be indistinguishable.[53] The number of comparison pairs can then be calculated as: $(n-1)/2$, where n represents the number of samples. The percent discrimination is given by the ratio of distinguished pairs over total number of pairs, multiplied by 100. This percentage of discrimination is typically reported in forensic science as it can help assess the potential of a technique (or analytical method) for the analysis and comparison of materials.

Spectra overlay is useful as it provides a visual representation of the main differences between two samples. In addition, spectral overlay is used to confirm association between duplicates and to check inter- and intra-day variations samples used as control. Moreover, spectra overlay allows the confirmation of the isotopic pattern of each element. In the case of LIBS, the presence of more than one emission line improves the certainty of identification of the presence of an element.

Although spectra overlay is user friendly and easily accessible, it presents disadvantages such as being subjective to the analyst's opinion and time consuming for several samples. Multivariate analysis of the integrated peak areas of the elements of interest can be used to determine if there is significant statistical difference between samples when the sample size is large.

1.6.2 Statistical analysis

Multivariate statistical methods allow the analysis of a large number of samples with several dependent variables automatically. Some examples of multivariate statistics methods include Principal Components Analysis (PCA), Cluster Analysis (CA), Linear Discriminant Analysis (LDA), and K-Nearest Neighbour (KNN). The multivariate statistical methods are divided in two groups: supervised and unsupervised methods. Supervised methods are those that start with a number of objects whose group membership is known.[54] Unsupervised methods are those that help to see whether objects fall into groups without any prior knowledge of the groups to be expected.[54]

Principal component analysis is an unsupervised technique for reducing the amount of data when there is correlation present.[54] In PCA, the set of correlated variables is

converted into linearly uncorrelated variables called principal components. For example, in the case of LA-ICP-MS analysis of tapes, up to 28 elements are found for be present in electrical tape samples. The comparison of samples of tapes using the 28 elements can be time consuming and confusing to interpret. However, the use of PCA allows to further reduce the data to three main principal components that account for the highest variability between the samples. Cluster analysis, just like PCA is an unsupervised technique. In CA, the distance between two points is used to determine the proximity of objects in the variable space. Cluster analysis produces dendrograms that cluster groups. Linear discriminant analysis consists in finding linear combinations within the sample set that can be used to associate or separate two or more samples to previously designed classes.[54] Linear discriminant analysis uses the linear discriminant function, which is a linear combination of the original variables. Linear discriminant analysis differs from PCA in that it is a supervised technique. The method of KNN predicts the test sample's category according to the nearest neighbors to the test sample and classifies it to the category that has the largest category probability. In KNN, a test sample is assigned the class most frequently represented among the k nearest training samples. If two or more such classes exist, then the test sample is assigned the class with minimum average distance to it.[55]

Univariate analysis is also useful to numerically compare different samples. As the name implies, in univariate analysis one element is compared at a time. Analysis of Variance (ANOVA) is a very useful method of comparing the means between samples. In addition, a post-hoc Tukey-Kramer test can be coupled to ANOVA in order to identify which sample mean is found significantly different from the rest. Analysis of variance was used for tape comparisons for reporting the differences between different sections of

selected tape rolls, different days of analysis for a same tape, and samples originating from different sources.

Aside from ANOVA, different match criteria can be used for the univariate comparison of tape samples. The match criteria typically used for tape comparisons for both LIBS and LA-ICP-MS data consisted of $K_{mean} \pm 3s$, 4s, or 5s where K_{mean} represents the mean of the "known" sample, and s represents the standard deviation of the "known" sample. If the mean of the "question" sample Q_{mean} falls within the range of the mean and the selected standard deviations for all the monitored elements, then the samples are said to be indistinguishable from each. If at least one element falls outside this range, the samples are differentiated from each other. A very simple schematic of this is shown in Figure 15; sample C would be reported as distinguished from sample A based on their differences is element X. Sample A and sample B would be reported as indistinguishable based on element X.

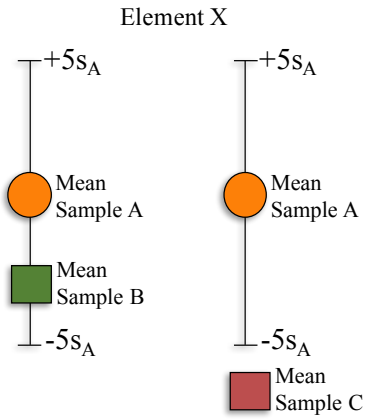

Figure 15 – Schematic representation of match criterion of mean ±5s for the comparison of two samples. Sample C is said to be distinguished from sample A based of their differences in element X.

Typically, $K_{mean} \pm 5s$ has been most useful for LIBS analysis, while $K_{mean} \pm 4s$, and 5s have been used for LA-ICP-MS analysis.

2 ELEMENTAL ANALYSIS OF ELECTRICAL TAPES BY LA-ICP-MS

2.1 Qualitative analysis of tapes

Qualitative analysis refers to the comparison of tapes using the intensity signals generated by the LA-ICP-MS instrument. Although the quantity of the components present in the samples are not reported by qualitative analysis, these constituents can be identified and used for comparison of the samples. Two tape samples are compared on the basis of spectral overlay (i.e., superimposing two spectra together to detect differences in the abundance and presence or absence of an isotope of interest). In addition, integration of the area under the curve for the selected isotopes allows to compare the samples numerically by statistical analysis such as ANOVA, PCA, match criteria comparisons, among others.

Qualitative analysis has been extremely useful in comparing samples of interest to forensic science such as inks and paper.[53] The present chapter section evaluates the use of LA-ICP-MS for the qualitative analysis of electrical tape samples.

The elemental composition of the electrical tapes examined in the chapter has been analyzed previously by SEM-EDS.[4] The elemental characterization by SEM-EDS allowed for 87% discrimination by pairwise comparison; SEM-EDS was the most discriminating tool for electrical tape backings.[4] Although SEM-EDS proved useful for the inorganic characterization of tapes, this technique presents some limitations such as low sensitivity and selectivity.

Laser ablation ICP-MS is proposed as a valuable complementary tool in tape examinations because of its superior sensitivity and selectivity, minimal sample destruction, short analysis time, and little to no sample preparation. Moreover, the current

study investigated if the chemical signature of tape backings could be used beyond comparative purposes to provide useful intelligence information about sources of origin.

2.1.1 Instrumentation and measurements parameters

The analysis by LA-ICP-MS was performed using a quadrupole ELAN DRC II (Perkin Elmer LAS, Shelton CT USA) ICP-MS coupled to a ns-Nd:YAG laser (NW UP213, New Wave, California). Data were acquired in mass scanning mode from m/z ^{7}Li to m/z ^{238}U and in transient mode using the following isotopes: ^{27}Al, $^{135, 137}$Ba, ^{13}C, $^{42, 44}$Ca, ^{111}Cd, ^{35}Cl, ^{57}Fe, ^{39}K, ^{139}La, ^{7}Li, $^{24, 26}$Mg, $^{95, 98, 100}$Mo, ^{23}Na, $^{206, 208}$Pb $^{121, 123}$Sb, $^{28, 29}$Si, $^{118, 119}$Sn, $^{86, 88}$Sr, $^{47, 48}$Ti, ^{232}Th $^{64, 66}$Zn, and $^{90, 91}$Zr. Performance checks were conducted daily and before each analysis. Standard reference material NIST 612 was used to monitor oxides (ThO/Th) and doubly-charged (Ca^{++}/Ca) ratios we monitored, as well as the intensity counts for the background (mass 220), and for light, medium, and heavier isotopes (Li, Ce, La, U). The final element list was reduced to 29 elements that were found to be relevant for characterization of the backing components. Table 1 shows the optimum instrumental parameters for LA-ICP-MS of electrical tape backings. Spectral regions that were anticipated to have large contribution from Ar isotopes and other polyatomic interferences were excluded from the scanning method. The isotopes selected for area integration were those with high abundance and small number of polyatomic and isobaric interferences.

Table 1 – Optimized parameters for the analysis of tape backings by LA-ICP-MS.[44]

Laser	ns-Nd:YAG (213 nm)
Energy	100% (2.6 mJ)
Stage Speed	40 µm/s
Spot Size	190 µm
Frequency	10 Hz
Ablation Mode	Line
Line Length	4 mm
Scanned Spectra	m/z 7 to m/z 238
Sweeps/Reading	40
Readings/Replicate	1
Carrier Gas	Helium
Gas Flow	0.9 L/min

The analysis by SEM-EDS was conducted using a Philips XL 30 scanning electron microscope (Philips, The Netherlands) coupled with an energy dispersive spectrometer detector (EDAX, USA) using a method previously reported.[4] The SEM-EDS was operated at 50X magnification, 15 mm working distance, 25 kV accelerating voltage and 200 seconds of acquisition time.

2.1.2 Sample collection and sample preparation

Six electrical tapes rolls (Table 2) were purchased at local retail stores. Each tape roll was divided into six sections and each section was further split into three (11 inches) subsections to constitute each analytical sample. The tape samples were placed on transparency films (Apollo, Acco Brands) and stored in plastic protectors. The local tapes were used to assess the intra-roll and inter-rolls variations in electrical tapes. Four out of the six tapes were also used as intra- and inter-day duplicate controls.

Table 2 – Locally purchased black electrical tapes.[44]

Sample Roll	Brand Name	UL
T02	Scotch (Super 88+)	539 H
T03	Scotch (Super 33+)	539 H
T04	Scotch	539 H
T05	Commercial Electric	E 305030
T06	General Electric	362 K
T07	General Electric	362 K

A selection of 90 black electrical tapes previously analyzed by Py-GC-MS, SEM-EDS, FTIR, and microscopical examination by Mehltretter et al.[3-4] was shared with our research group to assess the capabilities of SEM-EDS and LA-ICP-MS analyses. The samples were received as tape segments placed on plastic transparency films and were stored in plastic protectors prior to and after analysis.

In addition to the six electrical tape rolls locally purchased for the preliminary inter-roll and intra-roll studies, 45 electrical tapes were acquired for a more in-depth homogeneity study and to assess the variability within and between rolls for the different brands. A description of the 45 locally purchased tapes is included in Table 3. Packages containing as many as 100 rolls (e.g., T45 in Table 3) were used to analyze the homogeneity within rolls and between rolls of a same package, for different brands. The packages containing only one roll of tape were also used for within-source variation studies.

Prior to LA-ICP-MS analysis, a piece of ~1 cm by 2 cm of tape was cut and placed directly inside the ablation chamber.

Table 3 – Locally purchased black electrical tapes for in-depth inter- and intra-roll comparisons.

Sample Roll	Brand Name	UL	Country of Origin	Rolls Per Package
T08	Scotch 3M	539H	USA	1
T09	Scotch 3M	539H	USA	1
T10	Scotch 3M	539H	USA	1
T11	Scotch 3M	539H	USA	1
T12	Scotch 3M	539H	USA	1
T13	Duck	74HK	China	1
T14	Duck	21XH	USA	1
T15	Scotch 3M	539H	USA	1
T16	Scotch 3M	539H	USA	1
T17	Scotch 3M	539H	USA	1
T18	Scotch 3M	539H	USA	1
T19	Scotch 3M	539H	USA	1
T20	General Electric	362K	Taiwan	1
T21	Scotch 3M	539H	USA	1
T22	Utilitech	E219145	China	1
T23	Scotch 3M	539H	USA	3
T24	Scotch 3M	539H	USA	1
T25	Morris	3JHY	China	1
T26	General Electric	362K	USA	1
T27	Utilitech	E219145	China	1
T28	Frost King	906B	China	2
T29	Ace	74HK	China	1
T30	Temflex	539H	Mexico	1
T31	Victor	57RJ	China	1
T32	Morris	3JHY	China	1
T33	Shurtape	~	USA	1
T34	Duck	74HK	China	3
T35	Scotch 3M	539H	USA	3
T36	Steren	~	China	10
T37	Power First	590J	Taiwan	10
T38	Wonder	362K	Taiwan	10
T39	Scotch 3M	539H	USA	5
T40	Utilitech	E219145	China	10
T41	Pipeman's Installation Solution	590J	Taiwan	10
T42	3M Tartan	539H	USA	10
T43	Nitto	101K	Taiwan	10
T44	Scotch 3M	539H	USA	40
T45	Scotch 3M	539H	USA	10 rolls/10 pkgs. (100 rolls)

2.1.3 Data reduction and statistical analysis

Data pre-processing included the removal of non-relevant mass-to-charge peaks originating from polyatomic and isobaric interferences and normalization to the sum of the intensity peaks to account for any shot-to-shot variation and/or inter-day variations and as a mean to compensate for mass removal differences between replicates.[53] In the absence of an internal standard, the normalization strategy accounts for small differences in the ablated mass between samples and improves both repeatability and reproducibility of each individual sample.

Data reduction and statistical analyses were performed using Excel 2011 (version 14.6.1, Microsoft Corporation), JMP (version 12.0.0, SAS Institute Inc., NC), Plot2 for Mac (version 2.0.8, Berlin, Germany), and an in-house searchable database that uses machine-learning algorithms for classification and comparison of unknown samples to the database collection, specifically Partial Least Squares Discriminant Analysis (PLSDA) and K-Nearest Neighbor (KNN) spectral comparisons.[56] The search algorithms generate similarity scores that allow the user to identify the most similar samples in the data set. Moreover, the database reports the top five most similar spectra to the sample in question, therefore strengthening the confirmatory value of the comparison.

2.1.3.1 Estimation of discrimination power

The ability of a method to differentiate tape samples originating from different sources is evaluated by estimating the percent discrimination power (DP). The discrimination power was estimated as reported by Mehltretter et al.[4]

2.1.3.2 Estimation of percentage of correct associations

A total of 129 duplicates were used to calculate the percentage of correct associations to its corresponding tape roll. The 129 duplicates consisted of measurements from different sections of the 90 tapes and 39 duplicates from the inter-day and intra-day controls on four out of the six the locally purchased tapes. The 39 duplicates consisted of eight different days for the intra-day tapes (T04, T05, and T06) which accounted for 24 duplicates, and 15 for all the different days for the inter-day tape T07 was analyzed. Each duplicate was blind to the analyst and was compared by spectral overlay, PLSDA and KNN.

2.1.3.3 Estimation of the accuracy of the method

The percentage of accuracy of the method was estimated as:

$$\%\ Accuracy = \frac{true\ positives + true\ negatives}{total\ number\ of\ test\ samples} \qquad \text{Equation 1}$$

2.1.3.4 Comparison criteria

Spectral overlay analysis was conducted using Plot2 (version 2.0.8). The spectral overlay comparison method has been previously reported by our group.[53] In order to prevent bias in spectral overlay match decisions, the spectra were analyzed as a blind set by a second analyst. Relative natural abundance of different isotopes was used to confirm the identification of each element. The overlay comparisons accounts for variability within replicate measurements, which include instrumental variations and compositional variations in the sampled locations.

In addition to spectral overlay, Analysis of Variance (ANOVA) was performed on the integrated peak areas of different sections of the locally purchased tape rolls to assess inter-day and intra-day variations, as well as intra-roll and inter-rolls variations for the 45 locally purchased tapes.

2.1.4 Results and discussion

The evaluation of the utility of LA-ICP-MS of electrical tape backings consisted of two main phases: optimization and validation. The optimization phase carefully selected optimal and practical acquisition parameters suitable for the typical physical and chemical characteristics of electrical tape backings. For instance, aspects such as typical evidence size recovered at the scene, thickness and tape morphology, relevant chemical information and intra-roll variability were all considered during the method development and optimization.

The validation was designed to answer questions that could demonstrate the scientific validity of the method, such as:

- Is the intra-roll variability of the elemental composition of electrical tape backings smaller than the inter-roll variability?
- If so, which elements are relevant for discrimination and association of electrical tape backings?
- Are the elements detected correlated to components of the formulation?
- What is the capability of the method to differentiate electrical tape backings originating from different sources and to correctly associate tape sections that originated from the same roll or same source?

- Which methods of comparison can be applied to the semi-quantitative comparison of tape backings, and what is the estimated error rate?
- What is the overall value of LA-ICP-MS alone for the analysis of electrical tape backings?
- What is the overall improvement anticipated if LA-ICP-MS is incorporated as complementary tool to current analytical protocols?
- Could the elemental characterization of tape backings be used for the classification of tapes and to provide lead information?

2.1.4.1 Optimization of instrumental parameters

The optimization of the method was aimed to obtain the best precision and signal to noise ratio (SNR) with minimal destruction of the material. The ablation on the backing of electrical tapes was optimized to control the penetration depth of the laser ablation crater into the sample. The optimal penetration depth was selected to assure a general bulk characterization of the chemical composition of the tape while preventing cross contamination from adjacent layers (laser removal of backing layer without contribution from the adhesive). Figure 16 shows the microscopical images of the cross-section of an electrical tape after been ablated using a raster pattern with the selected optimal parameters; the images were taken using a digital microscope (Model VHX-1000, Keyence, USA). Penetration depth was controlled at ~30 μm. The thinnest tape in our collection set was ~80 μm; therefore, the optimal parameters would then be appropriate for the typical thickness of backings even after being stretched. Table 1 represents the final optimized parameters for the analysis of electrical tape backings by LA-ICP-MS.

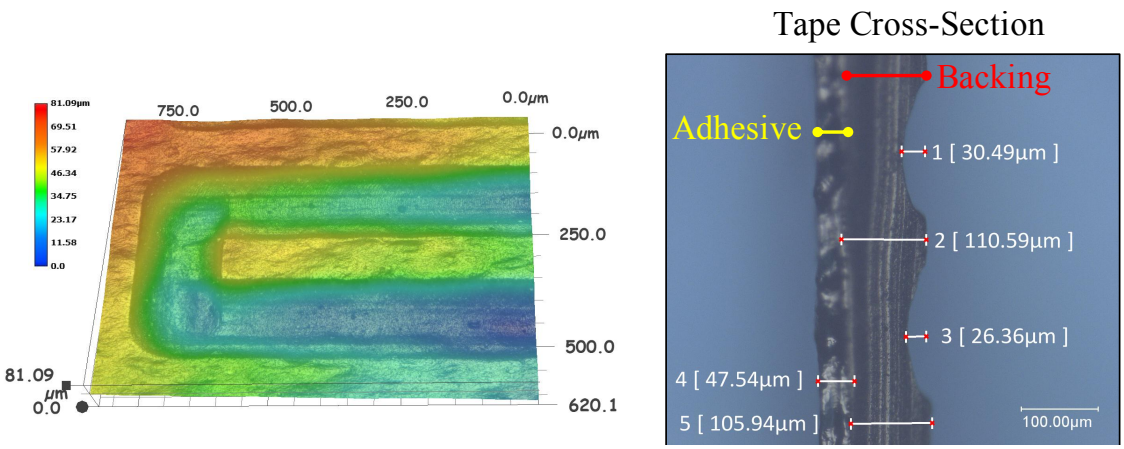

Figure 16 – Microscopical images of an electrical tape after being ablated using a raster pattern with the selected optimal parameters. Left: 3D image of the ablation pattern. Right: Cross-section of the tape. Images were taken using a Keyence digital microscope.[44]

2.1.4.2 Intra-roll studies (homogeneity studies)

To investigate the heterogeneity of the elemental composition on small sampling areas of a roll of tape (intra-roll variations), several of the locally purchased tape rolls were separated in six sections. Six replicates were performed per section, which generated a total of 36 replicates. Spectral overlay comparison was used to compare different sections of the electrical tape rolls. All replicate measurements overlapped the range of replicates of all the other sections of the tape, indicating small variability of the elemental profile across a single tape roll.

In addition to spectral overlay, analysis of variance (ANOVA) was performed on the integrated area for the element peaks for all the locally purchased tape rolls. No significant differences were found for the elements studied within the different sections within a single roll. Figure 17 illustrates the Tukey-Kramer analysis of the different sections of electrical tape T04 (Scotch, Made in USA, UL 539H) for magnesium and titanium. For both graphs, the horizontal line represents the overall mean between all the

tape sections. The diamonds illustrate the group mean and confidence intervals. The wider diamonds represent a larger number of replicates per group. No outliers were removed for the creation of the ANOVA plots.

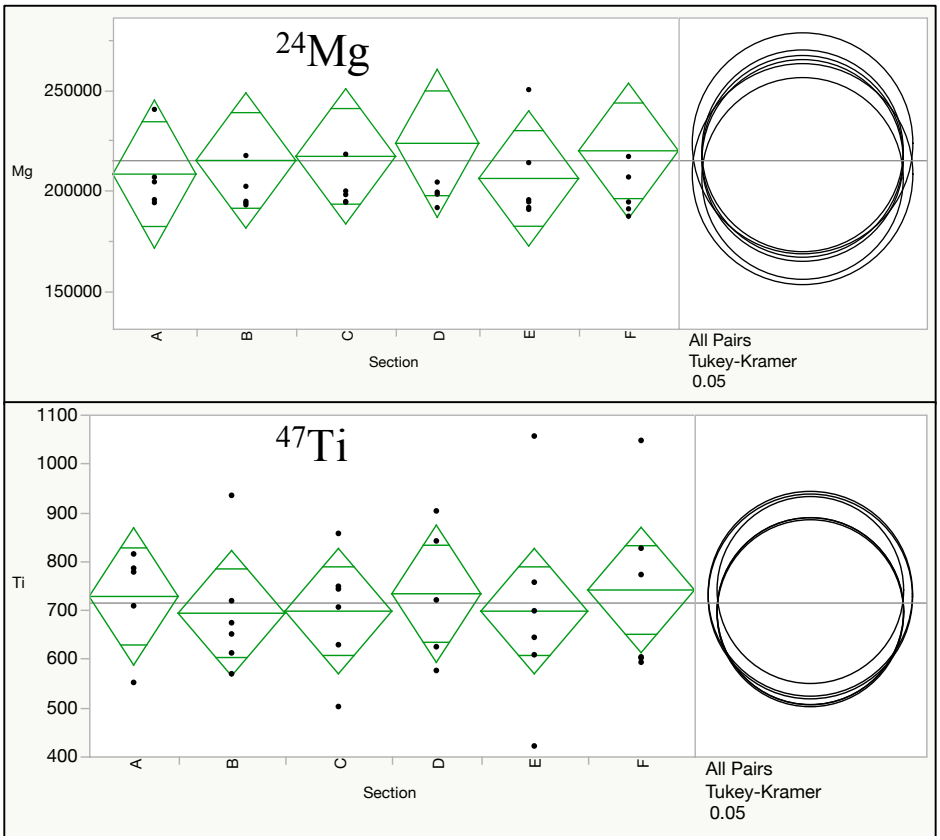

Figure 17 – ANOVA of LA-ICP-MS analysis of locally purchased Scotch electrical tape T04 within the different sections (A - F) of the roll for magnesium (top) and titanium (bottom) by Tukey-Kramer.[44]

Analysis of variance was also performed on the integrated areas of the isotopes of interest for the 45 locally purchased tape rolls. The sample set consisted of packages containing from 1 to 100 rolls. Analysis of variance was used to study within-roll and between-roll variations for all the packages. Figure 18 illustrates the ANOVA Tukey-Kramer analysis of the different sections and rolls of electrical tape T44 (Scotch 3M, Made in USA, UL 539H, Table 3) for antimony and strontium. No significant differences were

found for the elements studied for the different sections within a single roll (T44-R01 A-E), and among rolls in the 40-rolls package (T44 R01-R40). No significant differences resulted from t-Test performed on the roll pairs that showed the largest separation (e.g., T44 R11 vs. T44 R40 for ^{88}Sr).

No significant differences were observed for the rolls originating from the same package, or for different sections of the same tape roll for the 45 tape samples (Table 3). The lack of difference between rolls of a same package and within a single roll was extremely important, as it proved that the internal homogeneity within a sample of tape does not change for a whole batch, or within a tape roll. Homogeneity within a roll is needed before tape rolls from different sources (rolls) could be compared successfully.

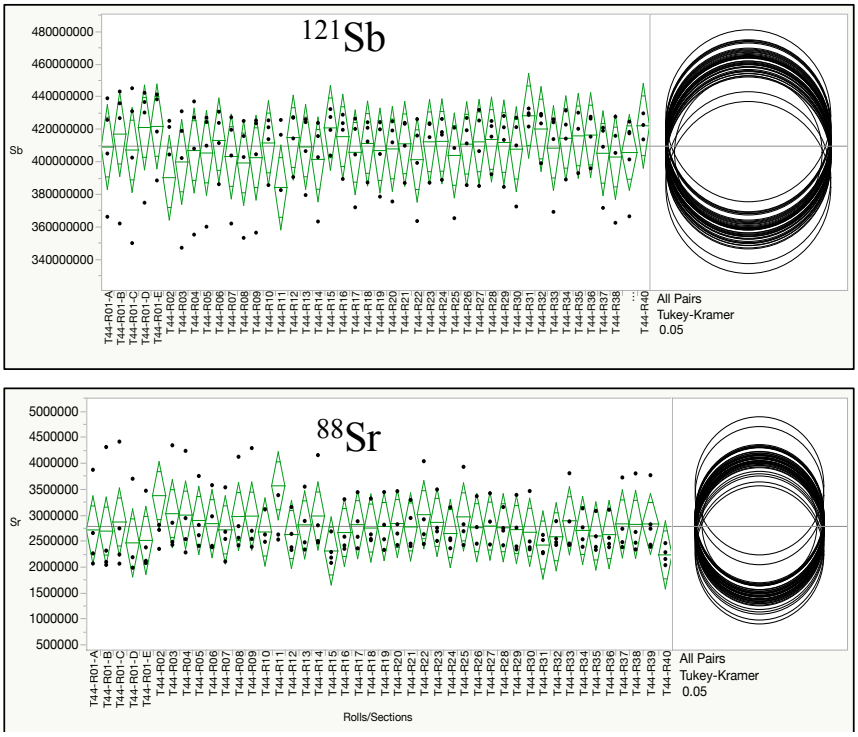

Figure 18 – ANOVA of LA-ICP-MS analysis of locally purchased Scotch electrical tape T44 within the different sections of a roll (T44-R01 A-E) and between the different rolls in the package (T44 R01-R40) for antimony (top) and strontium (bottom) by Tukey-Kramer.

2.1.4.3 Inter-roll variations (between source variations)

In order to evaluate the inter-roll variability and the discrimination capabilities of LA-ICP-MS, the elemental profiles of 90 electrical tapes backings were compared to each other. All 90 tapes were known to originate from different rolls. Elemental profiles obtained by SEM-EDS were compared to those obtained by LA-ICP-MS.

Figure 19 represents the spectral overlay comparison for SEM-EDS of tape 4 (Tesa Tape, Inc., Made in Taiwan, UL 362K) shown in blue and tape 32 (GE, Made in Taiwan, UL 206T) shown in red. Each spectrum shows three replicates measured. Elements such as calcium, antimony, barium, and titanium were often found as components of electrical tapes used in the present study. Nonetheless, antimony Lα (3.61) and calcium Kα (3.69) lines are not fully resolved as they are only 0.08 keV apart and typical SEM-EDS resolution is in the order of 0.1 keV. The same issue is observed when barium and/or titanium are present in the formulation. Moreover, barium and titanium were close to the detection limits (Signal to Noise Ratio (SNR) ~3) in these samples. After evaluation of the EDS spectra using spectra overlay, these two tapes were not distinguished by SEM-EDS using the detected elements (Ba, Ca, Ti, Sb, Cl, Si, and Al).

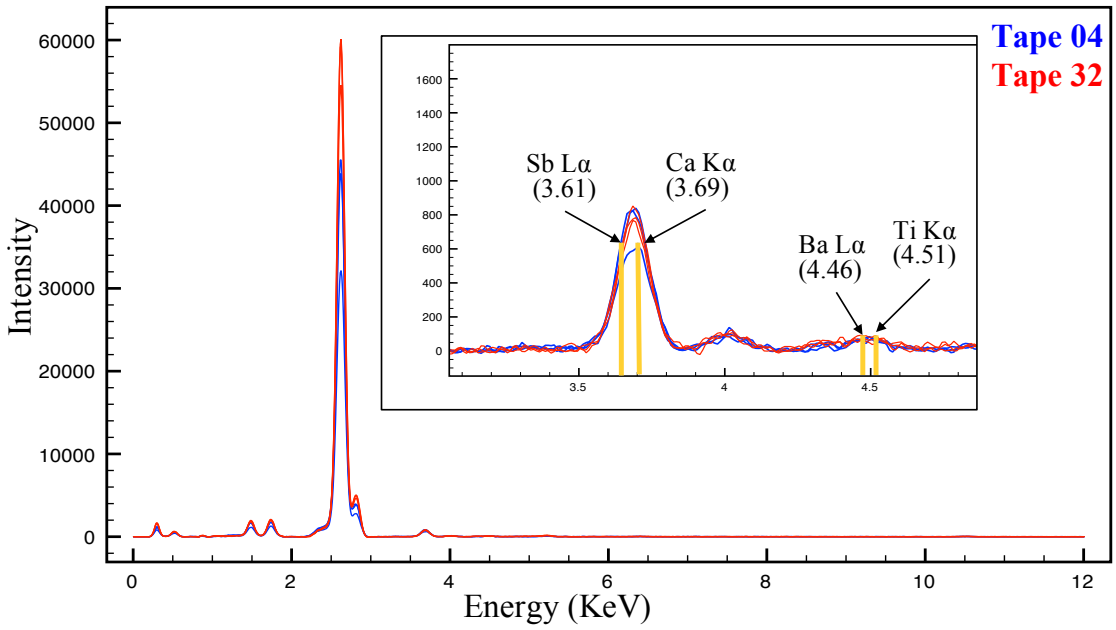

Figure 19 – Spectral overlay comparison for SEM-EDS of tapes 4 and 32.[44]

When the same tape samples were analyzed by LA-ICP-MS, the elemental profile was clearly differentiated. Figure 20 shows the LA-ICP-MS spectra, where significant differences were observed (e.g., tape 32 shows higher antimony and lower barium than tape 4). Additional elements were also detected in the samples (Li, Na, Mg, Al, Si, S, Cl, K, Cr, Cu, Zn, Br, Sr, Sn, Pb).

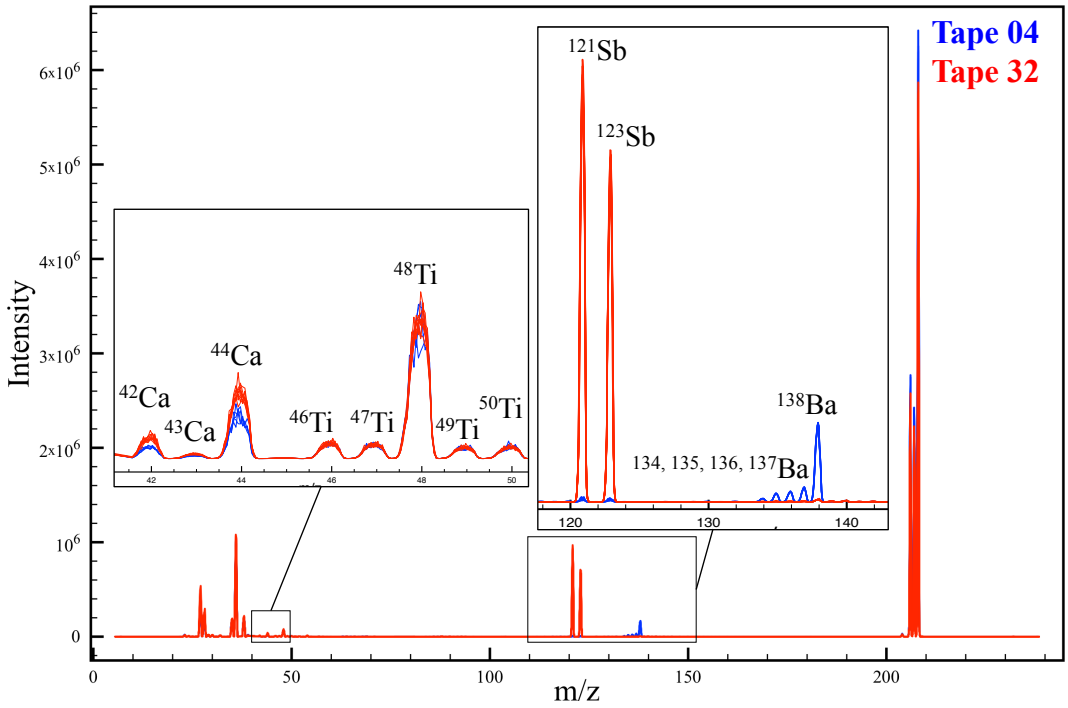

Figure 20 – Spectral overlay comparison of LA-ICP-MS of tapes 4 (blue) and 32 (red) showing the differences in the barium and antimony isotopes, and the identification of the calcium and titanium isotopes.[44]

Moreover, LA-ICP-MS not only provided superior discrimination capability, but also provided superior sensitivity and enhanced confirmatory value and selectivity. As shown in Figure 20, barium and titanium are detected with a SNR>10 (as opposed to SEM-EDS ~3 SNR). LA-ICP-MS was able to detect a greater number of elements on these tapes providing not only better discrimination, but also better characterization capabilities.

Selectivity is also improved in LA-ICP-MS, as the different isotopes of interest are resolved in the quadrupole. In addition to the ability to characterize the tape samples by providing an extensive elemental menu, LA-ICP-MS has the advantage of providing unambiguous identification of the elements by their m/z ratios and the relative abundance of natural isotopic signatures. Furthermore, the multiple isotopic profiles helped minimize potential interferences by comparing their ratios to natural abundance. Figure 21 shows the

spectral overlay comparison of tape samples 2 (Advance, Made in England) and 10 (3M Scotch Super 88, Made in USA, UL 539 H) and the relative abundance of the natural isotopes of molybdenum. Molybdenum isotope peaks were detected in tape 10 with a much higher intensity than in tape 2, and confirmation of molybdenum is possible by comparing the natural isotopic abundance ratios. From a forensic perspective, the detection of multiple isotopes per element adds certainty to the identification of inorganic compounds, providing additional scientific validity to the analysis.

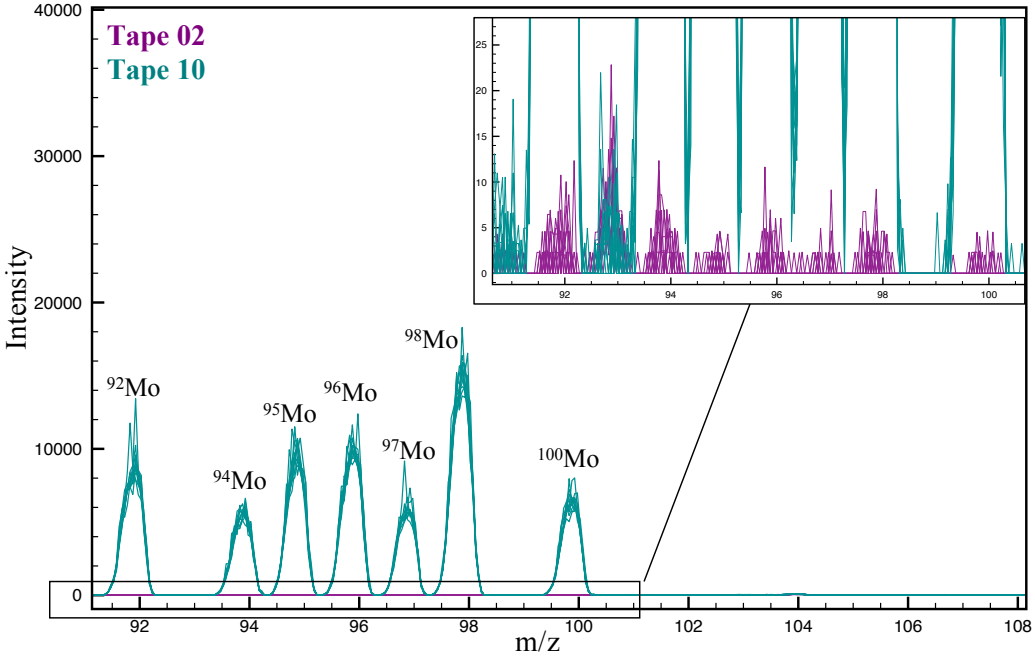

Figure 21 – LA-ICP-MS spectral overlay for tape 2 (purple) and tape 10 (green), demonstrating differences in molybdenum amounts and showing molybdenum natural isotopic abundances profile.[44]

2.1.4.4 Discrimination capabilities and error rates

Table 4 represents a summary of the discrimination power calculated for SEM-EDS and by LA-ICP-MS. Out of 4005 comparison pairs, SEM-EDS conducted in a previous study,[4] as well as corroborated in the current work, distinguished 87% of them. Since all

the samples originated from different sources, SEM-EDS by itself produced ~13% of false inclusions. The estimation of false inclusions assumes that all 90 samples originated from different sources, but there may be instances in which some of these samples may have originated from the same manufacturing plant (i.e., same product) or possibly the same jumbo roll. Interestingly, LA-ICP-MS distinguished 94% of the samples reducing false inclusions to ~6%. More importantly, the analysis of tapes by SEM-EDS allowed grouping of the samples into 15 distinctive groups and the determination of up to eight elements (Cl, Al, Si, Ca, Ti, Sb, Mg, Pb). Laser ablation ICP-MS allowed separation into 50 distinctive groups as a result of a superior characterization of the chemical components and the detection of up to 29 elements (Table 4).

Table 4 – Discrimination power, correct associations, grouping, and element menu found by SEM-EDS and LA-ICP-MS.[44]

	SEM-EDS	LA-ICP-MS
Number of Samples from Different Sources	90 (4005 pairs)	90 (4005 pairs)
Discrimination Power	87.3 % (3495 out of 4005)	93.9 % (3760 out of 4005)
Correct Associations	N/A	100% (129 out of 129 duplicates)
Number of Distinct Groups	15	50
Detected Elements	Cl, Al, Si, Ca, Ti, Sb, Mg, Pb	^{7}Li, ^{11}B, ^{23}Na, $^{24, 26}$Mg, ^{27}Al, $^{28, 29}$Si, ^{31}P, $^{32, 34}$S, $^{35, 37}$Cl, ^{39}K, $^{42, 44}$Ca, $^{47, 49}$Ti, ^{53}Cr, ^{55}Mn, $^{57, 58}$Fe, $^{63, 65}$Cu, $^{66, 68}$Zn, ^{81}Br, ^{85}Rb, ^{88}Sr, $^{90, 91}$Zr, ^{93}Nb, $^{95, 97, 98}$Mo, ^{111}Cd, ^{118}Sn, $^{121, 123}$Sb, $^{135, 137}$Ba, $^{206, 208}$Pb, ^{209}Bi

A review of several electrical tape and pressure sensitive adhesives patents confirmed the use of these elements as raw materials in tape formulations.[9-14] For instance, inorganic additives include fillers (aluminum oxide and aluminum silicate, barium sulfate,

cadmium oxides and silicates, calcium carbonate and calcium sulfate, iron oxide, lead oxides and silicates, magnesium oxide, silica, titanium oxides and silicates, zinc oxides and silicates), flame retardants (antimony oxide and molybdenum oxide), heat resistant components (aluminum, barium, calcium, chromium, iron, magnesium, niobium, sodium, strontium, tin, titanium, and zirconium oxides), pigments, catalysts and others (aluminum phosphate, calcium silicate, calcium stearate, iron salts, lead silicate, lithium catalysts, titanium dioxide, and zinc oxide). Until now, no other analytical method used in tape examinations allows for the comprehensive compositional characterization of tape backings. These inorganic components and their concentration were found to vary per brand and product.

The grouping found by SEM-EDS, LA-ICP-MS, and all the previously used techniques combined to LA-ICP-MS is represented in Table 5. The SEM-EDS group i was almost entirely separated by LA-ICP-MS into the individual tapes except for tapes 45 (Calterm, Made in Taiwan, 590J) and 55 (Manco, Made in Taiwan, 590J). Likewise, most of the tapes not differentiated by LA-ICP-MS were tapes from the same brand (Table 6).

Table 5 – Groups found by SEM-EDS, LA-ICP-MS and all the conventional techniques combined to LA-ICP-MS.[44]

SEM-EDS Groups	Sample Number	LA-ICP-MS Groups	Sample Number	All Techniques*	Sample Number
i	4, 8, 32, 42, 45, 51, 52, 53, 55, 56, 58, 70, 81, 82, 86	i	4	i	4
		ii	42	ii	42
		iii	45, 55	iii	45, 55
		iv	51	iv	51
		v	53	v	53
		vi	56	vi	56
		vii	58	vii	58
		viii	70	viii	70
		ix	81	ix	81
		x	82	x	82
		xi	86	xi	86
		xii	8	xii	8
		xiii	32	xiii	32
		xiv	52	xiv	52
ii	14, 35, 37, 50	xv	14, 37	xv	14, 37
		xvi	35	xvi	35
		xvii	50	xvii	50
iii	21, 38, 46, 67	xviii	21, 46	xviii	21, 46
		xix	38	xix	38
		xx	67	xx	67
iv	66	xxi	66	xxi	66
v	22, 69	xxii	22	xxii	22
		xxiii	69	xxiii	69
vi	72, 74, 76, 77, 79, 80, 83	xxiv	72	xxiv	72
		xxv	74, 79	xxv	74, 79
				xxvi	76, 77, 83
		xxvi	76, 77, 80, 83	xxvii	80
vii	62	xxvii	62	xxviii	62
viii	2, 10, 11, 12, 13, 15, 17, 18, 19, 20, 23, 24, 25, 26, 27, 28, 39, 41, 54, 61, 63, 64, 65, 68	xxviii	2	xxix	2
		xxix	10, 11, 12, 13, 15, 17, 18, 19, 20, 23, 24, 25, 26, 39, 41, 54, 61, 63, 64, 68	xxx	10, 23, 24, 61, 63
				xxxi	11, 12, 13, 15, 18, 20, 25, 26, 39, 41, 54, 64, 65, 68
				xxxii	17
				xxxiii	19
		xxx	65	xxxiv	65
		xxxi	27, 28	xxxv	27
				xxxvi	28
ix	16, 29, 30, 34, 36, 40, 43, 44, 47	xxxii	16, 29, 30, 34, 40, 43, 44, 47	xxxviii	34
				xxxvii	16, 29, 30, 40, 43, 44, 47
		xxxiii	36	xxxix	36
x	1, 5, 7, 48, 49, 57, 78, 84	xxxiv	1, 5, 7, 48, 49, 57	xl	1, 5, 7, 48, 49
				xli	57
		xxxv	78	xlii	78
		xxxvi	84	xliii	84
xi	3, 6, 31, 71, 87, 88, 89, 90	xxxvii	3	xliv	3
		xxxviii	6	xlv	6
		xxxix	31	xlvi	31
		xl	71	xlvii	71
		xli	87	xlviii	87
		xlii	88	xlix	88
		xliii	89	l	89
		xliv	90	li	90
xii	73, 85	xlv	73	lii	73
		xlvi	85	liii	85
xiii	9, 33	xlvii	9	liv	9
		xlviii	33	lv	33
xiv	59, 60	xlix	59, 60	lvi	59, 60
xv	75	l	75	lvii	75

*All techniques include physical examination, FTIR, SEM-EDS and Py-GC-MS, as reported by Mehltretter et al., [4] and LA-ICP-MS

Table 6 – Groups of tapes indistinguishable by all techniques.[44]

Indistinguishable Groups	Comments
45, 55	Taiwan, UL 590J
14, 37	Taiwan, UL 206T
21, 46	Manco®, Taiwan, UL 590J
74, 79	3M Scotch 700 commercial grade, USA, UL 539H
76, 77, 83	3M Scotch Super 33+, USA, UL 539H
10, 23, 24, 61, 63	3M Scotch Super, USA, UL 529H
11-13, 15, 18, 20, 25, 26, 39, 41, 54, 64, 65, 68	3M Scotch Super 33+ and 3M 700 commercial grade, USA, UL 539H
16, 29, 30, 40, 43, 44, 47	3M Tartan and 3M Temflex, USA, UL 539H
1, 5, 7, 48, 49	Tape It and Marcy Enterprises, Taiwan, unknown manufacturing source
59, 60	Tuff ™ Hand Tools, China

The elemental composition of electrical tapes analyzed by LA-ICP-MS provides enhanced discrimination, improved characterization capabilities and stronger conclusions than those provided by conventional methods, as a result of its superior sensitivity, selectivity and precision. In addition, LA-ICP-MS represents a complementary technique to the methods currently used (physical examination, FTIR, SEM-EDS, and Py-GC-MS). Table 7 shows the percentage of discrimination after LA-ICP-MS is combined with all the other techniques. Additional grouping was achieved (57 groups) with a discrimination power of 96.5%, and 3.5% of false inclusions, which is represented by the percentage of indistinguishable pairs.

Interestingly, LA-ICP-MS alone was able to classify the majority of the tape backings into the same groups as the combined conventional method (microscopic examination, SEM-EDS, FTIR and Py-GC-MS). These results indicate that the elemental signature detected by the laser ablation method has accurate classification capabilities and therefore could be used in forensic laboratories as a fast screening method that can reduce overall costs, time of analysis and reduce backlogs.

Table 7 – Discrimination power and grouping found by SEM-EDS, LA-ICP-MS, and the techniques combined, and percent of indistinguishable pairs for each method.[44]

	SEM-EDS	All Current Methods*	LA-ICP-MS	SEM + LA-ICP-MS	LA-ICP-MS + Current Methods*
Percent Discrimination	87.3%	94.3%	93.9%	93.9%	96.5%
Distinguished Pairs	3495	3777	3760	3760	3865
Distinct Groups	15	40	50	50	57
Percent of Indistinguishable Pairs	12.7%	5.7%	6.1%	6.1%	3.5%

*Current methods include physical examination, FTIR, SEM-EDS and Py-GC-MS as reported for the same sample set by Mehltretter et al. [4]

The comparison among the 50 different groups was performed by ANOVA to show the variability in elemental composition for selected isotopes and to identify which groups were different in each specific element. Antimony and strontium were selected because they offered great discrimination between tapes, and because they were previously used in the comparison between different rolls of a same package (see Intra-rolls studies section Figure 18).

In contrast with Figure 18, Figure 22 shows the significant differences found between the different groups for antimony and strontium. While the comparison between different rolls for a same package showed no significant differences between these two elements, the comparison between different sources showed clear differences for antimony (e.g., groups 09, 12, 13, 22, 25, 36 etc.) and strontium (e.g., groups 38, 40, 41, 42, 45, etc.). Most importantly, when combining both elements, increased discrimination is obtained between groups, showing the main advantage of multi-element analysis to classify samples into distinctive groups.

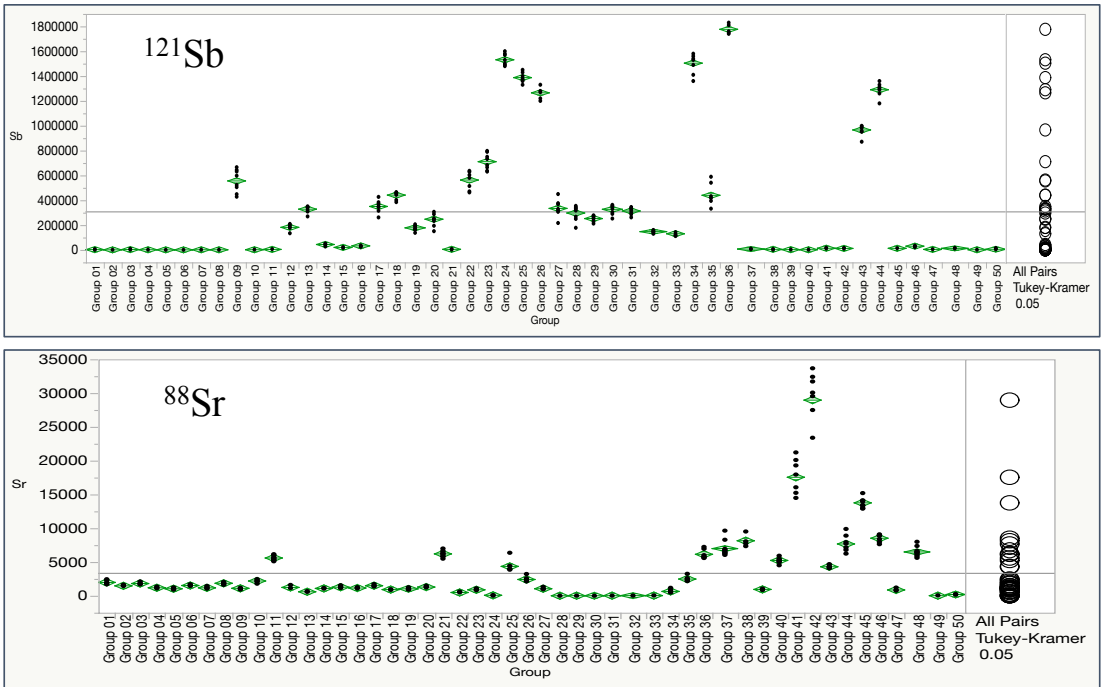

Figure 22 – ANOVA of LA-ICP-MS analysis of the 50 distinct groups for antimony (top) and strontium (bottom) by Tukey-Kramer.

2.1.4.5 Blind duplicate controls and evaluation of correct associations

The capability of the method to generate correct associations using the elemental profiles was studied by selecting 129 duplicate controls. These controls included 94 different electrical tapes, 90 tapes obtained from the FBI collection and four locally purchased tapes. The duplicates consisted of 4-6 replicates each, measured in different locations across a section of tape. Some blind duplicates were acquired months apart to account for any temporal variation or instrument drift. Figure 23 shows the spectra overlay of tape 8 and its duplicate (tape 8 D). All the replicates overlapped for all elements under study for the tapes and their duplicates, resulting in 100% correct association when using spectra overlay.

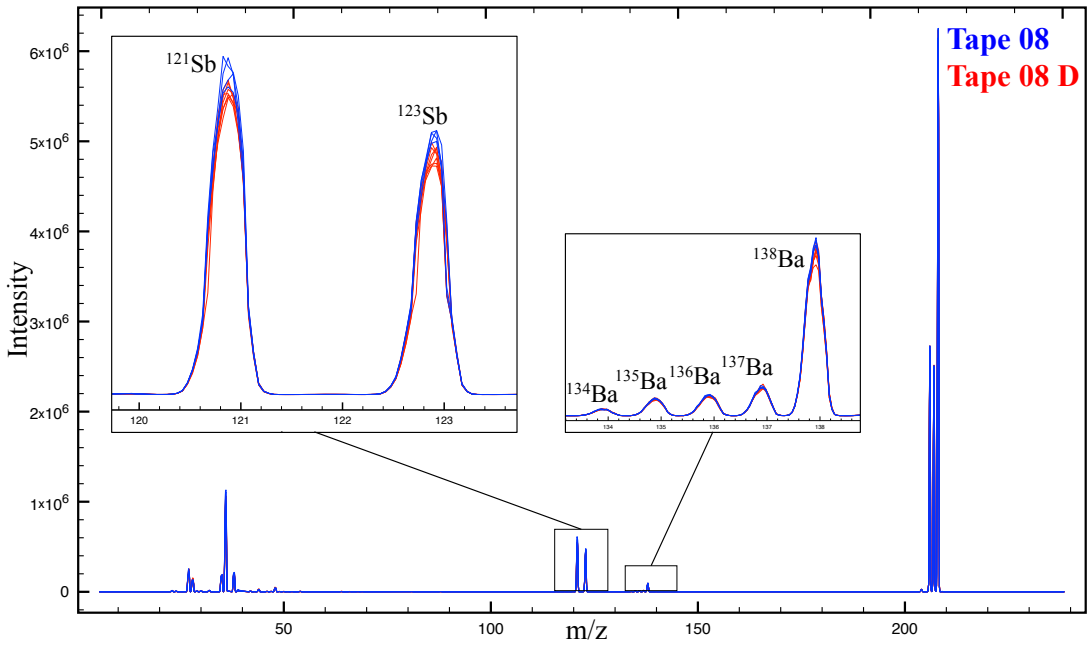

Figure 23 – Spectral overlay comparison of LA-ICP-MS of tape 8 (blue) and its duplicate 8 D (red) resulting in no significant differences for all the isotopes (antimony and barium isotopes shown as example).[44]

The locally purchased tapes used as controls consisted of 39 intra-day and inter-day blind duplicate controls analyzed on 14 different days, measured from two or three months apart. The control tapes were run at the beginning, in the middle and at the end of the analysis day. The spectra overlay plot shown in Figure 24; represents a control tape (General Electric, Made in Taiwan, UL 362K) for 14 different days of analysis for a period of three months. The results demonstrated that LA-ICP-MS provides good reproducibility and repeatability, with small inter-day and intra-day variations.

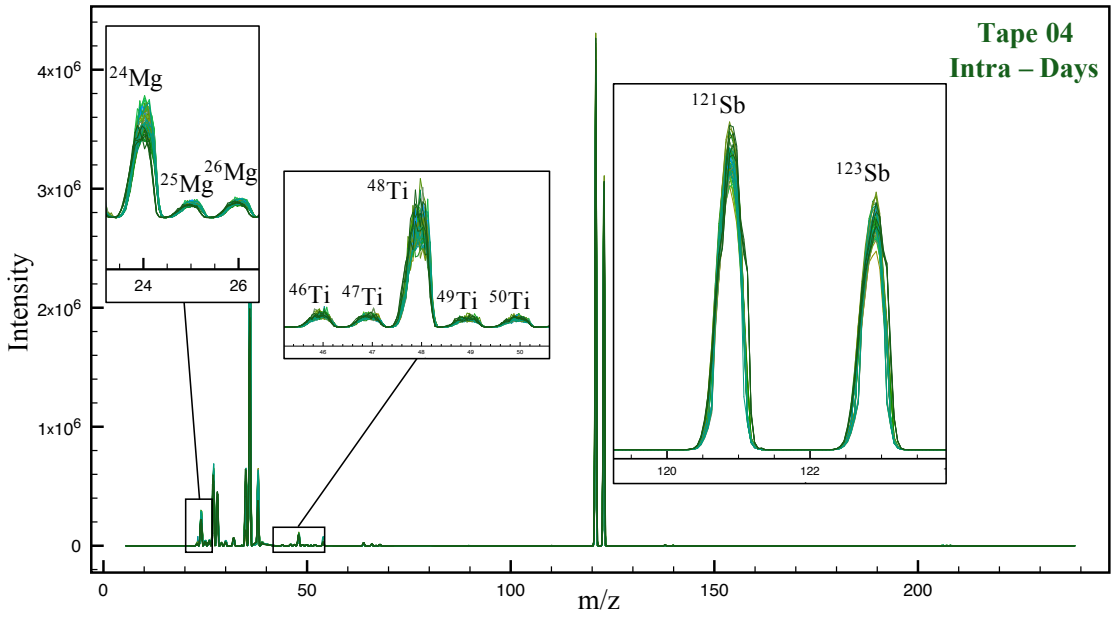

Figure 24 – Intra-day analysis of a locally purchased General Electric electrical tape in a period of three months (14 different days).[44]

2.1.4.6 Overall evaluation of the accuracy of the method

The accuracy of the method can be calculated by Equation 1, where the true positives are the samples that were correctly associated to their duplicates (129 duplicates representing 100% correct association), true negatives represent the samples that were distinguished from each other (3760 from Table 4), and the total number of test samples represent the sum of the true positives and the total number of pairs (129 + 4005 = 4134). The accuracy of the method was found to be 94.1% using spectral overlay.

2.1.4.7 Classification capabilities of LA-ICP-MS for the analysis of tapes

Principal component analysis was used to visualize the classification and grouping of tapes by country of manufacture. Tapes from different countries were clearly separated from each other, especially tapes manufactured in China (Figure 25). Moreover, a zoom-in on the United States and Taiwan region (Figure 26) shows two main clustering areas for

3M Scotch tapes manufactured in the USA. The main distinction between these groups (A and B in Figure 26) was found in the composition of lead, barium, antimony, magnesium and molybdenum, which might be due to differences in the source of the raw materials. It is important to note that tape labels do not necessarily represent the actual manufacturer. Tape distributors may provide their own label to a manufacturer, making it difficult to determine the manufacturer of the tape.[5] Therefore, the tapes labeled 3M made in Taiwan were likely not made by 3M but by a company located in Taiwan.

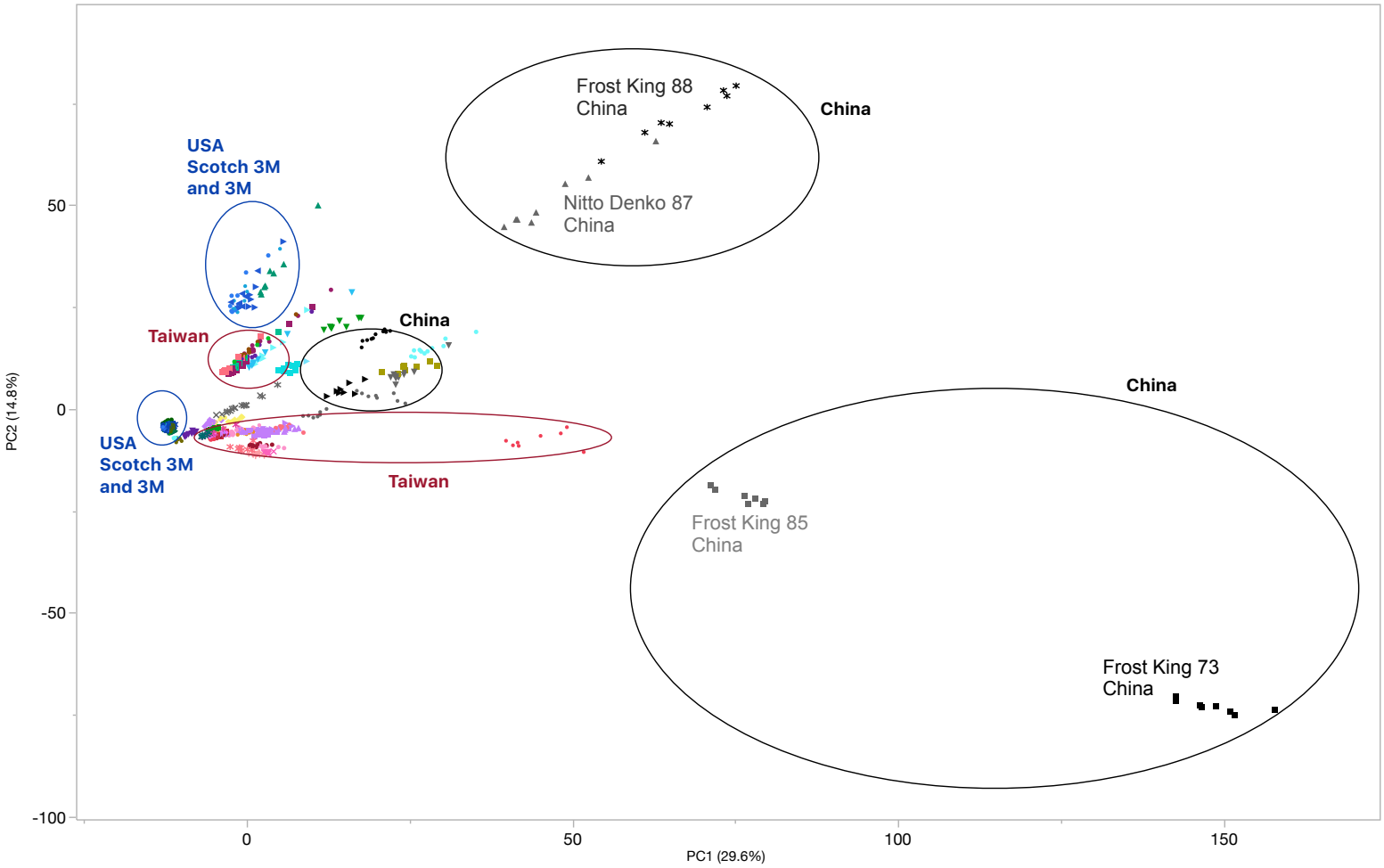

Figure 25 – PCA plot of the 90 electrical tapes selecting two principal components.[44]

Figure 26 – PCA plot of the 90 electrical tapes selecting two principal components. A: Scotch 3M tapes containing barium, antimony, and magnesium. B: Scotch 3M containing high amounts of lead.[44]

2.2 Quantitative analysis of electrical tapes by LA-ICP-MS

Quantitative analysis of tapes is necessary in order to create standard methods for the comparison and interpretation of tape samples. Once the concentrations of the elements present in tapes are known, a comprehensive database of tape samples can be populated and shared among laboratories. A database facilitates the use of likelihood ratios for the interpretation of tape evidence.

Two different quantitative methods were studied for the analysis of tapes. The first method consisted of an external calibration curve. Polyvinyl acetate (PVA) calibration point solutions were prepared using ICP-MS single element standards dissolved in 0.8 M HNO_3. Five calibration points were created; the linearity of the curves, percent bias compared to the certified material, and percent RSD among replicates were used to test the performance of the PVA external calibration method. External calibration curve methods have been thoroughly studied and applied to LA-ICP-MS analyses for a wide range of applications.[57-61] Most methods for external calibration require an internal standard to improve the precision of the quantitative analyses. In the present method, gold was used as a normalization standard by coating all the samples using a sputtering system. In addition, carbon (^{13}C) was also explored as an internal standard for this quantitative method of analysis of polymers.

The second procedure to determine the concentrations of the elements present in tapes and in other plastics consisted of the quantitative method without matrix-matched standards previously reported by Aeschliman et al.[62] In this method, the concentrations in an unknown solid can be found by using a known or standard solid to calculate a response

factor specific to each isotope. Solid samples of known concentrations used for the quantitative method without matrix-matched standards included: NIST SRM-610 and NIST SRM-612 glass standards, and BCR-680 and ERM®-EC681m polyethylene standards.

In order to test the performance of the quantitative methods, polyethylene films made of reference materials were created.

2.2.1 Polyethylene film standards preparation

Polyethylene standard films was prepared utilizing certified reference materials in pellet form (ERM-EC681m and BCR680) that were purchased from the Institute of Reference Materials and Measurements (IRMM, Geel, Belgium). The certified polyethylene pellets were melted on glass slides and cut into strips of ~1 cm by 2 cm. The thickness of the films was ~ 2 mm. Microwave digestion was performed using the SK-15 Ethos UP microwave digestion system (Milestone, Shelton CT USA) for both the films and the pellets to determine any loss of analytes during the melting process and to assess the performance of the digestion.

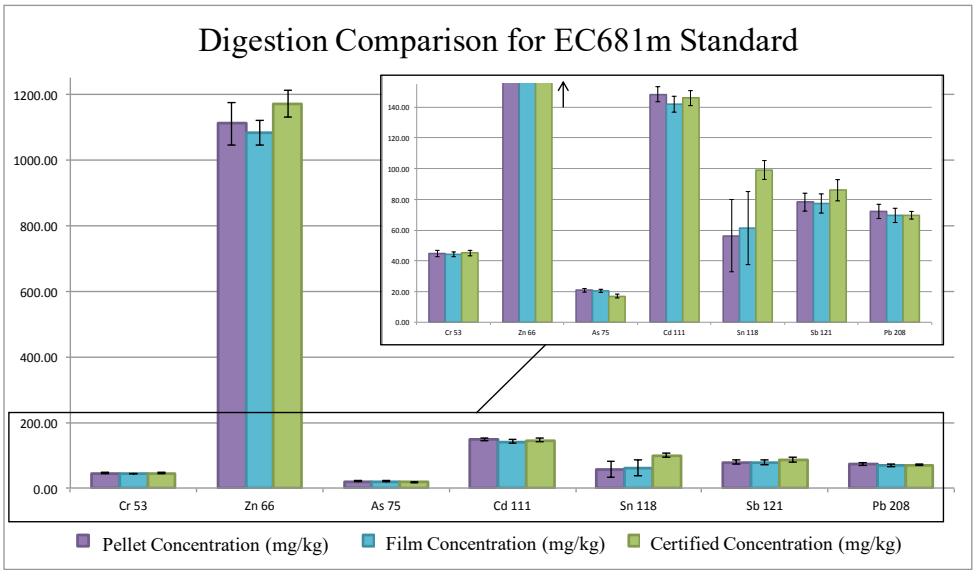

Figure 27 – Comparison of digestion recoveries from the pellets and the in-house prepared film.[44]

Figure 27 represents the comparison between the recovery for the pellets and the recovery of the prepared film for the ERM-EC681m standard. The recovered concentrations for the pellets and the films show no significant loss after the melting process. Arsenic and tin resulted in high bias compared to the reported concentrations (Table 8); however, the differences between the pellets and film are not significant. Therefore, the high percent bias is the result of the digestion process (i.e., caused by known interferences for arsenic in ICP-MS[63] or to volatilization from the digestion process for tin), and not to the preparation of the films by melting.

Table 8 – Precision and bias for polyethylene pellets and films after microwave digestion for a total of four digestion replicates.

Analyte	EC681m Film		EC681m Pellets	
	% RSD	% Bias	% RSD	% Bias
Cr 53	3.8	2.0	5.0	0.7
Zn 66	3.6	7.5	5.9	5.1
As 75	5.9	20.4	5.2	21.9
Cd 111	3.7	2.8	3.4	1.6
Sn 118	39.0	38.3	41.7	43.1
Sb 121	8.2	10.1	7.6	9.0
Pb 208	6.8	0.1	6.5	3.6

The plastic polyethylene films were created in order to test the performance of the calibration methods. Although the electrical tapes used for quantitative analysis were made of PVC backings, polyethylene represented a closer plastic alternative for comparisons in lack of a PVC plastic certified standard.

2.2.2 Quantitative method by LA-ICP-MS using PVA calibration standards

External calibration curves were created using poly-vinyl acetate (PVA) solutions at different concentrations (0 - 300 ppm). The samples were allowed to dry, and the new concentration was calculated after the liquid evaporated. The calibration standards, polyethylene films and tape samples were gold-coated using a sputtering system (Hummer 10.2, Anatech LTD, Michigan, USA). The samples were analyzed in the same manner as the calibration standards. The integrated signals (divided by the gold signal) were extrapolated to find the concentrations using the calibration curves for all the isotopes of interest. In the case of carbon as internal standard, the integrated signals were divided by the signal of carbon instead of the signal of gold, and a correction factor was applied to account for differences in carbon for the different polymers.

2.2.2.1 Reagents and standards

Polyvinyl acetate polymer (PVA, or PVAc) was provided by Celanese Corporation (Dur-O-Set® Emulsions, Celanese, Texas, USA). A multi-element standard mix of 800 ppm was prepared by diluting Al, Cr, Sb, Sr, Ti (10,000 ppm, Inorganic Ventures, Virginia, USA) and Ba, Cd, Fe, Mg, Mo, Pb, Zn (10,000 ppm, Ricca Chemicals, Texas, USA) single element solutions in 0.8 M HNO_3.

2.2.2.2 Sample preparation

The PVA polymer was in the form of a viscous white liquid capable of dissolving the ICP-MS (5% HNO_3) multi-element standards. A 400-ppm PVA mix was created by dissolving the pure polymer with the 800-ppm multi-element HNO_3 mix (1:1 volume/volume). The exact volume of the viscous liquid was determined using the mass and the density reported by the manufacturer. The 400-ppm PVA mix was vortexed exhaustively prior to the deposition of the polymer in the glass substrates. Solutions of PVA at different concentrations were prepared using a 1:1 (v/v) PVA polymer/0.8 M HNO_3 blank from the 400-ppm mix in order to create the calibration curves. The calibration points were created using 0, 50, 80, 150, and 300 ppm solutions.

Paper disks of 6 mm in diameter were cut from filter paper (GE Healthcare Whatman 542 Filter Paper, Fisher Scientific, Pennsylvania, USA) using a steel punching tool (Office Depot Brand Single-Hole Punch in Chrome, Office Depot, USA). The pre-cut disks were attached to double-sided adhesive tape (Double Sided Photo and Document Mending Tape, 3M Scotch, Minnesota, USA) and mounted on 18 mm by 18 mm glass slides (Fisherbrand Cover Glasses, Fisher Scientific, Pennsylvania, USA). A sample of 40

μL of the polymer solutions was deposited on the paper disks using a micro pipette for all the calibration point standards.

The weight measurements were recorded using a Mettler Toledo (XS Analytical Balance, Mettler Toledo, Ohio, USA) analytical balance. The weight of dried polymer consisted of the weight of the dried polymer in the glass slide subtracted from the weight of the glass slide (filter disk, double-sided tape, and glass slide). The weight of the wet polymer was recorded in order to calculate the new concentration of the elements in the dried polymer after evaporation of the liquid.

The polymer calibration standards, polyethylene films and tape samples were subsequently gold-coated using a sputtering system (Hummer 10.2, Anatech LTD, Michigan, USA). The samples were coated in pulse mode for 20 seconds at 1200 V. A schematic of the sample preparation process and of the analysis for this method is shown in Figure 28.

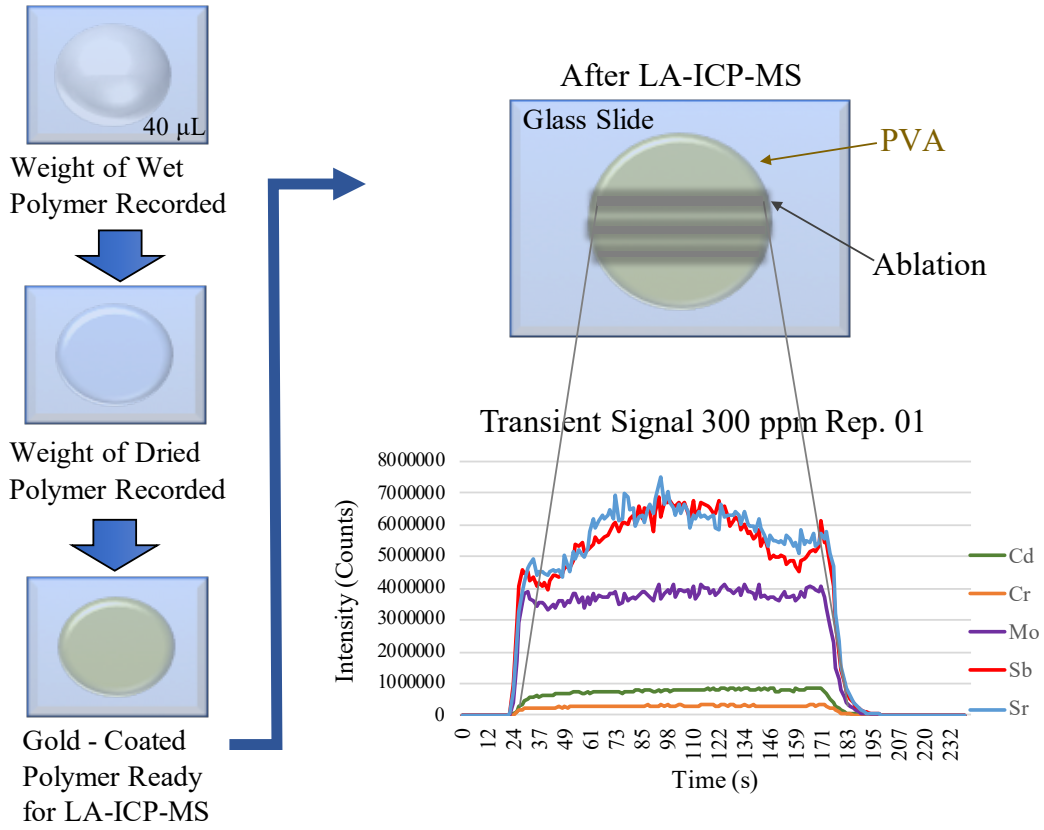

Figure 28 – Sample preparation schematic for the PVA external calibration method. A 40 µL drop was deposited on glass slides. The samples were allowed to dry overnight and subsequently coated with gold. After LA-ICP-MS analysis, the integration of the area under the curves were calculated and used to create the external calibration curves.

2.2.2.3 Instrumentation and measurement parameters

The analysis by LA-ICP-MS was performed using a quadrupole ELAN DRC II (Perkin Elmer LAS, Shelton CT USA) ICP-MS coupled to a ns-Nd:YAG laser (NW UP213, New Wave, California). Data were acquired in transient mode monitoring the following isotopes: ^{27}Al, $^{135, 137}$Ba, $^{111, 113}$Cd, ^{53}Cr, ^{57}Fe, $^{24, 26}$Mg, $^{95, 98, 100}$Mo, $^{204, 206, 207, 208}$Pb, $^{121, 123}$Sb, ^{88}Sr, $^{47, 49}$Ti, and $^{64, 66}$Zn. Performance checks were conducted daily and before each analysis to ensure the correct operation of the instrument. Standard reference material NIST 612 was used to monitor oxides (ThO/Th) and doubly-charged (Ca^{++}/Ca)

ratios were monitored, as well as the intensity counts for the background (mass 220), and for light, medium, and heavier isotopes (Li, Ce, La, U).

The instrumental parameters for the PVA external calibration method are summarized in Table 9. It was previously noticed that different element spread differently across the droplet (i.e., some elements concentrated more in the center, while other spread through the ends of the droplet). A 6 mm radial line was used for all replicates to account for the heterogeneity of the analytes in the droplet caused by chromatographic migration effects of the elements across the filter paper. The ablation method has previously been reported showing the advantages of radial scans for different types of liquids deposited on filter paper.[64]

Table 9 – Instrumental parameters for the PVA external calibration method.

LA-ICP-MS Parameters	
Laser	ns–Nd:YAG (213 nm)
Energy	100 % (2.6 mJ)
Stage Speed	40 µm/s
Spot Size	190 µm
Frequency	10 Hz
Ablation Mode	Line
Ablation Time	3 min
Analysis Time	4 min
Line Length	6 mm
Scan Mode	Transient
Sweeps/Reading	2
Readings/Replicate	177
Carrier Gas	Helium
Gas Flow	0.9 L/min

2.2.2.4 Results

To find the concentration of the dried polymer, Equation 2 was applied. The mass of the analyte could be calculated by dividing the initial liquid concentration (e.g., 50 mg/L) by the volume added (i.e., 40 µL = 40x10^{-6} L). The final solid mass was measured using the analytical balance after the subtraction of the paper/tape/glass slide substrate.

$$Concentration\ \left(\frac{mg}{kg}\right) = \frac{Mass\ of\ Analyte\ (mg)}{Mass\ of\ Dried\ Polymer\ (kg)} \qquad \text{Equation 2}$$

The concentrations after evaporation of the liquid are shown in Table 10. The samples were allowed to dry overnight inside a ventilated laboratory hood. An increase by a factor of 3.8, in average, was observed after evaporation.

Table 10 – Liquid and dried concentrations for the calibration point standards.

Calibration Point ID	Liquid Concentration (mg/L)	Solid Concentration (mg/kg)
0 PPM	0	0.0
50 PPM	50	141.8
80 PPM	80	227.6
150 PPM	150	452.8
300 PPM	300	748.1

Gold-coating as normalization standard

The calibration curves obtained for the PVA external calibration method for selected isotopes are shown in Figure 29. To create the calibration curves, the gold-normalized signals (y-axis) were plotted versus the solid concentrations reported in Table 10 (x-axis). The samples were previously coated with gold, as described in the sample

preparation section. The calibration curves showed good linearity ($R^2 > 0.98$) for all the isotopes monitored.

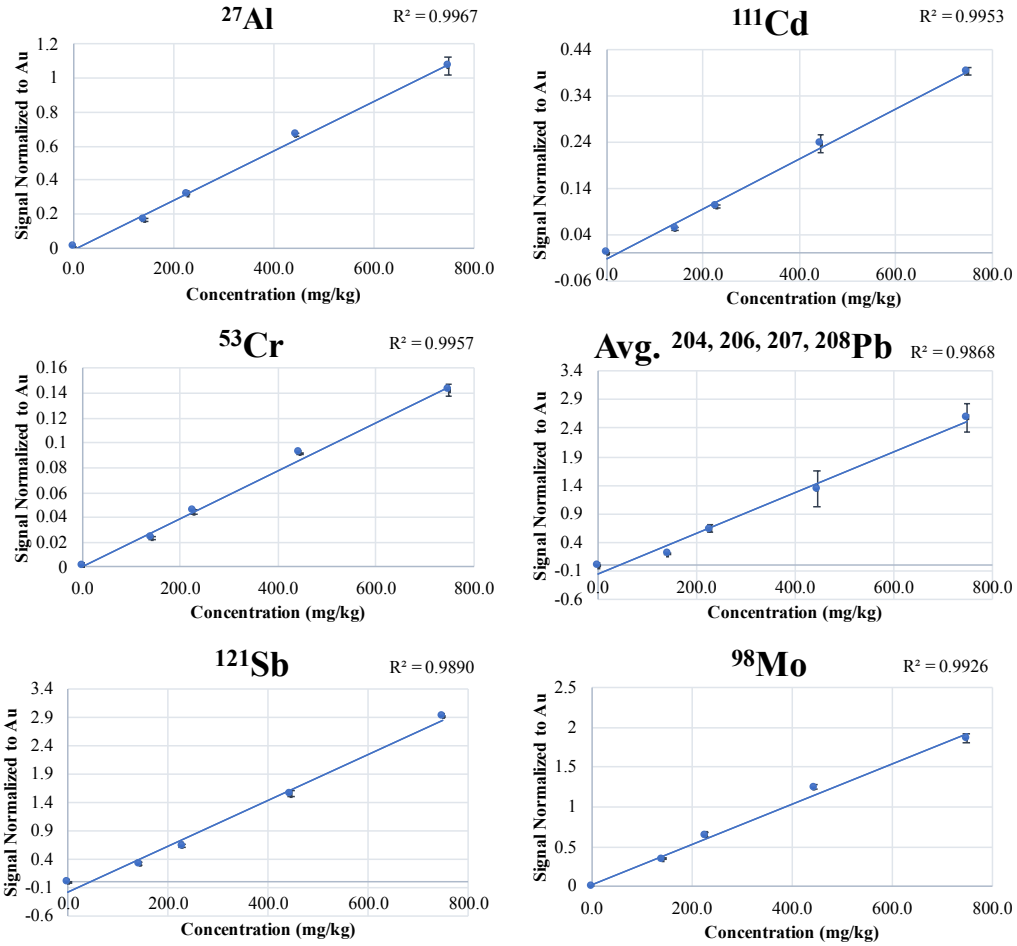

Figure 29 – Calibration curves for the PVA external calibration method for selected elements after gold normalization.

After extrapolating the normalized signals for the polyethylene standard EC681m, the concentrations could be calculated and compared to the certified concentrations reported in the plastic's certificate. Figure 30 shows the calculated and certified concentrations for the polyethylene film of the EC681m certified material. With the exception of cadmium and chromium, the bias obtained was less than 25%. The high

percent bias for cadmium and chromium could be reduced by using an internal standard that is embedded into the sample, as supposed to deposited on the surface, like in the case of gold coating.

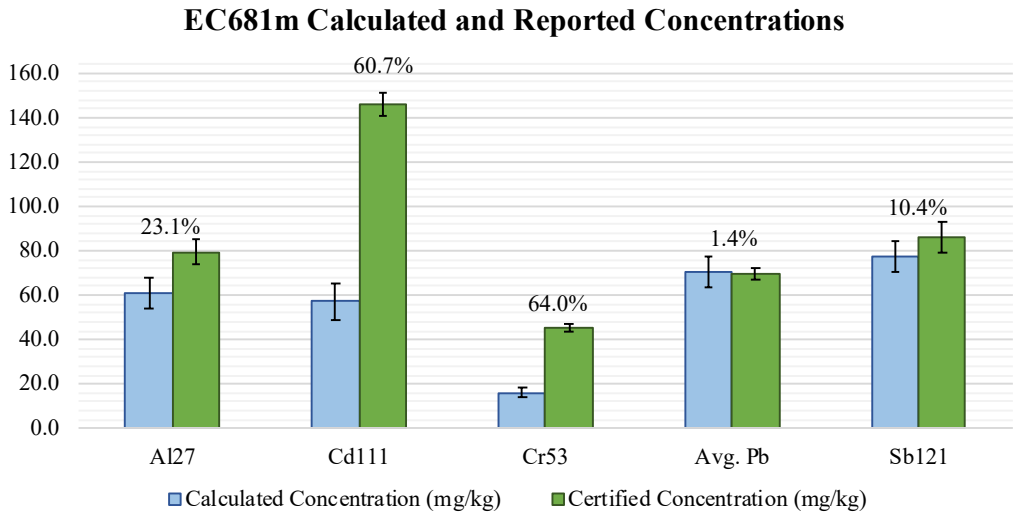

Figure 30 – Calculated (blue) and certified (green) concentrations for EC681m using the PVA quantitative method of external calibration with gold normalization. The values above the bars indicate the percent bias calculated with respect to the certified concentrations.

The concentrations of several tapes were calculated for selected isotopes and are shown in Table 11. The concentrations shown are those above the detection limits of this method. Signal limits of detection were calculated as the mean of the blank sample (0 ppm sample) plus three times the standard deviation of the blank sample (0 ppm sample). This signal was then converted to concentrations as for regular unknown samples by extrapolation using each calibration curve.

Table 11 – Calculated concentrations (mg/kg) for tape samples using the PVA external calibration method with gold as normalization standard.

	BPT11	BPT74	BPT43	BPT83	BPT73
^{27}Al	52 ± 5.9	592.5 ± 46.1	-	756.6 ± 27.3	423.9 ± 1.8
^{137}Ba	-	340 ± 11	-	415.2 ± 3	1020.7 ± 20
^{111}Cd	-	-	-	-	814.6 ± 14.1
^{53}Cr	-	-	-	-	37.6 ± 0.9
^{57}Fe	-	-	-	-	51.2 ± 2.3
^{24}Mg	25.6 ± 2.7	1267.9 ± 67.4	-	1509.8 ± 44.5	568.1 ± 5.3
^{98}Mo	138.1 ± 9.2	-	69.9 ± 1.2	115.6 ± 2.6	-
Avg. Pb	7028.5 ± 369.7	-	6494.1 ± 102.8	-	154.4 ± 3.2
^{121}Sb	5325.8 ± 9.6	5753.5 ± 191.8	2403.4 ± 72.5	5525.3 ± 65.4	171 ± 3
^{88}Sr	-	44 ± 1.5	-	43.4 ± 0.1	95 ± 1
^{47}Ti	-	-	-	-	2068.7 ± 217.2
^{66}Zn	306.2 ± 12.3	184.2 ± 3.2	179.6 ± 4.2	396 ± 9.7	701.7 ± 25.5

The PVA external calibration quantitative method shows great potential in terms of precision (RSD) and linearity of the calibration curves. However, the use of gold as normalization standard might not account for differences in the ablation process for all the analytes of interest between different samples. An internal standard that is present in the same concentrations in all the samples is needed in order to account for fractionation, instrumental drift, and differences in ablation for the different materials. In lack of an internal standard present in the samples at equal and known concentrations, the signal of gold was used for normalization. All the samples were coated with gold in the same manner and the signals for all isotopes were divided by the signal of gold. Gold-coating results in a thin layer (typically in Angstroms, Å), while the laser beam penetrates into the samples up to 100 μm. Therefore, gold coating does not account for most of the ablation process differences between samples. Nonetheless, if plastic samples of interest are known to have an analyte at very similar concentrations among the samples, such analyte can be easily added to the PVA calibration solutions and used as an internal standard for a more accurate

quantitative analysis. The PVA external calibration method can be used for different plastics, and it is not limited to polyvinyl acetate.

Carbon as normalization standard

Another approach to normalization for the PVA external calibration method was using the signal for ^{13}C as the normalization internal standard. The external calibration method with carbon as internal standard assumes that the concentration of carbon in all the different polymers (PVA, PVC, and polyethylene) is the same, and that is obviously not the case. Therefore, a correction factor was calculated as reported by Voss et al.[65] The carbon signals and correction factors are shown in Figure 31. All the signals for the isotopes of interest were divided by the carbon-13 integrated signal. After the concentrations were calculated from the calibration curves, they were multiplied by the corresponding correction factor. As an example, the calculated concentrations for the BCR680 polyethylene film were multiplied by a factor of 3.3 before reporting the final results.

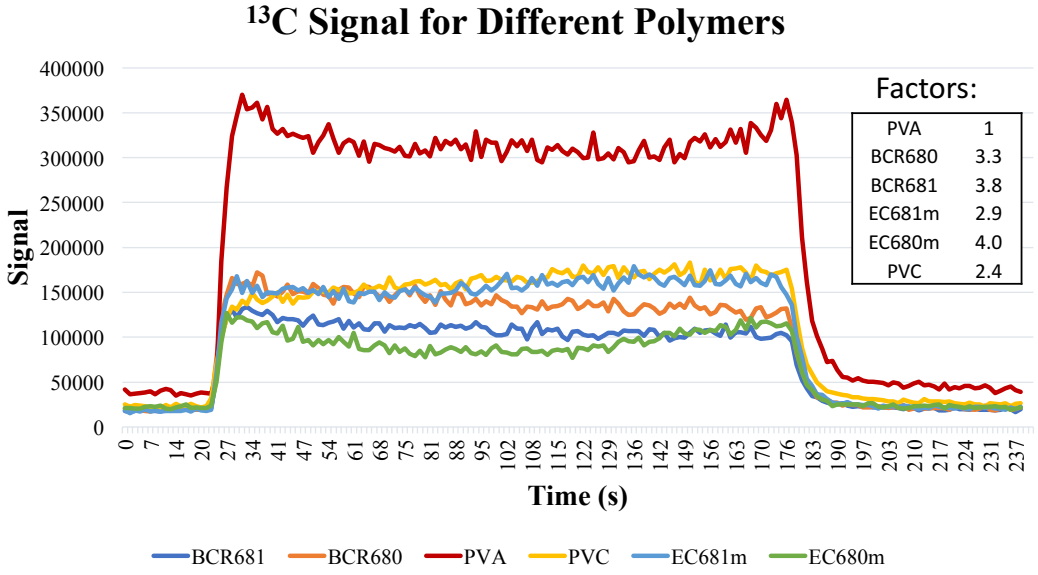

Figure 31 – Carbon signal for the different polymers showing the correction factors.

The linearity of the calibration curves for the carbon normalizations ranged from $R^2 = 0.92$ to $R^2 = 0.99$. The concentration and percent bias results for the EC681m polymer are represented in Figure 32. Although the percent bias for aluminum, cadmium and chromium improved with carbon normalization with respect to gold normalization, the calculated concentrations for lead and antimony resulted in very high percent bias. Lead and antimony are significant elements in tape analysis as they provide great discrimination between samples. Several reasons for the poor performance of carbon as an internal standard have been described before by Frick and Günther.[66] Carbon's ionization potential is significantly higher than those of commonly investigated elements, such as most transition metals, and an altered carbon load in the plasma may change the ionization efficiency of some of the analytes monitored. In addition, the transport of carbon into the ICP can partly occur in the form of carbon dioxide, which will lead to transport properties and efficiencies that can differ from those elements that are transported as particulate matter only.[66] For these reasons, carbon may not be suitable as an internal standard. Moreover, the calculations of the correction factors between carbon signals represents and approximation of the average for all the replicates of each polymer. The correction factor greatly impacts the concentration results; therefore, this method of correction should be regarded as an approximation to the actual concentration of the samples resulting in semi-quantitate rather than quantitative analysis.

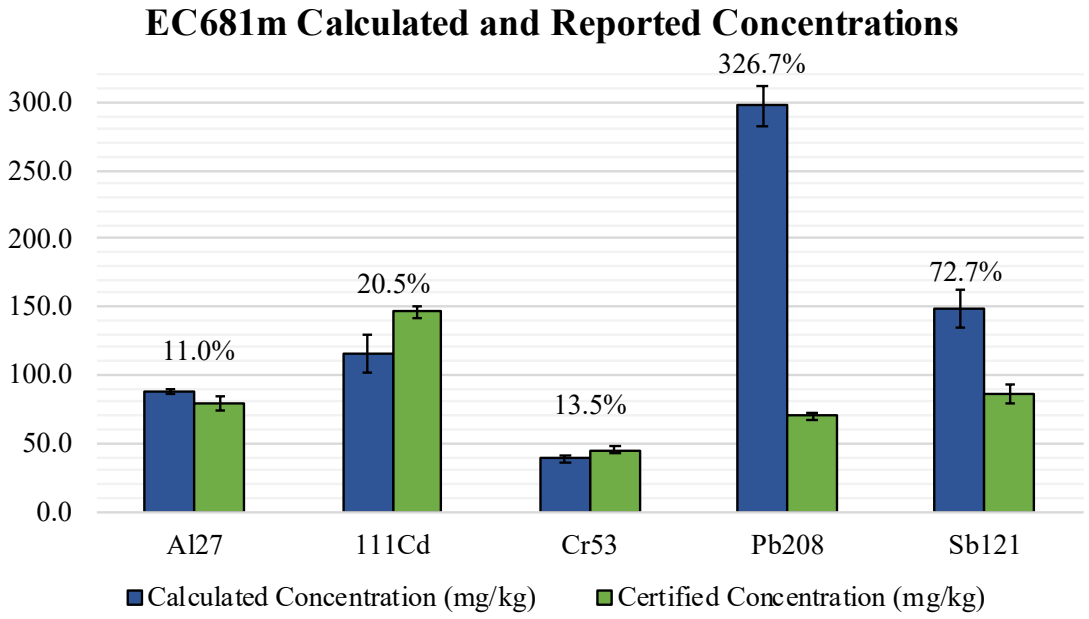

Figure 32 – Calculated (blue) and certified (green) concentrations for EC681m using the PVA quantitative method of external calibration with carbon normalization. The values above the bars indicate the percent bias calculated with respect to the certified concentrations.

2.2.3 Quantitative by LA-ICP-MS without matrix-matched standards

The instrumental set-up for the LA-ICP-MS method without matrix-matched standard is shown in Figure 33. In this quantitative method, a constant stream of standard solution containing a mixture of elements is introduced into a spray chamber, where it is mixed with the particles resulting from the laser ablation process of a solid sample. An online measurement of the solid particles' mass is achieved using a piezoelectric dust monitor (Kanomax, 3521). The solution and ablation mixture are then introduced into an inductively coupled plasma mass spectrometer where an intensity vs. time signal can be obtained for each isotope (see Figure 34).

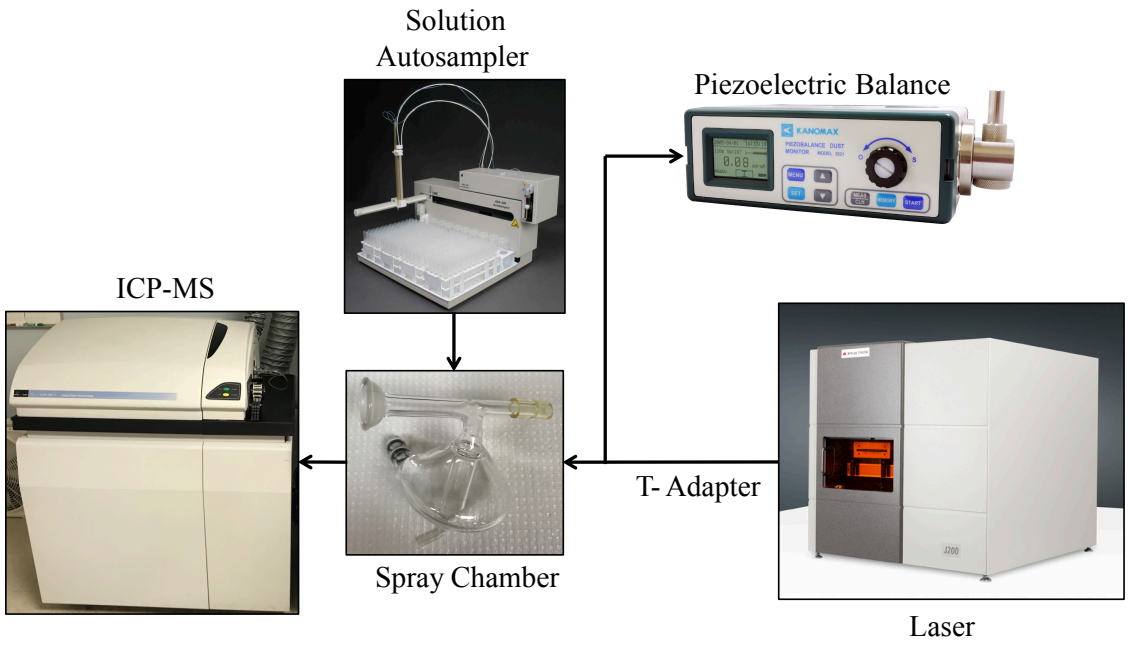

Figure 33 – Instrumental set-up for the LA-ICP-MS quantitative method without matrix-matched standard.

The total signal resulting from the analysis can be expressed as Equation 3 (see Figure 34).

$$Signal_{total} = Signal_{solid} + Signal_{solution} \qquad \text{Equation 3}$$

The total signal in Equation 3 can also be written as:[62]

$$Signal_{total} = R_x \times V \times [X]_{solution} + R_x \times m \times [X]_{solid} \qquad \text{Equation 4}$$

Where R_x is the response factor for the analyte (counts/ng), V is volume of the solution that reaches the ICP-MS (L), $[X]_{solution}$ represents the concentration of the analyte in the solution, m is mass measured by the piezobalance (ng) and $[X]_{solid}$ is the concentration of the analyte in the solid sample.

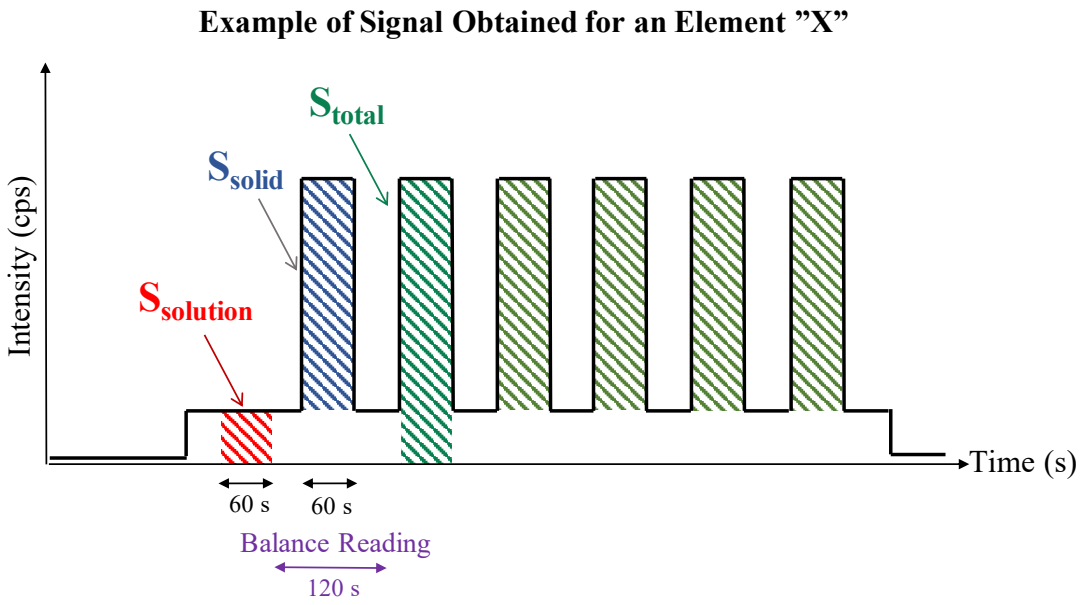

Figure 34 – Schematic example of the signal obtained by the use of the LA-ICP-MS quantitative method without matrix-matched standard representing the different parameters (integrated signals) used in the calculations. Total signal consists of the sum of the solution and solid signals. Six replicates were performed per sample.

Equation 4 can also be expressed as the equation of a straight line with "y" as the total signal, the slope as the response factor times the volume, and the y-intercept as the signal of the solid. Once the volume is known, the slope of the plot of S_{total} vs. $[X]_{solution}$ yields the response factor. Using the response factor with the horizontal intercept allows the calculation of the concentration of the solid in unknown samples.

Rearrangement of the signal of the solution equation allows to calculate the volume (Equation 5). And rearrangement of the signal of the solid for a known standard material allows to calculate the response factor for each analyte (Equation 6).

$$V = \frac{S_{solution}}{R_x \times [X]_{solution}} \qquad \text{Equation 5}$$

$$R_x = \frac{S_{solid}}{m \times [X]_{solid}} \qquad \text{Equation 6}$$

By using a solid of known concentrations, the response factor specific to each isotope can be found and the concentrations of the elements present in an unknown solid can be calculated after finding the transport volume. The response factor should correct for matrix effects, since the solid sample matrix is present when R_x is measured.[62]

2.2.3.1 Reagents and standards

Multi-element solutions at different concentrations were prepared using a 10-ppm mix (Inorganic Ventures, Virginia, USA) of ICP-MS standard solution containing the following elements: As, Ba, Cd, Cr, Cu, Fe, Pb, Sr, and Zn, and a 1000-ppm single element solutions (SPEX CertiPrep, New Jersey, USA) of Pb, Sb, Sr, Ti.

Solid standards samples used for this method included: NIST SRM-610 and NIST SRM-612 glass standards, and BCR-680 and ERM®-EC681m polyethylene standards

2.2.3.2 Instrumentation

The analysis by LA-ICP-MS was performed using a quadruple ELAN DRC II (Perkin Elmer LAS, Shelton CT USA) ICP-MS combined to a commercial LIBS system (J200, Applied Spectra, Freemont, CA) consisting of a ns-Nd:YAG 266 nm laser coupled to a CCD detector. Data were acquired in transient mode. The optimization for the laser was performed to account for the best signal to noise ratio (SNR), smaller percent RSD, while adjusting the laser energy to prevent contamination from the adhesive layer, in the case of tapes.

Measurement of the mass of solid particles was achieved using a piezoelectric dust monitor (Dust Monitor v. 3521, Kanomax USA Inc., NJ, USA).

2.2.3.3 Results

Optimization of instrumental parameters

The parameters for the laser analyses were optimized for tapes, as they are the thinnest material being analyzed among all the samples (i.e., glass standards, PE films, and tape samples). The optimization was performed by experimental design using the statistics software JMP (this optimization is described in Chapter 3).

The piezobalance dust monitor has an ingoing flow of 1 L/min that is achieved by a pump system inside the instrument. The optimized flow exiting the laser (J200) was found to be 0.6 L/min; therefore, different diameter tubing and flow rates were explored in order to obtain a flow rate of 0.6 L/min at the exit of the T-connector. The gas flow from the J200 for glass and tapes was optimized based of reproducibility among replicates (percent RSD) and signal-to-noise ratio (SNR). Ideally, the optimized flow would produce small variations (small percent RSD) and large intensity compared to the noise (large SNR). A flow of 0.6 L/min resulted good SNR and the smallest percent RSD.

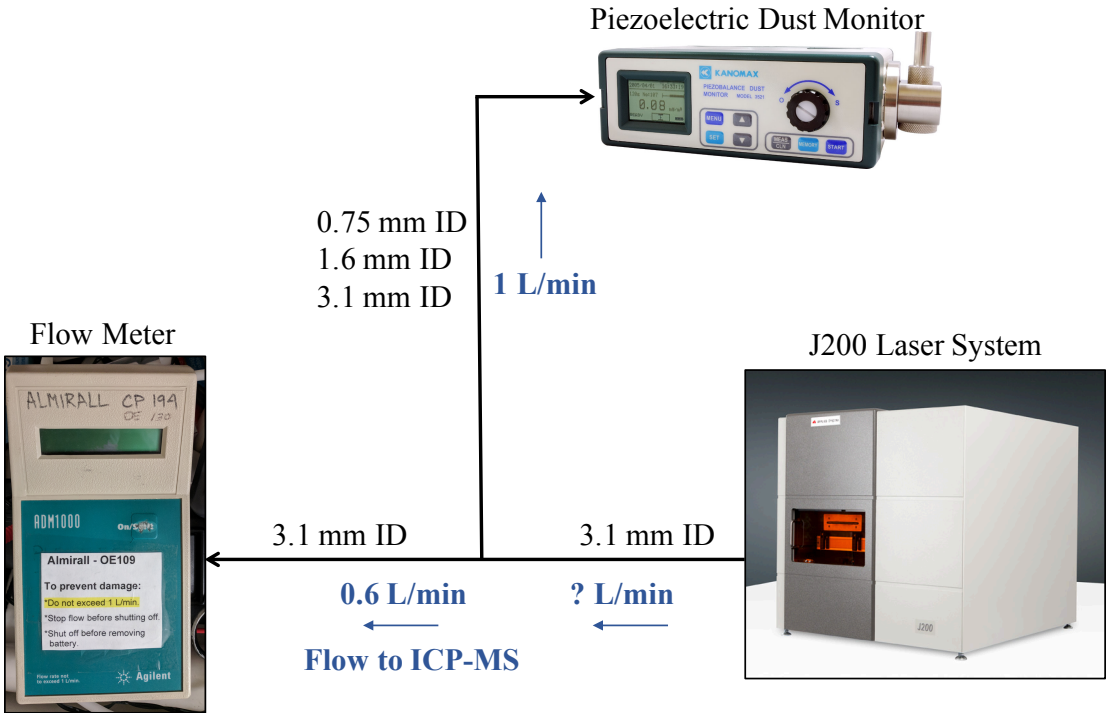

Figure 35 – Experimental set-up for the selection of the optimum flow rate exiting the T-connector towards the ICP-MS. Tubing of different inner diameters (ID) were utilized in order to obtain a final flow of 0.6 L/min into the spray chamber and ICP-MS.

The experimental set-up for the particle transport from the laser to the ICP-MS is shown in Figure 35. Tubing of different inner diameters (ID) were utilized in order to obtain a final flow of 0.6 L/min into the spray chamber and ICP-MS instrument. A flow meter was connected to the end of the T-connector in order to measure the resulting flow rate. Table 12 shows the variation of the flow exiting the T-connector after balance suction using different flow rates out of the laser ablation chamber. In order to obtain 0.6 L/min flow rate into the ICP-MS, three possible combinations were feasible: a 3.1 ID mm tubing and an inner flow of 1.6 L/min, a 1.6 mm ID tubing and an inner flow rate of 1.4 L/min, and finally a 0.75 mm ID tubing with an inner flow rate of 0.8 L/min. The 0.75 mm ID tubing with 0.8 L/min was selected as the best combination of tubing and flow rate set-up as it provided the best reproducibility between balance measurements and the smallest transport of

particles into the balance, therefore reducing the loss of sample that would otherwise reach the spectrometer.

Table 12 – Flow rate and tubing diameter optimization for the instrumental set-up of the LA-ICP-MS quantitative method without matrix matched standard.

Tubing to Balance (ID)	J200 Flow (L/min)	Flow to ICP-MS (Using Flow Meter)
3.1 mm	0.8	0
	1.5	0.525
	1.6	0.630
1.6 mm	0.8	0
	0.9	0.103
	1.0	0.200
	1.3	0.490
	1.4	0.594
	1.5	0.718
0.75 mm	0.8	0.559
	0.9	0.687
	1.0	0.816
	1.1	0.916

Once the flow rate was optimized, the velocity of the peristaltic pump was adjusted to account for the best reproducibility of solution signal while maintaining the spray chamber in the drier possible environment. A dry environment is desired in order to reduce the humidity that could transfer to the balance through the tubing and to imitate the dry aerosol resulting from the laser ablation, so that both laser and solution aerosols ionize in similar manner. Figure 36 shows the percent RSD comparison for six replicate measurements of the solution signal of a multi-element 10 ppb solution at 4 RPM and 6

RPM. A peristaltic pump speed of 6 RPM was selected, as it provided the best percent RSD while keeping minimum humidity in the spray chamber.

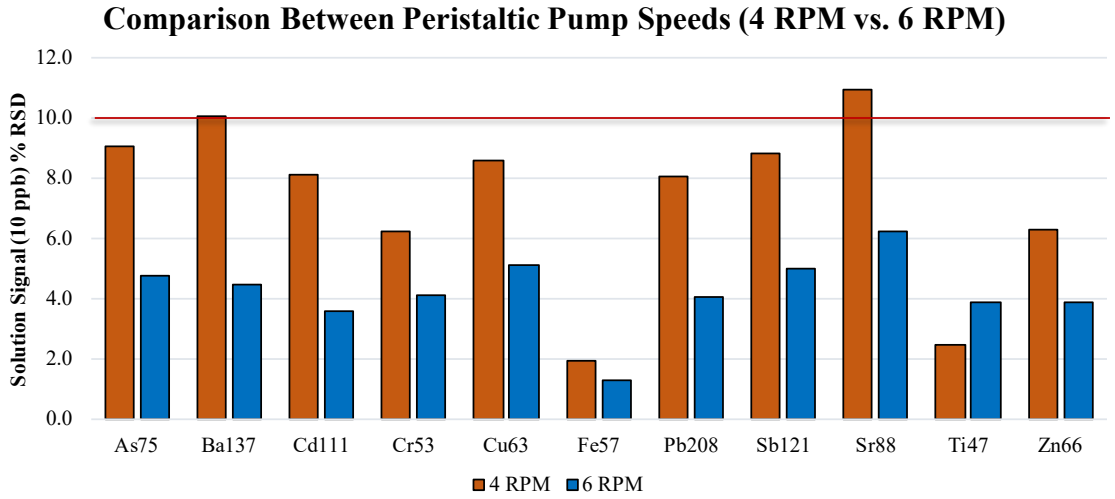

Figure 36 – Comparison of percent RSD for the delivery of 10 ppb multi-element solution into the ICP-MS at peristaltic pump speeds of 4 RPM (orange) and 6 RPM (blue). Six replicate measurements of the solution signal were recorded.

The laser energy was optimized to account for the best reproducibility (lower percent RSD) between replicate measurements for the solid signals, while delivering enough sample into the balance and ICP-MS for analysis. Two glass standards, NIST 612 and NIST 610, were ablated for 60 seconds at 50% and 100% energy with a line length of 6 mm at 100 µm/s and a frequency of 10 Hz. The solid signals resulting from 50% energy and 100% energy were both high enough to determine a signal-to-noise ratio larger than 3. Therefore, 50% energy was selected as the optimum value, as it produced the smallest variability between replicates, especially in the case of the NIST 610 glass (Figure 37, bottom).

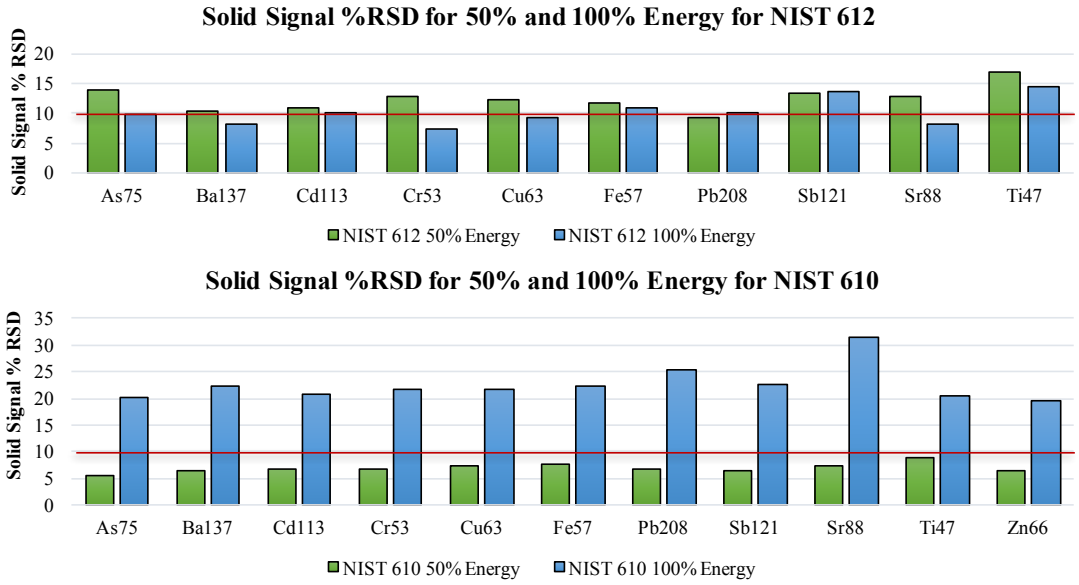

Figure 37 – Comparison of percent RSD for NIST 612 (top) and NIST 610 (bottom) glass standards at 50% (green) and 100% (blue) laser energy. The red line represents a 10% RSD. Six replicate measurements of the solid signal were recorded.

The final parameters used in the complete instrumental set-up are summarized in Table 13 for the laser system, ICP-MS and piezoelectric balance.

Table 13 – Optimized instrumental parameters for the LA-ICP-MS quantitative method without matrix-matched standard.

Laser Parameters (J200)	
Energy	50%
Stage Speed	100 µm/s
Spot Size	100 µm
Frequency	10 Hz
Ablation Mode	Line
Line Length	6 mm
Ablation Time	60 seconds
Shots	403
Medium/Gas	He (0.8 L/min into J200)
ICP-MS Parameters	
Nebulizer Flow	0.6 L/min
Scan Mode	Transient
Nebulizer Flow	0.6 L/min
Sweeps/Reading	2
Readings/Replicate	1285
Analysis Time	30 min (six replicates)
Peristaltic Pump Speed	6 RPM
Balance Parameters	
Measurement Time	120 sec
Tubing to Balance (Inner Diameter)	0.75 mm
Intake Flow	1 L/min

Glass comparisons

In order to optimize the parameters and to check the performance of the method, glass standards NIST 612 and NIST 610 were used both as "known" and "unknown" samples. Since the concentration of the elements present in NIST 610 is approximately ten times the concentrations reported in NIST 612, the solution concentration was also adjusted accordingly. Aeschliman et al.[62] and Umpierrez[67] applied this method to NIST 612 glass samples using 1 ppb solution. In order to determine the best concentration of solution to be used for the different samples, graphs of solid-to-solution ratios were created. The signal

ratios of solid-to-solution between ~3 and ~20 were selected as the acceptable range. This "threshold" was determined based on the percent bias of the final concentrations and precision (percent RSD) of the method.

The solid-to-solution ratios for NIST 610 at 10 ppb are shown in Figure 38. A solution of 10 ppb resulted in the best percent bias and reproducibility for the analysis of the NIST 610 glass, which presents concentrations in the range from ~250 mg/kg to ~500 mg/kg.

Glass NIST 610 was analyzed as an "unknown" sample, utilizing NIST 610 as the "known" standard. The glass samples were analyzed separately for a total of six replicates. The response factor (R_x) and volume (V) for the analytes of interest were calculated using the NIST 610 glass that was used as a "known" standard.

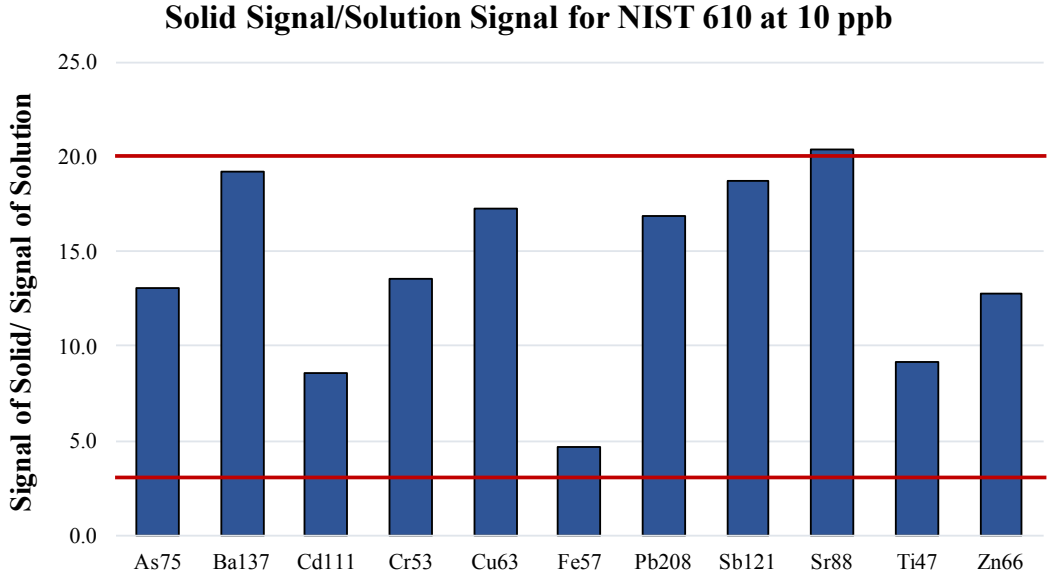

Figure 38 – Solid signal-to-solution signal ratio for NIST 610 glass sample using a 10 ppb multi-element solution. The red lines show the solid/solution ratios of 3 and 20.

The results for the LA-ICP-MS method without matrix-matched standard for NIST 610 are represented in Figure 39. The percent bias was found to be less than 15% for most elements. In the case of iron and titanium, the percent bias was higher than 15% and this can be a result of small solid-to-solution ratios for these elements (Figure 38), and also to the selection of low abundance isotopes in order to prevent polyatomic and isobaric interferences (i.e., $^{56}Fe^{+}$ and ArO^{+}, and ^{48}Ti and ^{48}Ca).

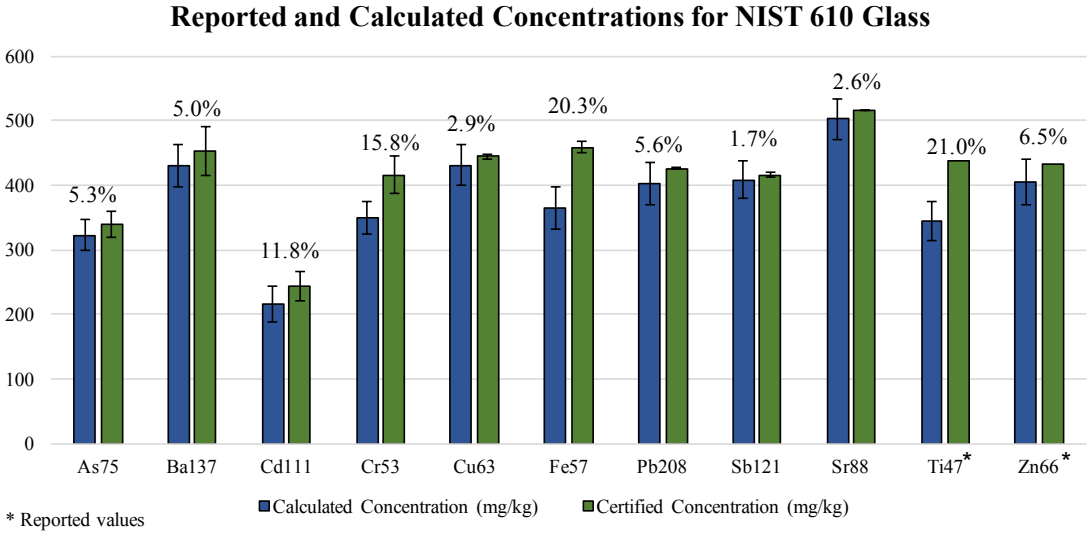

Figure 39 – Reported and calculated concentrations for NIST 610 glass using a 10 ppb multi-element solution. The values above the bars indicate the percent bias calculated with respect to the certified concentrations.

Similarly, the solid-to-solution ratios for NIST 612 were studied to determine the best concentration of solutions for the analysis of the NIST 612 glass. A mix solution of 1 ppb for As, Ba, Cd, Cr, Cu, Fe, Pb, Sb, Ti, and 5 ppb for Sr was selected as it provided the best results for NIST 612 analyses. A solution of 1 ppb for Sr resulted in a solid-to-solution ratio larger than 30, therefore the concentration in solution of strontium was increased to 5 ppb.

Increasing the concentration of the rest of the analytes to 5 ppb, resulted in a solid signal that was barely measurable with respect to the solution signal (Solid/solution < 3). The calculated percent bias for NIST 612 were found below 15% for all elements.

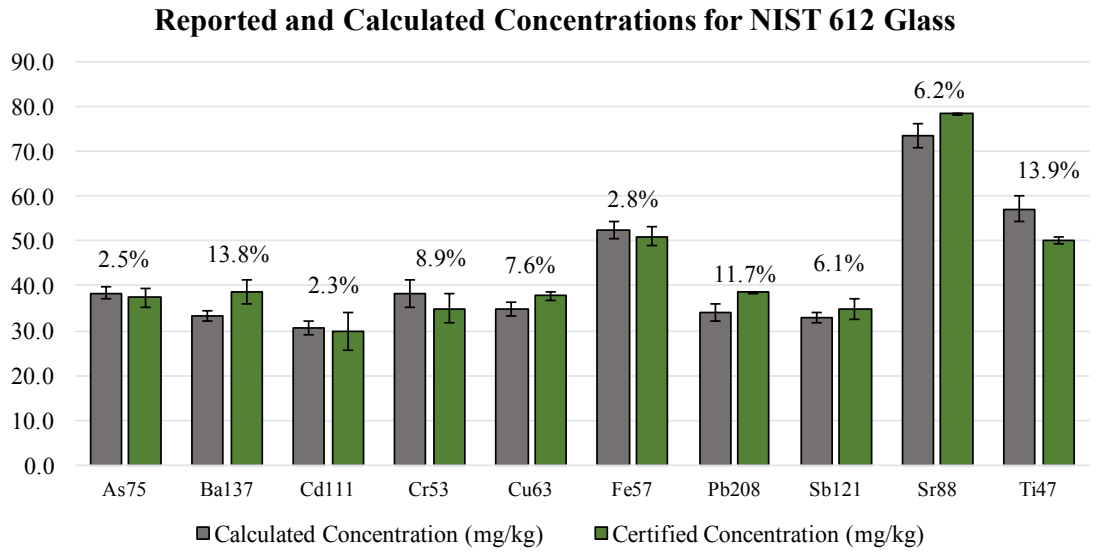

Figure 40 – Reported and calculated concentrations for NIST 612 glass using a 1 ppb multi-element solution and 5 ppb for Sr. The values above the bars indicate the percent bias calculated with respect to the certified concentrations.

The method provided good percent bias for most elements when comparing NIST 610 and NIST 612 glass samples as “known” samples, which evidently presented similar concentration ranges. Additionally, NIST 612 glass was analyzed using NIST 610 as the “known” standard to test the performance of the method to compare samples of different ranges in concentrations.

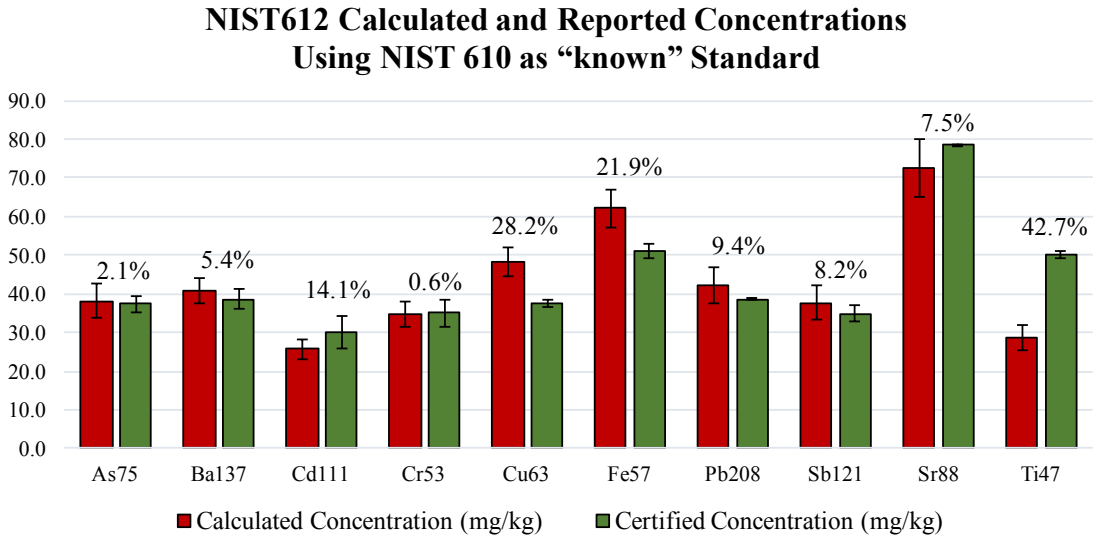

Figure 41 – Reported and calculated concentrations for NIST 612 glass using NIST 610 as "known" standard for R_x calculations. The values above the bars indicate the percent bias calculated with respect to the certified concentrations.

Calculating NIST 612 concentrations using NIST 610 as a standard solid for the calculations of the response factor R_x resulted in percent bias lower than 15% for most elements with the exception of copper, iron and titanium. Iron and titanium appeared to be problematic for NIST 610 as well, as they produced higher percent bias than the other analytes. Some reasons might be the difference in concentration between the standard and the sample, as well as the low abundance of these specific isotopes. Although the concentration ranges between NIST 610 and NIST 612 glasses varied significantly, both glasses can potentially be analyzed by this method using NIST 610 as the solid standard.

Polymer comparisons

The polyethylene films were analyzed in the same manner as the glass standards. The solution concentration that performed best for both plastics was a 5 ppb multi-element solution. The polyethylene film made of the BCR680 certified standard was analyzed using

the films made of EC681m certified standard as a “known” sample in the calculations of the response factor for each element (see Figure 42).

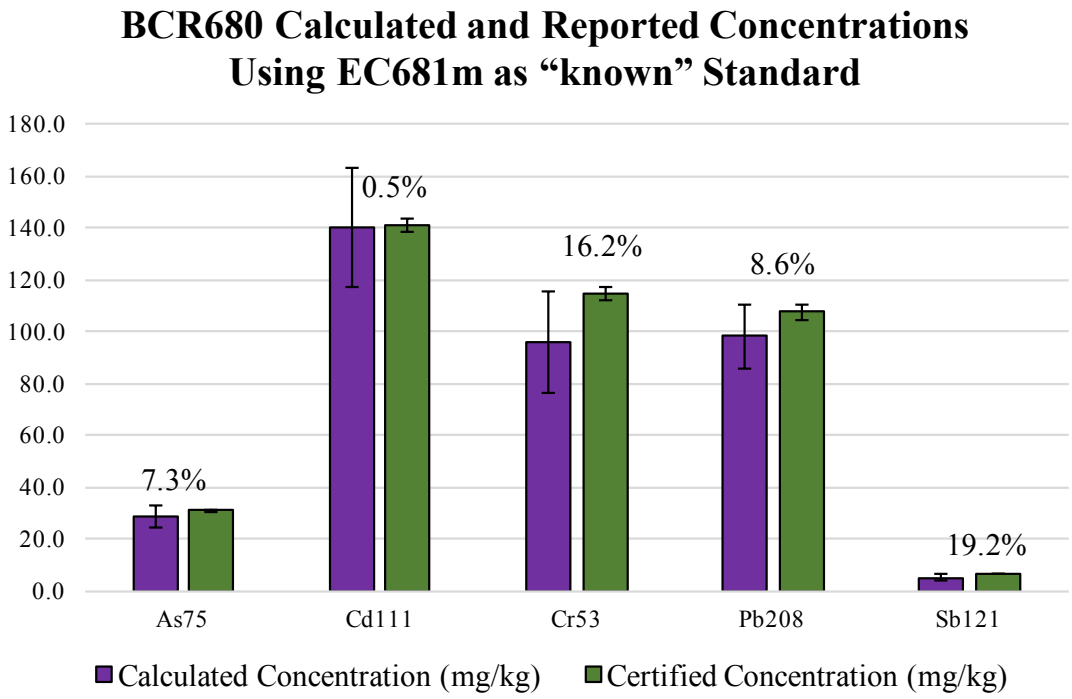

Figure 42 – Reported and calculated concentrations for BCR680 polyethylene film using EC681m as “known” standard for R_x calculations. The values above the bars indicate the percent bias calculated with respect to the certified concentrations.

Polyethylene film made of EC681m certified standard was subsequently used as a “known” sample for the response factor calculations in order to study the concentration of the elements present in PVC tape samples (Table 14).

Table 14 – Calculated concentrations for Frost King® electrical tape and polyethylene BCR680 film utilizing EC681m as "known" solid for R_x calculations.

		As75	Cd111	Cr53	Pb208	Sb121	Zn66
Frost King ® Electrical Tape	Concentration (mg/kg)	4	2104	39	5	37	1796
	Std. Dev. (mg/kg)	1	318	6	1	5	270
	% RSD	19	15	14	15	15	15
BCR680 Calculated Concentrations	Concentration (mg/kg)	28.6	140.1	96.0	98.4	5.0	-
	Std. Dev. (mg/kg)	4.3	22.8	19.3	12.4	1.2	-
	% RSD	14.9	16.3	20.1	12.6	24.0	-
BCR680 Certified Concentrations	Concentration (mg/kg)	30.9	140.8	114.6	107.6	6.2	-
	Std. Dev. (mg/kg)	0.7	2.5	2.6	2.8	-	-
	% RSD	2.3	1.8	2.3	2.5	-	-
	% Bias	7.3	0.5	16.2	8.6	19.2	-

Although good percent bias (<20%) was obtained for the polymer analysis, only five elements were monitored for the polyethylene films. In addition, caution must be taken when analyzing different materials by this method, as it does not account for elemental fractionation. [62] This method also works on the premise that the difference in the ablation process would be accounted for by the use of the piezoelectric balance. Daily performance checks on the balance should be performed to ensure the proper calibration of the sensor, as well as a good reproducibility between balance measurements for the different materials.

2.3 Conclusions for the elemental analysis of tapes by LA-ICP-MS

A novel LA-ICP-MS method was developed, optimized and evaluated for the chemical characterization and comparison of electrical tape backings. The results showed the ability of LA-ICP-MS to improve the comparison capabilities for the analysis of electrical tapes. The homogeneity studies in the tapes showed that the intra-roll elemental variation was smaller than the inter-roll variation. The optimization of the penetration depth accounted for the ablation of representative material without contamination from the adhesive layer. The backings of 90 black electrical tapes were analyzed using LA-ICP-MS

and the ability of the method to distinguish samples from different origin was evaluated by calculating the percentage of discrimination. The discrimination for the LA-ICP-MS analysis of the 90 samples was found to be 93.9%, which was greater than the discrimination power found using SEM-EDS alone (87.3%). Moreover, 100% correct association resulted for the 129 duplicate control samples evaluated in this study.

The great sensitivity of LA-ICP-MS provided improved discrimination over SEM-EDS and offered enhanced characterization of the tapes by detecting over 25 elements, most of which could not be detected by SEM-EDS. The discrimination between tapes originating from different sources is improved through LA-ICP-MS, and this method could be used to complement to organic methods for a full characterization of the tape samples. The fast analysis capabilities and minimal sample destruction of this laser-based technique makes it attractive for the analysis of this type of evidence. The increased sensitivity and selectivity of these methods will provide enhanced discrimination and a more complete characterization of the backing of electrical tape samples, making the method amenable to the development of a classification scheme of tape groups (possibly by country or by manufacturer) to support investigations. Finally, the numerical nature of the data generated is also amenable for the creation of databases in the future that can be searched to compare an unknown tape sample to tapes in a reference collection.

Two quantitative methods were developed for the analysis of tapes and other polymers. In order to test the performance of the quantitative methods, polyethylene films made of reference materials were created.

The first method consisted of an external calibration curve suing Polyvinyl acetate (PVA) solutions at different concentrations ranging from 0 ppm to 300 ppm. Five calibration points were created; the linearity of the curves, percent bias, and percent RSD were used to test the performance of this method. Due to lack of internal standard in the tape and PVA samples, gold was used as a normalization standard by coating all the samples using a sputtering system. Carbon (^{13}C) was additionally evaluated as an internal standard for this method.

The second procedure to determine the concentrations of the elements present in tapes and plastics consisted of the quantitative method without matrix-matched standards. In this method, the concentrations in an unknown solid can be found by using a known or standard solid to calculate a response factor specific to each isotope.

The accuracy of the method was tested using the different solid glass and plastic standards. The percent bias for the NIST 610 glass standard was found to be below 10% for most of the elements under study; the bias for the BCR-680 polyethylene plastic using ERM®-EC681m polyethylene plastic resulted in less than 10% for most elements under study. Tape concentrations were measured using ERM®-EC681m polyethylene as a known standard and were found to be: 4 ± 1 ppm for As, 2104 ± 318 ppm for Cd, 39 ± 6 ppm for Cr, 5 ± 1 ppm for Pb, 37 ± 5 ppm for Sb, and 1796 ± 270 ppm for Zn.

These quantitative methods can help in creating and populating databases which can lead to the use of likelihood ratios and the development of standard methods of analysis and interpretation for tape evidence. These methods also have the potential to be used for different types of solids without the need to conduct aggressive acid digestions.

3 ELEMENTAL ANALYSIS OF TAPES BY LIBS

3.1 Instrumentation and instrumental parameters

The analysis by Laser Induced Breakdown Spectroscopy (LIBS) was achieved using a commercial system (J200, Applied Spectra, Freemont, CA) consisting of a ns-Nd:YAG 266 nm laser coupled to a CCD detector. The optimization for LIBS was performed to account for the best signal to noise ratio (SNR), smaller percent RSD, while preventing contamination from the adhesive layer. The statistics analysis software JMP (version 12.0.0, SAS Institute Inc., NC) was utilized to create the most efficient design of experiment prior to the instrumental optimization. Design of experiment was used as an automated method to assess the impact of each parameter in the resulting output, as well as determining the combination of parameters that offers the best analytical results. A randomized series of experiments composed of different parameter values were conducted to determine the combination that accounted for maximizing the signal-to-noise ratio (SNR) and minimizing the percent RSD. The optimized parameters used for LIBS analysis are shown in Table 15.

Table 15 – Optimized parameters selected for LIBS analyses.

Laser	ns-Nd:YAG (266 nm)
Energy	100%
Stage Speed	100 µm/s
Spot Size	100 µm
Frequency	10 Hz
Ablation Mode	Line
Line Length	4 mm
Spectrum Range	180 nm to 1045 nm
Gate Delay	0.9 µs
Shots	403
Medium/Gas	Air

3.2 Sample collection and sample preparation

A selection of 90 black electrical tapes previously analyzed by Py-GC-MS, SEM-EDS, FTIR, microscopical examination,[3-4] was shared with our research group to assess the capabilities of LIBS and LA-ICP-MS analyses. The samples were received as tape segments placed on plastic transparency films and were stored in plastic protectors. Prior to analysis, a piece of ~1 cm by 2 cm of tape was cut and placed directly inside the ablation chamber.

3.3 Data pre-processing and statistical analysis

Data reduction and statistical analyses were performed using Excel 2011 (version 14.7.7, Microsoft Corporation), the Aurora software for LIBS data integration and peak identification (version 2.1, Applied Spectra, Freemont, CA), and Plot2 for Mac (version 2.3.7, Berlin, Germany).

The selection of the peaks of interest and comparison between the abundance for specific element line were performed by spectral overlay. The spectral overlay comparisons account for variability within replicate measurements, which includes instrumental variations and compositional variations in the sampled locations. Two samples were differentiated if there were differences in the spectral overlay for at least one element. The presence and abundance of two or more emission lines for the element in question confirmed its presence in the samples. The element lines selected for LIBS experimental design optimization were the following: Al 394.4 nm, Ca 393.4 nm, Ca 422.7 nm, K 766.5 nm, Li 670.8 nm, Mg 279.4 nm, and Na 589.5 nm.

3.4 Results and discussion

3.4.1 Optimization of instrumental parameters

Design of experiment was used to create a randomized series of experiments that would allow for a more efficient optimization of the LIBS instrumentation. The parameters selected were those that provided the best compromise between SNR and percent RSD. In the same manner as with LA-ICP-MS, the cross-section of the tapes was examined under the microscope to ensure that the laser beam did not penetrate into the adhesive layer.

Experimental design #1

The first experimental design consisted of 13 experiments and four factors: energy, frequency, speed, and gate delay (Table 16). The energy values tested were 60%, 75% and 90%. The frequency values were 8 Hz, 9 Hz, and 10 Hz. The speed values were 50 μm/s, 100 μm/s, and 150 μm/s and gate delay values were 0.01 μs, 0.05 μs, and 0.09 μs.

Table 16 – Experimental design #1 with four factors and 13 experiments.

Experiment	Energy (%)	Frequency (Hz)	Speed (μm/s)	Gate Delay (μs)
1	90	9	50	0.09
2	75	8	50	0.01
3	75	10	150	0.09
4	90	10	50	0.05
5	60	9	150	0.01
6	75	9	100	0.05
7	90	10	150	0.01
8	60	10	100	0.09
9	90	8	150	0.09
10	60	8	150	0.05
11	60	10	50	0.01
12	90	8	100	0.01
13	60	8	50	0.09

The first experimental design showed that, as expected, higher laser energy and higher frequency resulted in increased SNR. In order to keep a higher percentage of laser energy, the laser stage speed had to be increased in order to prevent contamination from the adhesive layer. Higher gate delay values resulted in better SNR for the majority of the elements monitored (both ionic and atomic lines were monitored). The RSD values remained below 5% for all the elements under study using the all the different parameter combinations.

Experimental design #2 was therefore focused of the effect of larger stage speed and higher gate delay while maintaining the energy constant at 100%.

Experimental design #2

The second experimental design consisted of 13 experiments and three factors: speed, gate delay, and frequency (Table 17). The energy of the laser was kept at 100%. The

speed values tested were 100 μm/s, 150 μm/s, and 200 μm/s. The gate delay values were 0.1 μs, 0.5 μs, and 0.9 μs. The frequency values tested were 8 Hz, 9 Hz, and 10 Hz.

Table 17 – Experimental design #2 with three factors and 13 experiments.

Experiment	Speed (μm/s)	Gate Delay (μs)	Frequency (Hz)
1	200	0.9	8
2	100	0.9	8
3	100	0.1	8
4	100	0.1	10
5	150	0.9	10
6	200	0.1	9
7	100	0.5	10
8	200	0.5	8
9	150	0.1	8
10	200	0.9	10
11	150	0.5	9
12	200	0.1	10
13	100	0.9	9

The second experimental design showed that higher gate delay values performed best for most of the element lines monitored. A speed of 100 μm/s and a frequency of 10 Hz resulted in the best SNR, while still preventing penetration of the beam into the adhesive layer. Higher gate delay values were monitored keeping a constant energy, frequency and speed. The best gate delay for most elements resulted in 0.9 μs.

The best parameters found after optimization are shown in Table 15. These parameters accounted to the best compromise in SNR and percent RSD, while considering the penetration of the laser beam onto the tape backing. Figure 43 shows the cross-section for tape 59, which is the thinnest tape in the collection. Tape 59 had an average backing thickness of 83.3 μm (measured in three replicates with the Keyence digital microscope).

Using the final optimized parameters, the laser beam penetrated about 50% into the backing of the thinnest tape in a collection set of more than 120 electrical tapes.

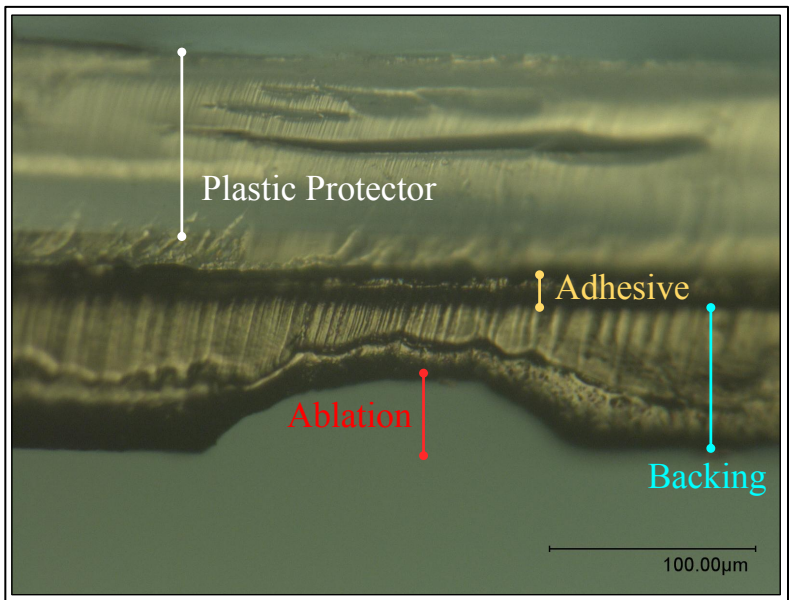

Figure 43 – Cross-section for tape 59 (thinnest tape in the collection, ~83 µm backing thickness) using the final optimized parameters for the J200 LIBS system shown in Table 15.

3.4.2 Discrimination capabilities and error rates

Tape comparisons for LIBS analysis were performed by spectra overlay. The grouping found by LIBS and LA-ICP-MS is shown in Table 18. By performing LIBS, 50 groups were found, which was the same number of distinctive groups found by LA-ICP-MS. However, LIBS allowed to separate some pairs of tapes that were not distinguished by LA-ICP-MS, such as tape pairs 45 and 55, 14 and 37, group xxix and 17 or 24, and 21 and 46.

Table 18 – Groups found by LIBS and LA-ICP-MS and both techniques combined.

LA-ICP-MS Groups	Sample Number	LIBS Groups	Sample Number	LA-ICP-MS + LIBS Groups	Sample Number
i	4	I	4, 42, 45, 51	*I*	4
ii	42			*II*	42
iii	45, 55			*III*	45
				IV	55
iv	51	II	55	*V*	51
v	53	III	53	*VI*	53
vi	56	IV	56	*VII*	56
vii	58	V	58	*VIII*	58
viii	70	VI	70	*IX*	70
ix	81	VII	81	*X*	81
x	82	VIII	82	*XI*	82
xi	86	IX	86	*XII*	86
xii	8	X	8	*XIII*	8
xiii	32	XI	32	*XIV*	32
xiv	52	XII	52	*XV*	52
xv	14, 37	XIII	14	*XVI*	14
		XIV	35, 37	*XVII*	37
xvi	35			*XVIII*	35
xvii	50	XV	50	*XIX*	50
xviii	21, 46	XVI	21	*XX*	21
		XVII	46	*XXI*	46
xix	38	XVIII	38	*XXII*	38
xx	67	XIX	67	*XXIII*	67
xxi	66	XX	66	*XIV*	66
xxii	22	XXI	22	*XXV*	22
xxiii	69	XXII	69	*XXVI*	69
xxiv	72	XXIII	72	*XXVII*	72
xxv	74, 79	XXIV	74, 79	*XXVIII*	74, 79
xxvi	76, 77, 80, 83	XXV	76, 77, 80, 83	*XXIX*	76, 77, 80, 83
xxvii	62	XXVI	62	*XXX*	62
xxviii	2	XXVII	2	*XXXI*	2
xxix	10, 11, 12, 13, 15, 17, 18, 19, 20, 23, 24, 25, 26, 39, 41, 54, 61, 63, 64, 68	XXVIII	10, 11, 12, 13, 15, 18, 19, 20, 23, 25, 26, 39, 41, 54, 61, 63, 64, 68	*XXXII*	10, 11, 12, 13, 15, 18, 19, 20, 23, 25, 26, 39, 41, 54, 61, 63, 64, 68
		XXIX	17, 24	*XXXIII*	17, 24
xxx	65	XXX	65	*XXXIV*	65
xxxi	27, 28	XXXI	27, 28	*XXXV*	27, 28
xxxii	16, 29, 30, 34, 40, 43, 44, 47	XXXII	16, 29, 30, 34, 40, 43, 44, 47	*XXXVI*	16, 29, 30, 34, 40, 43, 44, 47
xxxiii	36	XXXIII	36	*XXXVII*	36
xxxiv	1, 5, 7, 48, 49, 57	XXXIV	1, 5, 7, 48, 49, 57	*XXXVIII*	1, 5, 7, 48, 49, 57
xxxv	78	XXXV	78	*XXXIV*	78
xxxvi	84	XXXVI	84	*XL*	84
xxxvii	3	XXXVII	3	*XLI*	3
xxxviii	6	XXXVIII	6	*XLII*	6
xxxix	31	XXXIV	31	*XLIII*	31
xl	71	XL	71	*XLIV*	71
xli	87	XLI	87	*XLV*	87
xlii	88	XLII	88	*XLVI*	88
xliii	89	XLIII	89	*XLVII*	89
xliv	90	XLIV	90	*XLVIII*	90
xlv	73	XLV	73	*XLIX*	73
xlvi	85	XLVI	85	*L*	85
xlvii	9	XLVII	9	*LI*	9
xlviii	33	XLVIII	33	*LII*	33
xlix	59, 60	XLIX	59, 60	*LIII*	59, 60
l	75	L	75	*LIV*	75

Figure 44 shows the LA-ICP-MS and LIBS spectra of tapes 13 (3M Scotch Super 88, USA) and 17 (3M Scotch Super 33+, USA) and their comparison in lithium intensities. These two tapes were not distinguished by LA-ICP-MS due to the limitations of this technique for light elements such as lithium. Both lithium signals in LA-ICP-MS overlapped and the signal was too low (SNR<3) for both tapes in order to add lithium in the element menu. However, in the case of LIBS, the two samples were clearly differentiated by their difference in lithium. Both tapes had lithium signals above the detection limits (SNR>3). Lithium signal intensity for tape 13 was approximately six times the lithium signal intensity of tape 17 by LIBS analysis. LIBS was especially useful in detecting Li, which is a very difficult element to detect in LA-ICP-MS. Li can be difficult to detect in LA-ICP-MS due to space-charge effects between light and heavy ions in the mass spectrometer.[45] Li is a good emitter, easily detected by LIBS in most samples at very low concentrations.

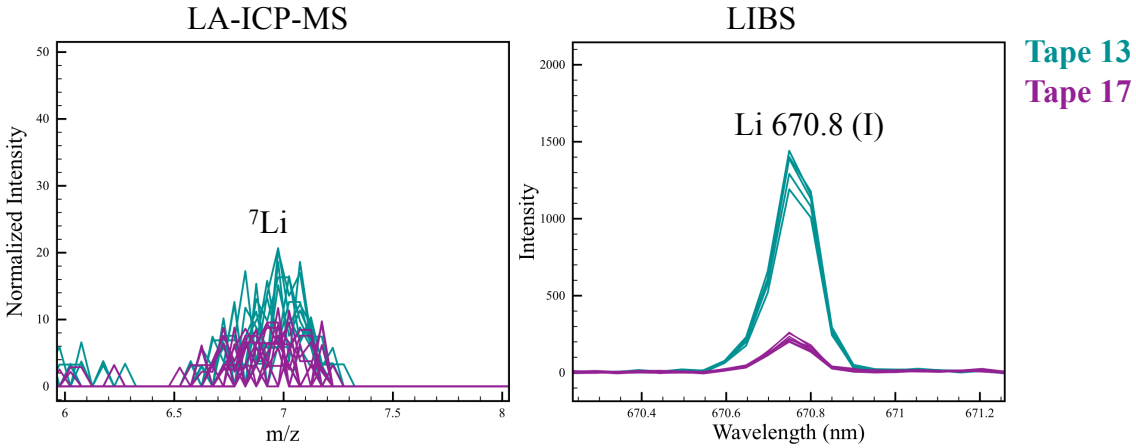

Figure 44 – Spectral overlay for LA-ICP-MS (left) and LIBS (right) for tapes 13 (green) and 17 (purple), showing their differences in lithium intensities.

Similarly, LIBS proved useful in detecting elements problematic to LA-ICP-MS such as potassium ($^{38}K^{+}$), which is the most abundant isotope that can be measured by ICP-

MS without $^{40}Ar^{+}$ interferences. Potassium is known to present interferences with Ar ($^{39}Ar^{1}H^{+}$) in ICP-MS but is easily detected by LIBS and confirmed by multiple lines throughout the spectra.

Figure 45 shows the spectral overlay comparison for LA-ICP-MS (left) and LIBS (right) for tapes 01 (Marcy Enterprises, Inc., Taiwan) and 02 (Advance, England) showing the differences in potassium intensities.

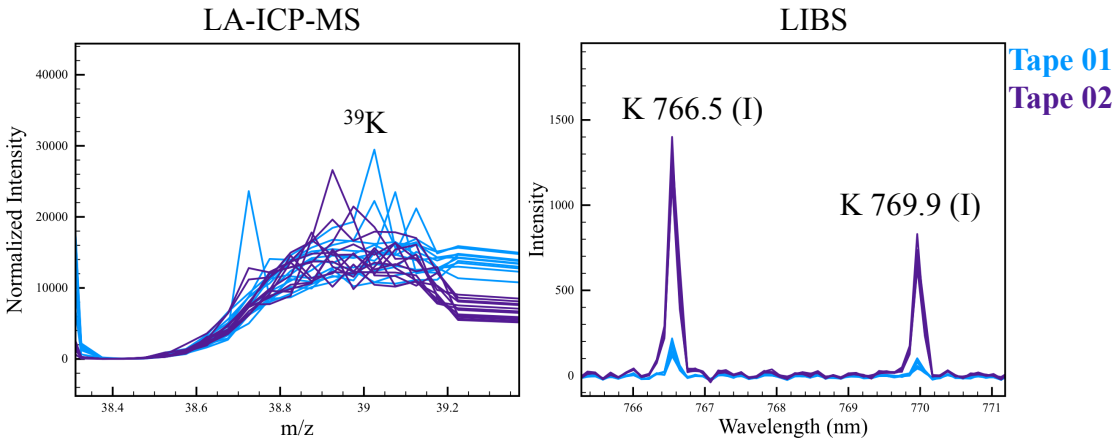

Figure 45 – Spectral overlay of LA-ICP-MS (left) and LIBS (right) for tapes 01 (blue) and 02 (violet), showing their differences in potassium intensities.

The element menu for LIBS for the set of 90 tapes is shown in Table 19. Although the element menu for LIBS (up to 14 elements) is smaller than the number of elements detected by LA-ICP-MS (up to 28 elements), it can be seen that elements such as lithium, sodium and potassium are added to the characterization of specific samples when combining both techniques.

The J200 tandem LIBS system allows to perform LIBS while also transporting the particles to the ICP plasma for mass spectrometry analyses. Therefore, by optimizing and performing these tandem experiments excellent characterization of the samples can be

achieved in a matter of seconds. Tandem LA-ICP-MS and LIBS would be of great benefit to forensic laboratories that currently perform time consuming analysis with poor sensitivity and selectivity, and even the destruction of the tapes in order to characterize the samples.

Table 19 – Element menu per tape group for LIBS for the set of 90 tape samples.

LIBS Groups	Sample Number	Elements Detected by LIBS
I	4, 42, 45, 51	Li, Na, Al, Si, K, Ca, Ti, Ba, Pb
II	55	Li, Na, Al, Si, K, Ca, Ti, Ba, Pb
III	53	Li, Na, Al, Si, K, Ca, Ti, Ba, Pb
IV	56	Li, Na, Al, Si, K, Ca, Ti, Ba, Pb
V	58	Li, Na, Al, Si, K, Ca, Ti, Ba, Pb
VI	70	Li, Na, Al, Si, K, Ca, Ti, Ba, Pb
VII	81	Li, Na, Al, Si, K, Ca, Ti, Sb, Ba, Pb
VIII	82	Li, Na, Al, Si, K, Ca, Ti, Ba, Pb
IX	86	Li, Na, Al, Si, K, Ca, Ti, Ba, Pb
X	8	Li, Na, Al, Si, K, Ca, Ti, Sb, Ba, Pb
XI	32	Li, Na, Al, Si, K, Ca, Ti, Sb, Pb
XII	52	Li, Na, Al, Si, K, Ca, Ti, Zn, Mo, Sb, Ba, Pb
XIII	14	Li, Na, Al, Si, K, Ca, Ti, Cr, Ba, Pb
XIV	35, 37	Li, Na, Al, Si, K, Ca, Ti, Cr, Ba, Pb
XV	50	Li, Na, Al, Si, K, Ca, Ti, Cr, Sb, Ba, Pb
XVI	21	Li, Na, Al, Si, K, Ca, Ti, Cr, Sb, Ba, Pb
XVII	46	Li, Na, Al, Si, K, Ca, Ti, Cr, Sb, Ba, Pb
XVIII	38	Li, Na, Al, Si, K, Ca, Ti, Sb, Ba, Pb
XIX	67	Li, Na, Al, Si, K, Ca, Ti, Sb, Ba, Pb
XX	66	Li, Na, Al, Si, K, Ca, Ti, Zn, Ba
XXI	22	Na, K, Ca, Sb, Ba, Pb
XXII	69	Na, Al, K, Ca, Sb, Ba, Pb
XXIII	72	Na, Mg, Al, K, Ca, Zn, Sb, Ba
XXIV	74, 79	Li, Na, Mg, Al, K, Ca, Zn, Sb, Ba
XXV	76, 77, 80, 83	Li, Na, Mg, Al, K, Ca, Zn, Mo, Sb, Ba
XXVI	62	Li, Na, Al, K, Ca, Ti, Cr, Sb, Ba, Pb
XXVII	2	Li, Na, Al, K, Ca, Zn, Sb, Pb
XXVIII	10, 11, 12, 13, 15, 18, 19, 20, 23, 25, 26, 39, 41, 54, 61, 63, 64, 68	Li, Na, Al, K, Ca, Zn, Mo, Sb, Pb
XXIX	17, 24	Li, Na, Al, K, Ca, Zn, Mo, Sb, Pb
XXX	65	Li, Na, K, Ca, Sb, Pb
XXXI	27, 28	Li, Na, K, Ca, Zn, Mo, Sb, Pb
XXXII	16, 29, 30, 34, 40, 43, 44, 47	Li, Na, K, Ca, Zn, Mo, Sb, Pb
XXXIII	36	Li, Na, K, Ca, Cr, Zn, Mo, Sb, Pb
XXXIV	1, 5, 7, 48, 49, 57	Na, Mg, Al, K, Ca, Zn, Sb
XXXV	78	Li, Na, Mg, Al, K, Ca, Zn, Mo, Sb, Ba
XXXVI	84	Li, Na, K, Ca, Zn, Sb, Ba
XXXVII	3	Li, Na, K, Ca, Ti, Ba, Pb
XXXVIII	6	Na, Al, K, Ca, Ba, Pb
XXXIV	31	Na, K, Ca, Pb
XL	71	Na, K, Ca, Cr, Zn, Ba, Pb
XLI	87	Na, K, Ca, Zn, Ba
XLII	88	Na, K, Ca, Zn, Ba
XLIII	89	Na, K, Ca, Zn, Sb, Ba, Pb
XLIV	90	Na, K, Ca, Zn, Sb, Ba, Pb
XLV	73	Li, Na, K, Ca, Ti, Cr, Zn, Ba
XLIV	85	Li, Na, Mg, Al, K, Ca, Ti, Cr, Zn, Ba, Pb
XLVII	9	Na, K, Ca, Ba, Pb
XLVIII	33	Na, K, Ca, Zn, Ba, Pb
XLIX	59, 60	Na, K
L	75	Li, Na, Al, K, Ca, Zn

3.5 Normalization strategies

Two normalization strategies were applied to LIBS analyses: normalization to the total emission light (see Chapter 5) and Standard Normal Variate (SNV) normalization.

Standard normal variate (SNV) normalization has been previously used for LIBS analyses.[68-71] This method has assisted in reducing the standard deviation (and percent RSD) between replicate measurements that occurs due to signal fluctuations or matrix effect.

The mathematical form of the SNV normalization method is shown in Equation 7.

$$I_{SNV}(\lambda) = \frac{[I_{Raw}(\lambda) - I_{BL}(\lambda)] - \mu}{\sigma} \qquad \text{Equation 7}$$

Where I_{BL} (λ) is the background or baseline intensity for a specific wavelength point, I_{Raw} is the raw intensities for a specific wavelength point, μ is the average of the net intensities (I_{Raw} - I_{BL}) and σ is the standard deviation of the net intensities. The baseline intensities and the net intensities were calculated by using the statistical software R, as described by D. Syvilay et al.[69] In order to perform the normalization, a baseline correction constant had to be selected. Three different correction constants were evaluated: 10^4, 10^5, and 10^6. The best correction constant used for the analysis of electrical tapes by LIBS was 10^5 (Figure 46); the baseline is shown in blue. Using the larger constant did not fit the wider background bands, while using the smaller constant resulted in over-correction of some of the signals of interest.

Figure 47 shows the comparison between two spectra before and after SNV normalization.

The resulting normalized spectra can be used for further data processing and statistical analysis, but also for spectral overlay comparisons.

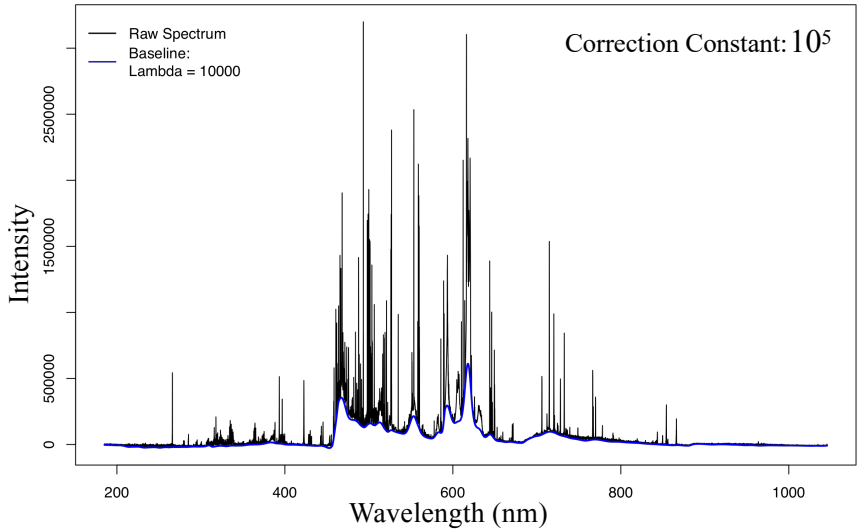

Figure 46 – SNV normalization for a tape samples using 10^5 as the baseline correction constant.

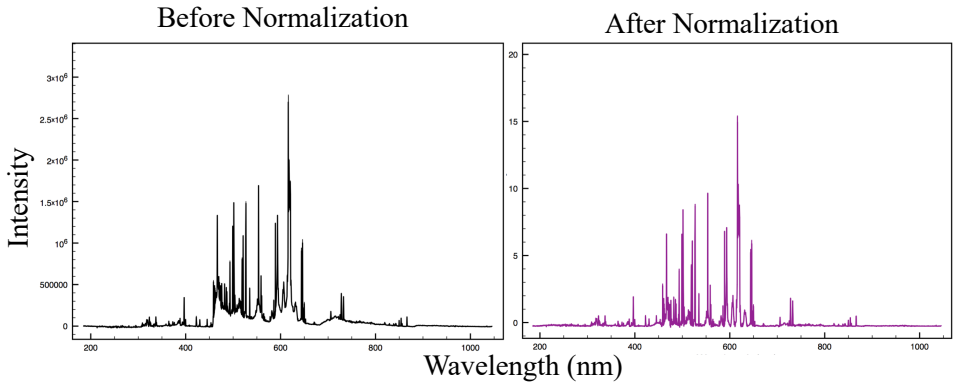

Figure 47 – LIBS spectra before (left) and after (right) SNV normalization for an electrical tape sample.

3.6 Conclusions for the elemental analysis of tapes by LIBS

The method of analysis for laser induced breakdown spectroscopy was developed for electrical tape backings. Design of experiment was used for the optimization of LIBS instrumental parameters. The different factors used for the experimental design included

energy, gate delay, stage speed, and frequency. The best parameters were those that provided a good compromise between maximizing the SNR, minimizing the percent RSD, and preventing the laser beam penetration into the adhesive layer of the tapes. The optimized parameters accounted for a penetration of about 50% into the backing of the thinnest tape in the collection (~83 μm).

After the optimization of the instrumental parameters, a set of 90 electrical tapes previously examined by LA-ICP-MS was analyzed by LIBS. Fifty (50) groups were found by LIBS analysis, which was the same number of distinctive groups found by LA-ICP-MS. Moreover, LIBS allowed to separate some pairs of tapes that were not previously distinguished by LA-ICP-MS by detecting differences in lithium, calcium, and potassium. These elements are problematic in ICP-MS analysis, but typically good emitters in optical spectroscopic techniques such as LIBS. Although the element menu for LIBS was found to be smaller than of LA-ICP-MS, elements such as lithium, sodium and potassium were added to the characterization of specific samples when combining both techniques.

Standard normal variate normalization was applied to LIBS spectra. The SNV method assisted in reducing the standard deviation (and percent RSD) between replicate measurements that occurs due to signal fluctuations or matrix effect.

The tandem analysis of LIBS and LA-ICP-MS provides excellent characterization of the samples in a matter of seconds and would greatly benefit to forensic community in reducing the analysis time and destruction of the samples, while obtaining improved characterization of the samples by detecting up to 14 elements by LIBS, and up to 29 elements by LA-ICP-MS.

4 INTERLABORATORY EXERCISES FOR THE COMPARISON OF TAPES

Adhesive tapes are occasionally received in forensic laboratories as substrates to different types of evidence such as DNA, fingerprints, fibers, and trace evidence. The tape itself, however, represents a very important type of evidence that can assist investigations in a variety of crimes that include the use of tapes in bindings, drug packaging, and the construction of improvised explosive devices, for example. The construction- and composition-related comparison of adhesive tapes in forensic laboratories consists typically of physical and microscopic examination followed by the analysis of the organic and inorganic components.

The physical and microscopic examination of tapes include the description of the texture of the backings, the color of the adhesive, the thickness of the different layers of the tapes, the number of different layers present, and when possible, the examination of potential physical fit between torn edges.[3-5, 16-18, 24] For most laboratories, visual examination is the first step of the analytical scheme and is usually followed by a supplemental instrumental method of analysis. The identification of the organic components of the tapes is usually accomplished by Infrared spectroscopy (IR) and Pyrolysis Gas Chromatography Mass Spectrometry (Py-GC-MS).[2-4, 30, 37, 72-73] These two methods are almost orthogonal and therefore, when combined, provide improved characterization of the organic constituents and superior discrimination.[4] The inorganic analysis of tapes is commonly conducted by Scanning Electron Microscopy with Energy Dispersive Spectroscopy (SEM-EDS) and X-ray Fluorescence (XRF).[3-5, 16-17] These techniques have proved useful in characterizing the elemental composition of tape samples.

SEM-EDS has shown to produce the best discrimination compared to physical examination, IR, and Py-GC-MS for the analysis of the backings of 90 electrical tapes.[4]

More recently, the methods of analysis incorporating Laser Ablation Inductively Coupled Plasma Mass Spectrometry[44] and Laser Induced Breakdown Spectroscopy[43] have been developed for the chemical analysis of tape samples. These techniques have shown promising results for the analysis of tapes by increasing the detected element menu, the confirmatory value of the results, and the sensitivity and selectivity of the analysis. The present work evaluates the informing power of the conventional methods (physical examination, IR, Py-GC-MS, and SEM-EDS), and of LA-ICP-MS and LIBS for the analysis of electrical tapes by different laboratories.

Elemental analysis provided valuable information about the inorganic components present in tapes. These components were found to be part of the fillers, stabilizers, flame retardants, driers and other additives that are incorporated to the formulation of tapes. The formulation of tapes varies significantly between manufactures and products and this information can be used in forensic examinations of tapes to characterize and classify tapes into groups of similar composition. Elemental profile of tapes has shown to be an informative analytical step that adds certainty to the conclusions derived from the complete examination and comparison of tape samples.

Two interlaboratory exercises were designed to study the performance of different analytical methods for the forensic analysis of electrical tapes. The exercises were developed with the objective to imitate forensic case scenarios where known (K) samples are compared to question (Q) samples following the laboratory's analytical scheme. Seven

laboratories participated in two interlaboratory exercises. The participants were asked to compare the tape samples as in a regular forensic case, using their standard protocol for the analysis of tapes by the available techniques.

4.1 Interlaboratory tests design

Interlaboratory test #1 consisted of seven participant laboratories. Six samples of tapes: three known samples (K1, K2, and K3) and three questioned samples (Q1, Q2, and Q3) belonging to 3M Scotch and GE brands were sent out to the participant laboratories. There was a total of three pairs corresponding to the same rolls: K1 and Q2, K2 and Q3, and K3 and Q1 (Table 20). The participants were asked to compare the tape samples as in a regular forensic case, using their regular standard protocol for the analysis of tapes and available techniques. Four laboratories performed SEM-EDS analysis, three performed LIBS analysis, two performed LA-ICP-MS analysis. All laboratories performed physical/microscopic examination of the tapes and IR spectroscopy. Four laboratories performed Py-GC-MS to analyze the tape samples.

The results of interlaboratory #1 were discussed and evaluated among the participants before the design of interlaboratory test #2. The first interlaboratory test showed the potential of the elemental methods (mainly LIBS and LA-ICP-MS) to not only correctly distinguish the different pairs of tapes and associate the tapes from the same rolls, but also to increase the characterization of the samples. Interlaboratory test #2 was therefore focused on testing the performance of the different elemental techniques for the analysis of similar samples of tapes not previously distinguished by the organic analysis methods.

The effect of different parameters in the performance of a specific technique was also evaluated.

Interlaboratory test #2 consisted of five participant laboratories performing only elemental methods of analysis (SEM-EDS, LIBS and LA-ICP-MS). In order to produce a more challenging set of samples, interlaboratory #2 consisted of four samples of tapes: a known sample (K1) and three questioned samples (Q1, Q2 and Q3) all belonging to the same brand (3M Scotch). The pairs K1 and Q2 originated from the same roll of tape (3M Scotch 700) (Table 20). These samples were selected from a set of tapes formerly analyzed by most of the techniques in question, and were not previously differentiated by physical and microscopic examination, IR spectroscopy, or Py-GC-MS.[3-4] Four participant laboratories performed SEM-EDS analysis, five performed LIBS analysis, and three performed LA-ICP-MS analysis.

The participant laboratories provided their conclusions as to which pair of tapes could be distinguished and which ones were not differentiated. False positive and false negative error rates were estimated by documenting any disagreement between the anticipated conclusion (e.g., known source of origin to be considered a true association or exclusion) and the conclusion reported by the participants based on their measured data. In addition, the raw instrumental data from interlaboratory #2 was re-processed to compare the spectral data quantitatively using different match criteria: ±3s, ±4s and ±5s.

4.2 Sample set description for interlaboratory test #1 and #2

The samples of tapes were prepared by selecting a section (~20 cm) of the tape rolls and attaching them to a plastic substrate (Apollo Plain Paper Copier Transparency Film).

The individual samples consisted of six (~2 cm by ~2 cm) pieces of tapes labeled as K1, K2, K3, Q1, Q2, and Q3 for interlaboratory test #1 and K1, Q1, Q2 and Q3 for interlaboratory test #2. Table 20 shows the sample description for both interlaboratory exercises. Each laboratory was asked to compare the known sample to all the questioned sample, for a total of nine comparison pairs for interlaboratory test #1, and three comparison pairs for interlaboratory test #2.

Table 20 – Sample description and expected results for interlaboratory test #1 and #2.

Test	Comparison Pair	Sample Origin	Expected Results
1	K1 vs. Q1	Same brand, different model, different roll (3M Scotch Super 88/3M Scotch 700)	Different elemental composition
	K1 vs. Q2	Same brand, same model, same roll (3M Scotch Super 88, made in USA)	Same elemental composition
	K1 vs. Q3	Different brand, different model, different roll (3M Scotch Super 88/GE)	Different elemental composition
	K2 vs. Q1	Different brand, different model, different roll (GE/3M Scotch 700)	Different elemental composition
	K2 vs. Q2	Different brand, different model, different roll (GE/3M Scotch Super 88)	Different elemental composition
	K2 vs. Q3	Same brand, same model, same roll (GE, made in Taiwan)	Same elemental composition
	K3 vs. Q1	Same brand, same model, same roll (3M Scotch 700, made in USA)	Same elemental composition
	K3 vs. Q2	Same brand, different model, different roll (3M Scotch 700/3M Scotch Super 88)	Different elemental composition
	K3 vs. Q3	Different brand, different model, different roll (3M Scotch 700/GE)	Different elemental composition
2	K1 vs. Q1	Same brand, different model, different roll (3M Scotch 700/3M Scotch Super 33+, made in USA)	Different elemental composition
	K1 vs. Q2	Same brand, same model, same roll (3M Scotch 700, made in USA)	Same elemental composition
	K1 vs. Q3	Same brand, same model, different roll (3M Scotch Super 33+, made in USA)	Different elemental composition

Samples for interlaboratory test #1 were selected in order to include three different situations: two tape samples originating from a same roll that should be indistinguishable, two different tape samples of a same brand that may be differentiated by some of the most selective and sensitive methods, and two different samples from different brands that should be distinguishable by most techniques.

Samples for interlaboratory test #2 were selected in order to include tape fragments originating from a same tape roll, and tape samples from the same brand which could not be distinguished by physical examination or IR spectroscopy, but that showed differences in their elemental composition. The purpose of interlaboratory test #2 was to evaluate the performance of the different elemental techniques for the comparison of similar tapes from the same brand.

4.3 Instrumental parameters

Participants were asked to compare each known and question samples by their available methodology. For the participants without a protocol for a specific instrumentation, a set of parameters were suggested for the analysis of tapes by such technique, based on previous studies.[4, 44] The participant laboratories were asked to provide detailed description of the parameters used for the elemental analysis techniques; this would allow to estimate the effect of some parameters in the sensitivity and selectivity of the method. Table 21, Table 22, and Table 23 show the parameters for SEM-EDS, LIBS and LA-ICP-MS, respectively. The instrumental parameters for the different instrumentation were optimized in order to obtain the best signal to noise ratio (SNR) and smaller relative standard deviation (% RSD). The identification code (A, B, C, …) for the

laboratories was randomly assigned for each individual technique; this identification code was also rotated among analytical methods so that lab A performing SEM-EDS was not the same as lab A performing LIBS, etc.

Table 21 – Parameters for SEM-EDS for interlaboratory tests #1 and #2.

SEM-EDS Instrumental Parameters				
Lab ID	Lab A	Lab B	Lab C	Lab D
Instrument	Tescan Vega 3	FEI Explorer	Zeiss EVO 40	JEOL JSM 6490LV
Detector	Apollo V EDS	OmegaMax EDS	Oxford INCA EDS	INCA x-Sight
Magnification	50	Variable	180	50
Acceleration Voltage (kV)	25	25	20	25
Working Distance	15	15	25	15
Take off Angle	30	37	35	30
Dead Time (%)	30	16	-	30
Counting Time (s)	200	100	152	120

Table 22 – Parameters for LIBS for interlaboratory test #1 and #2.

LIBS Instrumental Parameters					
	LAB A	LAB B	LAB C	LAB D*	LAB E*
Instrument	J200	J200	RT100	J200	J200
Laser	Nd:YAG 266 nm	Nd:YAG 266 nm	Nd:YAG 266 nm	Nd:YAG 266 nm	Nd:YAG 266 nm
Laser Energy	100% (19 mJ)	100% (19 mJ)	100% (~30 mJ)	100%	50%
Spot Size (µm)	100	100	100	100	100
Gas Used	Air	Ar	Air	Air	Ar
Shots	403	403	403	403	325
Gate Delay (µsec)	0.9	0.9	0.9	0.5	1.0
Frequency (Hz)	10	10	10	10	10
Stage Speed (µm/s)	100	150	100	100	300
Line Length (mm)	4	6	4	4	2

*Data reported for interlaboratory test # 2

Table 23 – Parameters for LA-ICP-MS for interlaboratory test #1 and #2.

LA-ICP-MS Instrumental Parameters			
	LAB A	LAB B	LAB C*
MS Instrument	Agilent 7700x	PE ELAN 6100	PE NEXION 350X
Laser	193 NWR ESI (193 nm)	New Wave ns–Nd:YAG (213 nm)	Applied Spectra ns–Nd:YAG (266 nm)
Energy	0.7 mJ	2.6 mJ	19 mJ
Stage Speed	40 µm/s	40 µm/s	40 µm/s
Spot Size	150 µm	190 µm	200 µm
Repetition Rate	20 Hz	10 Hz	10 Hz
Ablation Mode	Line	Line	Line
Line Length	5.6 mm	4 mm	4 mm
Sampling Time	140 s (2 min 20 sec)	180 s (3 min)	150 s (2 min 30 sec)
Blank Time (Laser Off)	30 sec	40 sec	40 sec
Carrier Gas	Helium	Helium	Helium
Gas Flow	0.8 L/min	0.9 L/min	0.6 L/min

*Data reported for interlaboratory test # 2

4.4 Data reduction and statistical analysis

Data reduction and statistical analyses were performed using Excel 2011 (version 14.7.7, Microsoft Corporation), the Aurora software for LIBS data integration and peak identification (version 2.1, Applied Spectra, Freemont, CA), and Plot2 for Mac (version 2.3.7, Berlin, Germany) for spectral overlay comparisons.

Each data file originally obtained from the instrument was converted into a .csv file for further data processing. The .csv files consisted of a column for the intensity/counts representing the y axis and a column for the measurement variables representing the x axis (e.g., energy in eV for SEM-EDS, mass/charge ratio for LA-ICP-MS in mass scan mode, time in seconds per each isotope for LA-ICP-MS in transient mode, wavenumbers in nm^{-1} for IR, and retention time for Py-GC-MS). The .csv files were used to further graph the data for spectral comparison and for integration of the area under the curve for the selected element peaks, emission lines, and isotopes.

4.4.1 Data pre-processing

The data collected for SEM-EDS was in the form of energy spectra (counts vs. x-ray energy). Data pre-processing included background subtraction and estimation of SNR as reported by Ernst et al.[74]

All of the emission lines selected for LIBS were confirmed by the presence, and abundance, of two or more emission lines for each element. The emission lines selected were those with no known interferences, smaller percent RSD, and larger SNR.

All of the emission lines selected for LIBS were confirmed by the presence, and abundance, of two or more emission lines for each element. The emission lines selected were those with no known interferences, smaller percent RSD, and larger SNR. Integration of the area under selected peaks of the elements of interest followed by the ratio of the elements was applied to the data used for numerical comparison. The element lines selected for LIBS match criteria comparison were the following: Sb 259.8 nm, Si 288.2 nm, Ti 334.9 nm, Mo 386.4 nm, C 247.8 nm, Ca 393.4 nm, Al 396.2 nm, Cr 427.5 nm, Cd 480.0 nm, Zn 481.1 nm, Pb 405.8 nm, Sr 407.8 nm, Mg 518.4 nm, Na 589.0 nm, Ba 614.2 nm, Li 670.8 nm, K 766.5 nm. These elements were determined to be present if the SNR>3.

The data collected for LA-ICP-MS was in the form of mass scan (intensity counts vs. mass-to-charge ratio) and transient mode (intensity counts vs. time).

The spectra in mass scan mode for LA-ICP-MS were especially useful for spectral overlay comparison. Data pre-processing for LA-ICP-MS for spectral overlay included the removal of non-relevant mass-to-charge peaks originating from polyatomic and isobaric interferences and normalization to the sum of the intensity peaks as a mean to compensate

for any shot-to-shot variation and inter-day variations.[44, 53] In the absence of an internal standard, normalization to the sum of the intensity peaks accounts for small differences in the ablated mass between samples and improves both repeatability and reproducibility of each individual sample.[44] All of the isotopes selected for LA-ICP-MS were confirmed by their isotopic pattern and natural abundance.

The data collected for LA-ICP-MS in transient mode (intensity vs. time) is not suitable for spectral overlay comparison. Instead, the GeoPRO (CETAC Technologies, v 1.0, NE) software was used to integrate the area under the curve for the selected isotopes for further statistical analysis using different match criteria. The elements were determined to be present if the SNR>3. The isotopes selected were those with larger abundance and no known interferences. The isotopes used for LA-ICP-MS match criteria comparison are the following: ^{27}Al, $^{135, 137}$Ba, ^{13}C, $^{42, 44}$Ca, ^{111}Cd, ^{35}Cl, ^{57}Fe, ^{39}K, ^{139}La, ^{7}Li, $^{24, 26}$Mg, ^{23}Na, $^{206, 208}$Pb $^{121, 123}$Sb, $^{28, 29}$Si, $^{118, 119}$Sn, $^{86, 88}$Sr, $^{47, 48}$Ti, ^{232}Th $^{64, 66}$Zn, $^{90, 91}$Zr.

4.5 Comparison criteria

Physical and microscopic examination comparison criteria varied greatly between laboratory. Most laboratories compared tapes based on the thickness of the backing and adhesive layer and the texture of the backing.

The laboratories comparing backing texture determined that tapes were distinguished base on the shiny or matte finish, and on dimples or marks on the surface. Physical examination and microscopy were, however, followed by a more confirmatory technique (IR, Py-GC-MS, SEM-EDS, LIBS, or LA-ICP-MS).

IR comparisons were performed by spectral overlay between the samples. The samples were differentiated by the presence or absence of peaks in the overlay comparison. In some cases, these peaks were attributed to adipates or phthalates present in the tapes.

Py-GC-MS samples were differentiated by the retention time, fragmentation pattern, and confirmation of the presence of specific organic components using the different fragmentation patterns. The identified organic components were present in some tapes and not others, therefore allowing to differentiate the tape pairs originating from different sources.

The comparisons by SEM-EDS, LIBS and LA-ICP-MS were performed by spectral overlay. The spectral overlay comparisons account for variability within replicate measurements, which includes instrumental variations and compositional variations in the sampled locations. Two samples were differentiated if the variation of the spectral peaks of the replicates of the questioned item did not fall within the observed range of variation of the respective spectral peaks of the replicates of the known sample. The variability was documented for the x-axis of the analyte peaks (e.g., identification of elements by energy, wavelength or m/z) and for the y-axis (e.g., counts, peak intensity or area correlated with the concentration of each element on the samples). Two samples were differentiated if at least one element fall outside the spectral overlay criteria.

In the case of LIBS comparisons, the presence and abundance of two or more emission lines for the element in question confirmed its presence in the samples. For LA-ICP-MS, relative natural abundance of different isotopes was used to confirm the identification of each element.

In addition to spectral overlay comparisons, different match criteria were tested for the numerical comparison of tapes for LIBS and LA-ICP-MS. Although spectral overlay provides a visual comparison of the samples and allows for the identification of the element menu in the samples, it can be subjective when samples are very similar to each other. Spectral overlay is also time consuming when the sample comparison set is large.

In efforts to numerically compare the elements in the samples for LIBS and LA-ICP-MS, different match criteria were studied: ±3s, ±4s and ±5s, where s represents the standard deviation of the known sample. If the mean of at least one element or ratio in the sample in question falls outside these ranges of the mean and standard deviation of the known sample, the two tapes are said to be distinguished from each other by the measured properties. If all elements in the question sample fall within the range of standard deviation of the known sample, the two tapes are indistinguishable from each other.

In order to perform the different match criteria for all laboratories, the data was processed in the same manner for all laboratories and the selected elements or ratios were those detected by the laboratories in at least one sample.

The best match criterion for LIBS and LA-ICP-MS was found to be the ±5s interval. The ±5s match criterion allowed to correctly associate the tapes belonging to the same rolls and differentiate the tapes from different rolls.

In the case of LIBS comparisons, the match criteria were applied to the ratios of the peak areas. The variability between replicate measurements for LIBS, as well as the effect of the sample matrix in the resulting spectra can be minimized by the use of ratios. The element ratios method works on the premise that ratios between different elements should

remain relatively constant, regardless of the matrix composition and instrumental variations.

4.6 Results and Discussion

The results for both interlaboratory tests are summarized by technique. Interlaboratory test #1 consisted of SEM-EDS, LIBS, LA-ICP-MS, physical and microscopic examination, IR spectroscopy, and Py-GC-MS. Interlaboratory #2 consisted only of the elemental methods of analysis (SEM-EDS, LIBS and LA-ICP-MS).

4.6.1 Interlaboratory test #1

Four laboratories performed SEM-EDS analysis, three performed LIBS analysis, two performed LA-ICP-MS analysis for interlaboratory test #1. All laboratories performed physical/microscopic examination of the tapes and IR spectroscopy. Four laboratories performed Py-GC-MS to analyze the tape samples.

4.6.1.1 SEM-EDS

All the laboratories performing SEM-EDS in interlaboratory #1 were able to correctly associate K1 to Q2 (3M Scotch Super 88, USA), K2 to Q3 (GE, Taiwan), and K3 to Q1 (3M Scotch 700, USA), therefore the rate of false negatives was zero; these pairs of tapes belong to the same rolls and based on predistribution analysis were expected to be indistinguishable (Table 20). However, laboratories C and D were not able to detect enough differences between the different models of 3M Scotch tapes (K1 vs. Q1, and K3 vs. Q2). In the case of K2 (GE, made in Taiwan), this tape was always correctly distinguished from the 3M Scotch tapes based on its elemental profile.

The total number of comparison pairs for interlaboratory test #1 was 9 (Table 20) for a total of 4 participating laboratories. From these 36 comparison pairs, 12 correspond to same roll comparisons, and 24 correspond to different roll comparisons. Two of the laboratories performing SEM-EDS incorrectly associated two pairs of tapes belonging to different rolls, therefore 4 comparison pairs contributed to a 16.7% false positives rate (4 undistinguished pairs out of 24 comparison pairs) (Table 24).

Table 24 – False positive rate (FPR) and false negative rate for the elemental techniques for interlaboratory test #1 and #2.

Method	Test # 1		Test # 2	
	FPR (%)	FNR (%)	FPR (%)	FNR (%)
SEM-EDS	16.7 (4 out of 24)	0	12.5 (1 out of 8)	0
LIBS	0	0	0	0
LA-ICP-MS	0	0	0	0

Figure 48 shows the SEM-EDS spectral overlay comparison for Lab D for K1, Q1, Q2, and Q3. Sample K1 was differentiated from sample Q3 based on the higher amounts of Al (1.486 Kα) and Si (1.740 Kα) present in Q3. Sample K1 was not distinguished from Q1 and Q2 using SEM-EDS by laboratory D.

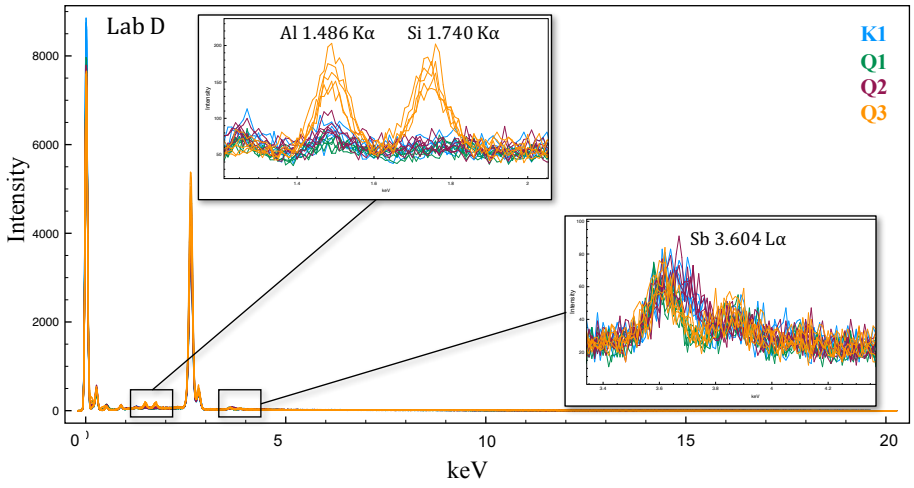

Figure 48 – SEM-EDS spectral overlay comparison of K1 vs. Q1, Q2, and Q3 for Lab D for interlaboratory test #1. Sample K1 was differentiated from sample Q3 based on the higher amounts of Al (1.486 Kα) and Si (1.740 Kα) present in Q3. Sample K1 was not distinguished from Q1 and Q2 by SEM-EDS by this laboratory.

In contrast, Lab A was able to differentiate the 3M Scotch tapes (Super 88 and 700) (see Table 20). Figure 49 shows the SEM-EDS spectral overlay comparison of K1, Q1, Q2, and Q3 by Lab A for interlaboratory test #1. Sample K1 was differentiated from Q3 based on the presence of a shoulder next to the largest Sb (3.606 Lα) peak, due to the higher amounts of Ca (3.691 Kα) in K1 and Q2. The difference in Ca (3.691 Kα) was detected by Lab C and Lab D, but not considered enough for an exclusion due to the lack of resolution among the Ca and Sb peaks and the relatively low SNR of the signal. It is worth noting that the SNR for the Sb Lα /Ca Kα peak observed by laboratories C and D was at least one order of magnitude lower than the respective SNR observed by laboratories A and B, indicating that the sensitivity of the SEM-EDS instruments is highly dependent on instrumental configurations.

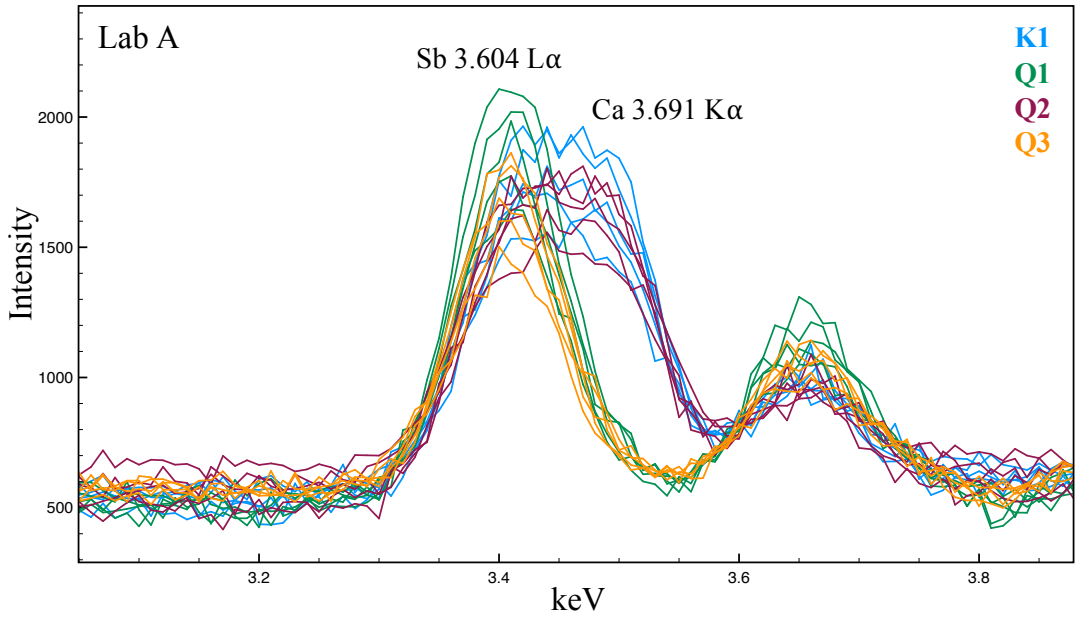

Figure 49 – SEM-EDS spectral overlay comparison of K1 vs. Q1, Q2, and Q3 for Lab A for interlaboratory test #1. Sample K1 was differentiated from Q2 based on the presence of Ca (3.691 Kα) in K1 and Q2.

The relatively lower sensitivity of instrumental configurations C and D in comparison to those of laboratories A and B is also reflected in the overall element menu detected by SEM-EDS for the participant laboratories (Table 25). Although the laboratories selected up to 4-7 elements by SEM-EDS, only Ca appeared to differentiate the 3M Scotch tapes for laboratories A and B. One factor that contributed in the discrepancy of calcium content is the relatively low selectivity and sensitivity observed by the Ca Kα peak. Laboratories C and D did not differentiate the pair K1 and Q1 based on just the wider signal around the 3.4 keV area (Figure 49); the difference between the samples was not considered large enough to constitute an exclusion. In the case of the GE tape, all laboratories differentiated this tape from the 3M Scotch tapes based on Al and Si.

Table 25 – Element menu detected for the elemental techniques for each tape pair by the different laboratories in interlaboratory exercise #1.

Lab	Tape Pairs	SEM-EDS	LIBS	LA-ICP-MS
A	K1, Q2	Cl, Ca/Sb, Mg, Al, Si, Zn	Al, Ba, C, Ca, K, Li, Mg, Mo, Na, Sb, Sr, Zn	Al, Ba, Co, Cu, La, Mn, Mo, Ni, Pb, Sb, Sr, Ti, W, Y, Zn
	K2, Q3	Cl, Ca/Sb, Mg, Al, Si	Al, C, Ca, K, Li, Mg, Mo, Na, Sb, Si, Ti	Al, Ba, Co, Cu, La, Mn, Mo, Nd, Ni, Pb, Pr, Sb, Sr, Ti, W, Y, Zn
	K3, Q1	Cl, Ca/Sb, Mg, Al, Si	Al, Ba, C, Ca, K, Li, Mg, Mo, Na, Sb, Sr	Al, Ba, Cu, La, Mn, Mo, Ni, Pb, Sb, Sr, Ti, W, Y, Zn
B	K1, Q2	Cl, Ca/Sb, Mg, Al, Si, Zn	Al, Ba, C, Ca, K, Li, Mg, Mo, Na, Sb, Sr, Ti, Zn	Al, Ba, Ca, Cl, K, Mg, Na, Sb, Si, Sn, Sr, Zn
	K2, Q3	Cl, Ca/Sb, Mg, Al, Si	Al, C, Ca, K, Li, Mg, Mo, Na, Sb, Si, Ti, Zn	Al, Ca, Ce, Cl, Fe, K, Mg, La, Na, Nb, Sb, Si, Ti, Th, Zn
	K3, Q1	Cl, Ca/Sb, Mg, Al, Si, Zn	Al, Ba, C, Ca, K, Li, Mg, Mo, Na, Sb, Sr, Zn	Al, Ba, Ca, Cl, K, Mg, Na, Sb, Si, Sn, Sr, Zn
C	K1, Q2	Cl, Ca/Sb, Mg, Al, Si	Al, Ba, C, Ca, K, Li, Mg, Na, Sr, Zn	-
	K2, Q3	Cl, Ca/Sb, Mg, Al, Si	Al, C, Ca, K, Li, Mg, Mo, Na, Sb, Si	
	K3, Q1	Cl, Ca/Sb, Mg, Al, Si	Al, Ba, C, Ca, K, Li, Mg, Na, Sr	
D	K1, Q2	Cl, Ca/Sb, Mg, Al	-	-
	K2, Q3	Cl, Ca/Sb, Mg, Al, Si		
	K3, Q1	Cl, Ca/Sb, Mg, Al		

4.6.1.2 LIBS

The pairs of tapes belonging to the same rolls: K1 and Q2 (3M Scotch Super 88, USA), K2 and Q3 (GE, Taiwan), and K3 and Q1 (3M Scotch 700, USA) were all correctly associated by LIBS analysis in interlaboratory test #1. All the laboratories correctly differentiated the two different 3M Scotch tape pairs (K1 vs. Q1 and K3 vs. Q2) (Table 20). In contrast with SEM-EDS, Ca was easily detected by LIBS (Figure 50). Moreover, LIBS allowed to detect the same elements identified by SEM-EDS with the addition of C, Ca, Ba, K, Li, Na, Mo, Si, Sr, and Ti.

Figure 50 shows the LIBS spectral overlay comparison for samples K1, Q1, Q2, and Q3 for laboratory A. Sample K1 was differentiated from Q1 based on the higher amounts of Mo and Ca in sample K1. Also, K1 was differentiated from Q3 based on Ba, Ca and Ti. Additionally, the three pairs of tapes originated from the same roll were correctly associated and the element menu detected is shown in Table 25. The main differences between the two 3M Scotch tapes (Super 88 and 700) consist of the higher amounts of Mo and Ca in K1 and Q2 (3M Scotch Super 88). The Super 88 electrical tape is of a higher quality compared to the commercial grade 3M Scotch 700, therefore some extra components might have been added to the formulation in order to improve its performance. A review of several electrical tape and pressure sensitive adhesives patents[9-14] confirmed the use of calcium carbonate and calcium sulfate, as well as zinc oxides and silicates and inorganic fillers. Similarly, molybdenum oxide is known to be a flame retardant added to the formulation of tapes. These differences in Ca were not always resolved from the Sb peaks by SEM-EDS due to lower selectivity of the technique. In the same manner, Mo and Zn were not always detected in SEM-EDS due to the lower sensitivity of the technique compared to LIBS.

The higher sensitivity and selectivity of LIBS allowed to detect more elements per sample and this permitted to further distinguish the similar 3M tapes that belong to different rolls (K1 vs. Q1 and K3 vs. Q2), which were not always distinguished by SEM-EDS.

The rate of false negatives and false positives for LIBS was found to be zero (see Table 24) as LIBS allowed to correctly associate all tapes belonging to the same rolls and differentiate the tapes from different rolls of the present study.

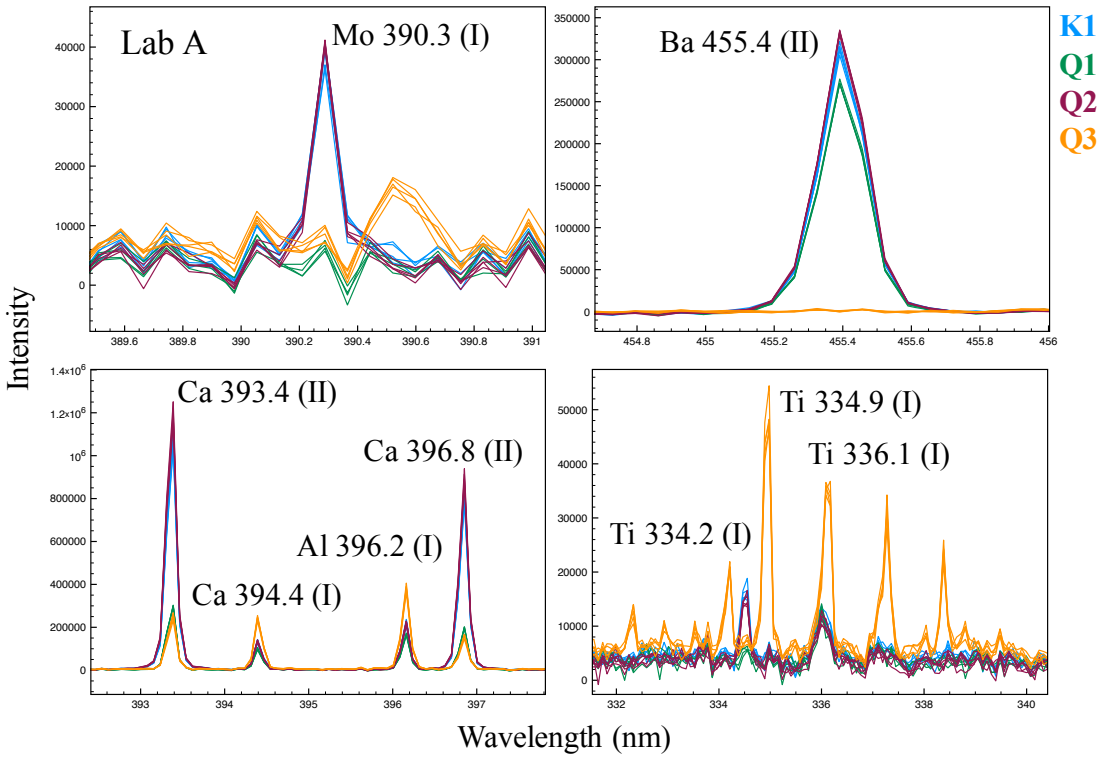

Figure 50 – Spectral overlay comparison by LIBS of K1 vs. Q1, Q2, and Q3 for Lab A for interlaboratory test #1. Sample K1 was differentiated from Q1 based on the higher amounts of Mo and Ca in sample K1. K1 was differentiated from Q3 based on Ba, Ca and Ti.

4.6.1.3 LA-ICP-MS

All the laboratories performing LA-ICP-MS were able to correctly associate pairs of tapes belonging to the same rolls which were expected to be indistinguishable (Table 20). The 3M Scotch tapes belonging to different rolls (K1 vs. Q2 and K3 vs. Q2) were correctly differentiated by LA-ICP-MS analysis as well. Table 25 shows the element menu obtained by LA-ICP-MS for interlaboratory test #1 for each pair of tapes. The element menu obtained by LA-ICP-MS increased compared to LIBS by the addition of Ce, Co, Cu, Cl, Fe, La, Mn, Nb, Nd, Ni, Pr, Sn, W, and Y. These elements are present in the tapes at concentrations below the limits of detection of LIBS but could be detected by LA-ICP-MS due to the improved sensitivity and selectivity of this method. The rate of false positives

and false negatives for LA-ICP-MS comparisons were found to be zero (Table 24). It is important to note that LIBS was especially useful in detecting Li, which is a very difficult element to detect in LA-ICP-MS. Li can be difficult to detect in LA-ICP-MS due to space-charge effects between light and heavy ions in the mass spectrometer.[45] Li is a good emitter, easily detected by LIBS in most samples at very low concentrations. Similarly, LIBS proved useful in detecting elements problematic to LA-ICP-MS such as potassium ($^{38}K^{+}$), which is the most abundant isotope that can be measured by ICP-MS without $^{40}Ar^{+}$ interferences. Potassium is known to present interferences with Ar ($^{39}Ar^{1}H^{+}$) in ICP-MS but is easily detected by LIBS and confirmed by multiple lines throughout the spectra.

Figure 51 shows the LA-ICP-MS spectral overlay comparison between K1, Q1, Q2, and Q3 for laboratory B for interlaboratory test #1. K1 was differentiated from Q1 based on the higher amounts of Sr and Sn in K1. K1 and Q3 were differentiated based on the higher amounts of Ti in Q3, and the higher amounts Mo, Sr and Sn in K1. K1 and Q2 were not distinguished by LA-ICP-MS based on spectral overlay comparisons; this pair of tapes belong to the same roll.

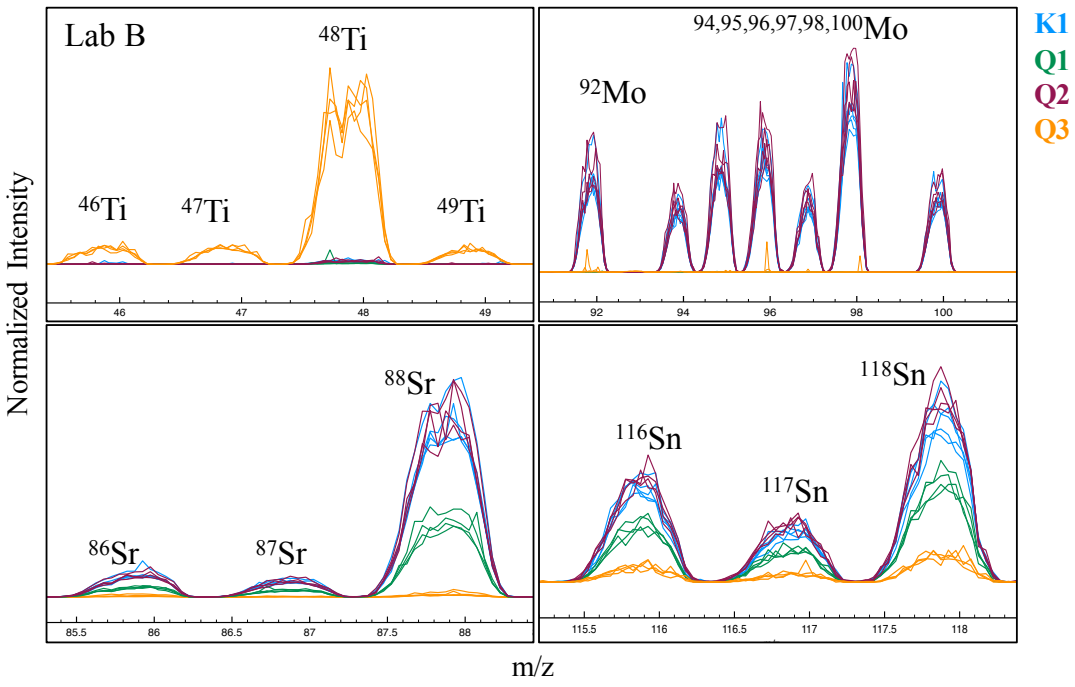

Figure 51 – LA-ICP-MS spectral overlay comparison of K1 vs. Q1, Q2, and Q3 for Lab B for interlaboratory test #1. K1 was differentiated from Q3 based on Ti, Mo, Sr, and Sn Sample K1 was differentiated from Q1 based on the higher amounts of Mo, Sr, and Sn in sample K1.

Interlaboratory #1 showed the potential of the elemental methods (mainly LIBS and LA-ICP-MS) to not only correctly distinguish the different pairs of tapes and associate the tapes from the same rolls, but also to increase the characterization of the samples by detecting up to 14 elements by LIBS and 20 elements by LA-ICP-MS.

4.6.1.4 Additional techniques

Physical examination was performed as part of interlaboratory test #1 by all seven participant laboratories. Although each lab used a different method for comparing the tapes, they all correctly associated the tape pairs belonging to the same rolls. However, physical examination alone was not always able to differentiate the 3M Scotch tapes belonging to different rolls (3M Scotch Super 88 and 700). Further tests (IR, Py-GC-MS,

SEM-EDS) were needed to confirm if there were chemical differences between the tapes. Microscopic and physical examination of tapes typically include the measurement of the thickness and width of the tapes, the number of layers present, and the description of colors of the backing and the adhesive. In addition, the backing texture is described according to its shine and individual characteristics or imperfections such as dimples, craters, lines, etc. Moreover, the tape ends are evaluated to determine if a fracture match is present.

Infrared analysis was performed by all the laboratories for interlaboratory test #1. Out of the seven participant laboratories, six correctly associated the tapes belonging to the same rolls. One laboratory reported false exclusions between K1 and Q2 and between K3 and Q1 based on their IR spectra. Out of the seven laboratories, four could not differentiate the different 3M Scotch tape pairs belonging to different rolls. All laboratories correctly associated the GE tapes (K2 and Q3).

IR spectroscopy is a quick universal technique that provides identification of organic compounds without the need for sample preparation. By using IR spectroscopy, the backing polymer can be identified as polyvinyl chloride, polyethylene, or butyl rubber. Components in the tapes such as phthalates and adipates could also be detected when present at higher concentrations.[2-4, 30, 72] However, in some instances, FTIR presents some limitations for the analysis of electrical tape backings because primary components of the plasticizer may mask the detection of other components, and the carbon black in the PVC backing creates sloping baselines for the IR spectrum.[1]

Pyrolysis gas chromatography was performed by four laboratories. The laboratories compared the chromatograms between tapes. Furthermore, the fragmentation spectra

obtained from the mass spectrometry analysis allowed to identify specific components in the tapes such as the backing polymer, phthalates, adipates, mixtures of phthalates and adipates, sebacate, trimellitate, among others.[2-4, 37, 72-73] Py-GC-MS allowed for the correct association of the tapes belonging to the same rolls, and correctly differentiated the pairs of tapes from different rolls.

The main advantage of Py-GC-MS is that it provides separation (retention time) and identification (mass spectrometry) of the organic compounds present in tapes. However, Py-GC-MS is a destructive and time-consuming technique, and therefore is recommended as the last analytical step in tape examinations.

SEM-EDS produced the best discrimination power compared to physical examination, IR, and Py-GC-MS for the analysis of the backings of 90 electrical tapes.[4] LIBS and LA-ICP-MS show the potential for even better discrimination than all of these techniques combined.

4.6.2 Interlaboratory test #2 results

In order to produce a more challenging set of samples, interlaboratory #2 consisted of four tapes: a known sample (K) and three questioned samples (Q) all belonging to the same brand (3M Scotch), but from different rolls (Table 20). The pairs K1 and Q2 belong to the same roll of tape (3M Scotch 700). These samples were selected from a set of tapes that was previously analyzed by most of the techniques in question, and were not previously differentiated by physical and microscopic examination, IR spectroscopy, or Py-GC-MS, but were differentiated by LA-ICP-MS.[4, 44]

Four participant laboratories performed SEM-EDS analysis, five performed LIBS analysis, and three performed LA-ICP-MS analysis.

4.6.2.1 SEM-EDS

The four laboratories performing SEM-EDS compared the samples by spectral overlay. Figure 52 shows the spectral overlay by SEM-EDS for Lab B for interlaboratory test #2. Sample K1 was differentiated from sample Q1 based on the higher amounts of Mg (1.254 Kα) in K1, and P (2.013 Kα), Pb (2.342 Mα) and Ca (3.69 Kα) present in Q1. Sample K1 was distinguished from Q3 for based on the Ca (3.691 Kα) shoulder on the Sb (3.604 Lα) peak. K1 was not distinguished from Q2 by SEM-EDS; K1 and Q2 belong to the same tape roll (Table 20).

In the case of Laboratory D, the difference in the Ca shoulder between the signals was reported as inconclusive and not enough to differentiate the two samples for the same issues of selectivity and sensitivity discussed for the first test.

The total number of comparison pairs for interlaboratory test #2 was 3 (Table 20) for a total of 4 participating laboratories. From these 12 comparison pairs, 4 correspond to same roll comparisons, and 8 correspond to different roll comparisons. One of the laboratories performing SEM-EDS incorrectly associated two pairs of tapes belonging to different rolls, therefore 1 comparison pair contributed to a 12.5% false positive rate (1 undistinguished pair out of 8 comparison pairs) (Table 24). The element menu obtained by SEM-EDS analysis for interlaboratory test #2 is reported in Table 26.

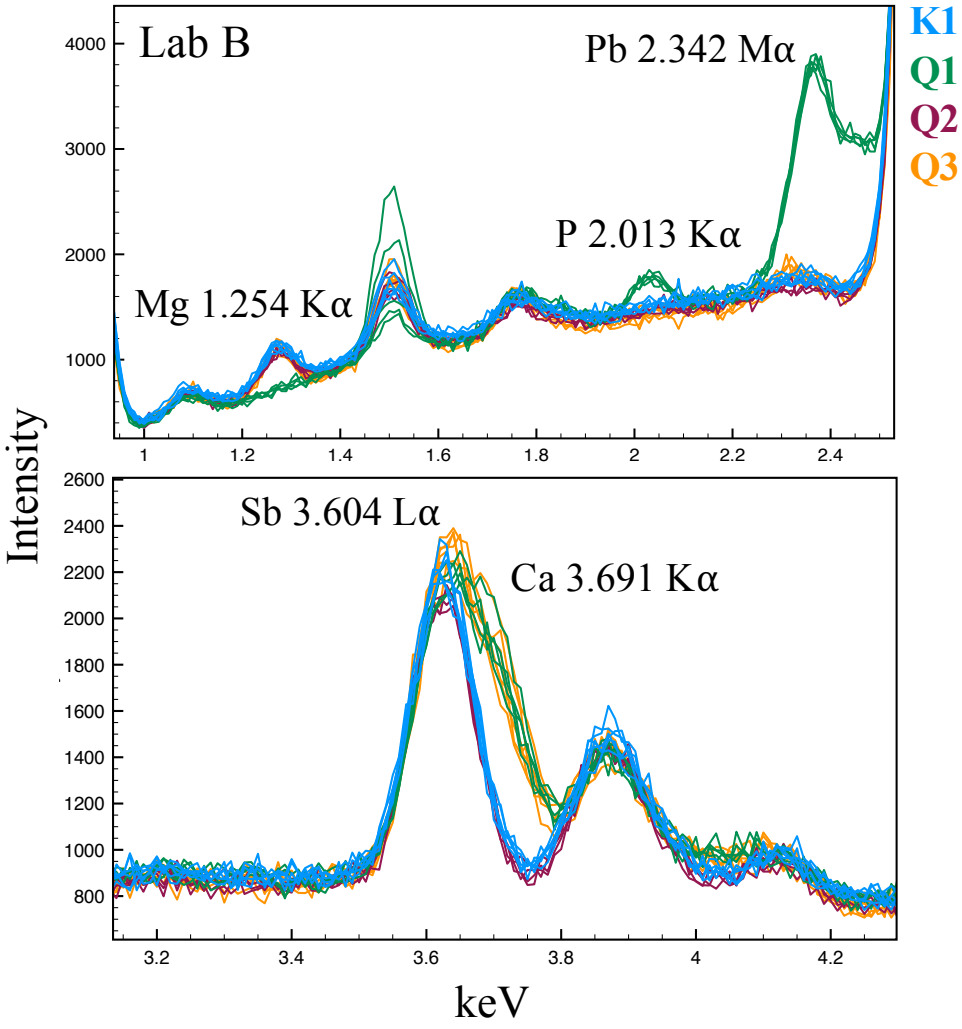

Figure 52 – SEM-EDS spectral overlay comparison of K1 vs. Q1, Q2, and Q3 for laboratory B for interlaboratory test #2. Sample K1 was differentiated from sample Q1 based on the lower amounts of Mg (1.254 Kα) and higher amounts of P (2.013 Kα) and Pb (2.342 Mα), and the Ca (3.691 Kα) shoulder in Q1. Sample K1 was distinguished from Q3 based on the Ca (3.691 Kα) shoulder on the Sb (3.604 Lα) peak.

Table 26 – Element menu detected for the elemental techniques for each tape sample by the different laboratories in interlaboratory exercise #2.

Lab	Tape Pairs	SEM-EDS	LIBS	LA-ICP-MS
A	K1, Q2	Cl, Ca/Sb,Mg, Al, Si	Al, Ba, C, Ca, K, Li, Mg, Mo, Na, Sb, Sr, Zn	Al, Ba, C, Cr, K, Li, La, Mg, Mo, Na, Nb, Ni, Pb, Rb, Sb, Sr, Ti, Tl, W, Y, Zn, Zr
	Q1	Cl, Ca/Sb,Mg, Si, Pb	Al, Ba, C, Ca, K, Li, Mo, Na, Pb, Sb, Zn	Al, Ba, Bi, C, Ca, Cd, Cr, Cu, K, Li, La, Mg, Mn, Mo, Na, Nb, Nd, Ni, Pb, Pr, Rb, Sb, Si, Sr, Ti, Tl, W, Y, Zn, Zr
	Q3	Cl, Ca/Sb,Mg, Al, Si	Al, Ba, C, Ca, K, Li, Mg, Mo, Na, Sb, Sr, Zn	Al, Ba, C, Ca, Cd, Co, Cr, Cu, K, Li, La, Mg, Mn, Mo, Na, Nb, Nd, Ni, Pb, Pr, Rb, Sb, Si, Sr, Ti, Tl, W, Y, Zn, Zr
B	K1, Q2	Cl, Ca/Sb,Mg, Al, Si	Al, Ba, C, Ca, K, Li, Mg, Na, Sb, Si, Sr, Ti, Zn	Al, Ba, Ca, Cd, Cl, Cr, Fe, K, Mg, Na, Pb, Sb, Sn, Sr, Ti, Zn, Zr
	Q1	Cl, Ca/Sb,Mg, Al, Si, Zn, Pb	Al, C, Ca, K, Li, Mg, Mo, Na, Pb, Sb, Si, Ti, Zn	Al, Ba, Ca, Cd, Cl, Fe, K, Mg, Na, Pb, Sb, Sn, Sr, Ti, Zn, Zr
	Q3	Cl, Ca/Sb,Mg, Al, Si, Zn	Al, Ba, C, Ca, K, Li, Mg, Mo, Na, Sb, Si, Sr, Ti, Zn	Al, Ba, Ca, Cd, Cl, Fe, K, Mg, Na, Pb, Sb, Sn, Sr, Ti, Zn, Zr
C	K1, Q2	Cl, Ca/Sb,Mg, Al, Si	Al, Ba, Ca, Cd, Cr, K, Li, Mg, Mo, Na, Sr, Ti	Al, Ba, Ca, Cd, Cl, K, Mg, Na, Pb, Sb, Sn, Sr, Ti, Zn, Zr
	Q1	Cl, Ca/Sb,Mg, Al, Si, Pb	Ca, K, Li, Mo, Na, Pb	Al, Ba, Ca, Cd, Cl, K, Mg, Na, Pb, Sb, Sn, Sr, Ti, Zn, Zr
	Q3	Cl, Ca/Sb,Mg, Al, Si	Al, Ba, Ca, K, Li, Mg, Mo, Na	Al, Ba, Ca, Cd, Cl, K, Mg, Na, Pb, Sb, Sn, Sr, Ti, Zn, Zr
D	K1, Q2	Cl, Ca/Sb,Mg, Al	Al, Ba, C, Ca, K, Li, Mg, Na, Sb	-
	Q1	Cl, Ca/Sb,Mg, Al, Si, Pb	Al, C, Ca, K, Li, Mo, Na, Pb, Sb	
	Q3	Cl, Ca/Sb,Mg, Al	Al, Ba, C, Ca, K, Li, Mg, Mo, Na, Sb	
E	K1, Q2	-	Al, Ba, Ca, K, Li, Mg, Mo, Na, Sb	-
	Q1		Al, Ba, Ca, K, Li, Mo, Na, Pb, Sb	
	Q3		Al, Ba, Ca, K, Li, Mg, Mo, Na, Sb	

4.6.2.2 LIBS

All the tape samples belonging to different rolls (K1 vs. Q1, and K1 vs. Q3) were correctly differentiated by LIBS analysis for interlaboratory #2.

The samples K1 to Q2, which belong to the same roll, were always correctly associated by LIBS.

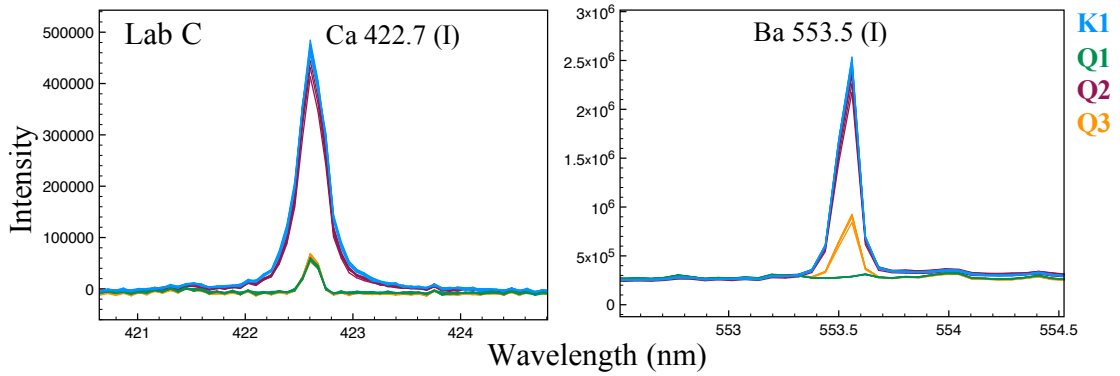

Figure 53 – Spectral overlay comparison by LIBS of K1 vs. Q1, Q2, and Q3 for Lab C for interlaboratory test #2. Sample K1 was differentiated from Q1 and Q3 based on the higher amounts of Ca and Ba in K1.

Figure 53 shows the spectral overlay comparison of K1 vs. Q1, Q2, and Q3 for Lab C for Interlaboratory test #2 for Ca and Ba lines. Sample K1 was differentiated from Q1 and Q3 based on the higher amounts of Ca and Ba in K1. Samples K1 and Q2 were indistinguishable for all the elements examined, these samples belong to the same tape roll (Table 20).

All laboratories performing LIBS analysis compared the samples by spectral overlay. Some laboratories further compared the samples using ±3s, ±4s and ±5s match criteria for the peak area and peak ratios comparisons.

The element lines and ratios selected varied greatly between laboratories. In order to further study the best match criterion, the data obtained from the five different laboratories was re-processed and analyzed in the same manner for all laboratories. Table 27 shows the match criterion results for interlaboratory test #2 for LIBS.

Table 27 – Distinguished ratios by ±5s match criteria comparison for LIBS for interlaboratory test #2.

Tape Pairs	Lab A	Lab B	Lab C	Lab D	Lab E
K1, Q1	Mo/Sb, Ca/Sb, Ca/Mo, Al/Ca, Al/Pb, Pb/Sr, Sr/Zn, Na/Mg, Ba/Li	Mo/Sb, Ca/Sb, Ca/Mo, Al/Ca, Al/Pb, Pb/Sr, Sr/Zn, Na/Mg	Ti/Mo, Ca/Mo, Al/Pb, Ba/Li	Mo/Sb, Ca/Sb, Ca/Mo, Al/Ca, Al/Pb, Na/Mg, Ba/Li, K/Li	Mo/Sb, Ca/Sb, Al/Ca, Na/Mg, Ba/Li
K1, Q2	None	None	None	Na/Mg	None
K1, Q3	Mo/Sb, Ca/Sb, Ca/Mo, Al/Ca, Sr/Zn, Na/Mg, Ba/Li	Mo/Sb, Ca/Sb, Ca/Mo, Al/Ca	Ti/Mo, Ca/Mo, Al/Ca, Na/Mg, K/Li	Mo/Sb, Ca/Sb, Ca/Mo, Al/Ca, Na/Mg, Ba/Li, K/Li	Mo/Sb, Ca/Sb, Ba/Li

Using the proposed match criterion for the comparison of ratios, four out of the five laboratories correctly associated samples K1 and Q2 which belong to the same roll of tape. In the case of laboratory D, the two tapes originating from the same roll were distinguished based on the Na/Mg ratio. Sodium has been found to be detected in tapes due to handling contamination (sweat), which might have caused the false exclusion between K1 and Q2. If Na is removed from the element menu before ratio analysis, the two samples are indistinguishable from each other. Sodium differences found emphasize the importance of selecting a representative element menu that explains the variations between samples due to the manufacturing process of different tapes, and not due to contamination interferences. The match criterion allowed to correctly discriminate the tape samples belonging to different rolls (K1 vs. Q1, and K1 vs. Q3). The element menu obtained by each laboratory for LIBS is shown in Table 26. The elements present were those with a SNR>3.

4.6.2.3 LA-ICP-MS

All the laboratories performing LA-ICP-MS correctly differentiated the tape samples from different rolls (K1 vs. Q1, and K1 vs. Q3).

All laboratories correctly associated K1 to Q2, which belong to the same roll (Table 20).

Figure 54 shows the LA-ICP-MS spectral overlay comparison for Lab B for interlaboratory test #2 using the mass scan mode. Sample K1 was differentiated from Q1 based on their differences in Mo, Sr, Cd, Sn, Cu, and Zn. K1 was distinguished from Q3 based on Mo, Nb, Sr, Cd, Sn, and Cu. K1 and Q2 were not distinguished by LA-ICP-MS, both belong to the same tape roll. The element menu detected (SNR>3) by LA-ICP-MS for interlaboratory test #2 for each laboratory is summarized in Table 26.

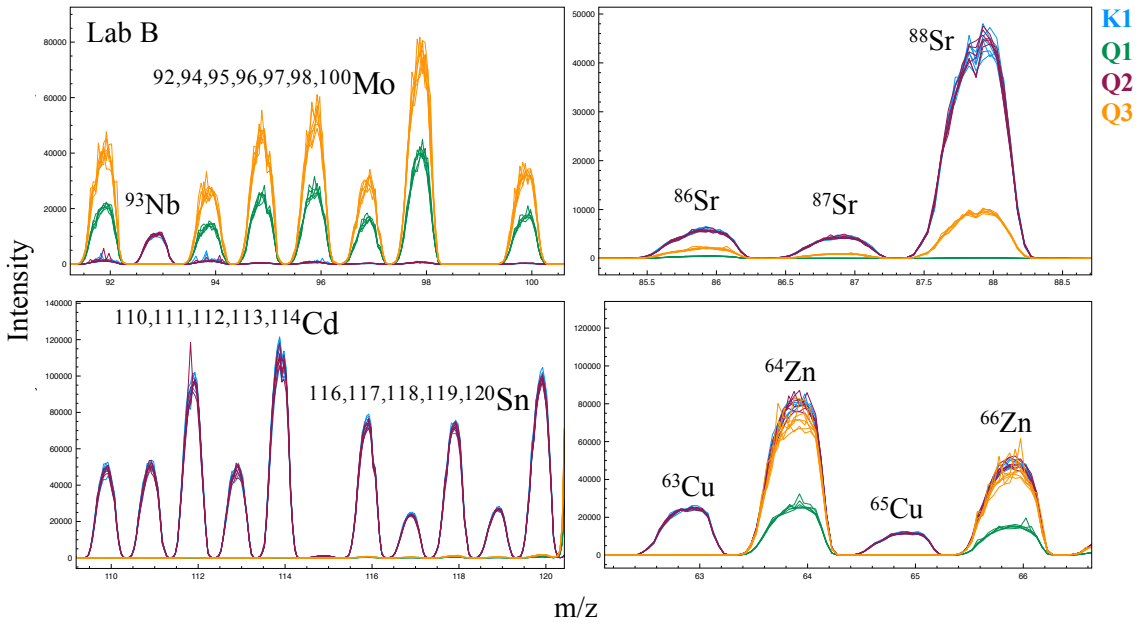

Figure 54 – Spectral overlay comparison for LA-ICP-MS of K1 vs. Q1, Q2, and Q3 for Lab B for interlaboratory test #2. Sample K1 was differentiated from Q1 based on their differences in Mo, Sr, Cd, Sn, Cu, and Zn. K1 was distinguished from Q3 based on differences in Mo, Nb, Sr, Cd, Sn, and Cu.

Using the proposed match criterion (± 5s) for the comparison of integrated signal, all the laboratories performing LA-ICP-MS correctly associated samples K1 and Q2. The method also allowed to correctly discriminate the tape samples belonging to different rolls.

Match criteria comparisons allowed to objectively compare two samples and report the elements that produced the highest variability between sample pairs. The method can be automated to facilitate the comparison between several sample pairs without the need of performing one-to-one spectral overlay comparisons.

Analysis by LA-ICP-MS allowed detecting most of the elements identified by LIBS with the addition of Cl, Co, Cu, Fe, La, Mn, Nb, Nd, Ni, Pr, Rb, Sb, Sn, Sr, Tl, W, Y, Zn and Zr, which were not detected by LIBS due to the lower sensitivity of this method. Similarly to interlaboratory #1, LIBS proved useful in detecting problematic elements for LA-ICP-MS such as Li, Ca, and K.

Table 28 – Distinguished ratios by ±5s match criteria comparison for LA-ICP-MS for interlaboratory test #2.

Tape Pairs	Lab A	Lab B	Lab C
K1, Q1	Al, Ba, Ca, Fe, K, Mg, Pb, Sr, Ti, Zn, Zr	Al, Ba, Ca, Cd, Cr, Fe, K, Mg, Pb, Sb, Sr, Ti, Zn, Zr	Al, Ba, Ca, Cd, K, Mg, Na, Pb, Sr, Ti, Zn, Zr
K1, Q2	None	None	None
K1, Q3	Ca, Fe, Pb, Ti, Zn	Al, Ba, Ca, Cd, Cr, Fe, K, Mg, Na, Pb, Sb, Sr, Ti, Zn, Zr	Ca, Cd, Na, Pb, Ti, Zn

4.7 Conclusions for interlaboratory tests

Two interlaboratory exercises were designed to study the performance of different analytical methods for the forensic analysis of electrical tapes. The exercises simulated forensic case scenarios where known (K) samples are compared to question (Q) samples following the laboratory's analytical scheme.

Two of the laboratories performing SEM-EDS for the first interlaboratory test incorrectly associated two pairs of tapes belonging to different rolls, therefore resulting in

a 16.7% false positives rate. One of the laboratories performing SEM-EDS for interlaboratory test #2 incorrectly associated two pairs of tapes belonging to different rolls, resulting in a 12.5% false positive rate. These false inclusions were the result of the lower selectivity of the method which prevented from detecting differences in calcium and antimony for selected samples, as well as the lower sensitivity of the technique which prevented the detection of elements present in tapes below SEM-EDS detection limits. It is important to clarify that these false positive and false negative rates were calculated for a small number of comparison pairs with the purpose of evaluating the performance of the different instrumental methods for this sample set. A larger set of comparison pairs is needed to fully assess type 1 and type 2 errors. Up to 7 and 8 elements were detected by SEM-EDS for interlaboratory test #1 and #2, respectively.

Elemental analysis of electrical tape backings provided valuable information about the inorganic components added to the formulation of tapes. The increased sensitivity and selectivity of LIBS and LA-ICP-MS methods allowed to always distinguish the pairs of tapes originating from different sources, to correctly associate the tapes belonging to the same rolls, and to increase the characterization of the samples by detecting up to 14 elements by LIBS and 27 elements by LA-ICP-MS for interlaboratory test #1, and 17 elements by LIBS and 32 elements by LA-ICP-MS for interlaboratory test #2.

Elemental analysis alone seems to have informative capability similar to combined organic analytical tools (i.e., IR and Py-GC-MS) with the advantage that analyses are less destructive and faster than Py-GC-MS, therefore it may be used as a fast screening step early in the analytical protocol to reduce backlog.

A match criterion of ±5s allowed to objectively compare LIBS ratios and LA-ICP-MS signal areas. The method proved useful in providing an automated way to show the elements/ratios responsible for the distinction of tapes originating from different sources, as well as confirmation of the level of association for tape samples originating from the same roll.

The informing power, discrimination capabilities, classification potential, and certainty in the identification of elemental components increased with superior sensitivity and selectivity of the methods in the following order SEM-EDS < LIBS < LA-ICP-MS.

Standardized methods currently exist for SEM-EDS, IR and Py-GC-MS. The present study is a first effort towards standardization of the LA-ICP-MS and LIBS analytical and comparison methods. The results show there is good analytical agreement among the participating laboratories. Further developments in the standardization of methods for comparison of spectrochemical data will improve the overall forensic utility of the methods described.

5 ANALYSIS OF PACKAGING TAPES BY LA-ICP-MS AND LIBS

Pressure-sensitive adhesive tapes are often submitted as evidence as they are used for packaging drugs, in the manufacture of improvised explosive devices, to immobilize victims in assault and rape cases, among other criminal activities.

Packaging tapes are usually composed of a backing layer and a pressure sensitive adhesive layer. The backing material for packaging tapes is usually polypropylene, but polyethylene can also be used. There may be colorants, fillers, cross-linkers, plasticizers, stabilizers, and fire retardants added to the polymer.[1] The backing composition varies greatly depending on the type of tape and the manufacturer. Colorants commonly used include titanium dioxide, aluminum oxide, and iron oxide. Antimony trioxide has been used as a flame retardant, and fillers such as calcium carbonate can also be present.[1]

Typically, the investigator is asked to compare a tape fragment found at the crime scene to a tape roll in the possession of a suspect. If the known and question samples belong to different brands or manufacturer, the differences may be clearly observed by the naked eye, microscopy, or molecular spectroscopic techniques.[3-5, 32] However, similar tapes from different sources such as different tapes from the same brand may only be distinguished using more advanced techniques. Different analytical methods have been applied to the analysis of adhesive tapes including XRF[75], SEM-EDS[3-5], Py-GC-MS[2-4, 32, 73], and FTIR[2-4, 32, 73]. SEM-EDS presents limitations in terms of sensitivity for detecting the elements in tapes below detection limits (approximately 1000 ppm). In addition, SEM-EDS has shown selectivity limitations, not being able to detect differences between elements such as antimony and calcium, and barium and titanium.[44] Py-GC-MS is complementary to IR and

allows for the identification of the organic components of tapes, however it is a destructive and time-consuming technique.

Laser Ablation Inductively Coupled Plasma Mass Spectrometry has been previously applied to the analysis of electrical tape, and has been found capable of detecting over 20 elements therefore increasing the characterization and discrimination potential over more conventional elemental analysis methods such as SEM-EDS.[44] In addition, LA-ICP-MS analysis has been used for the analysis of several materials of interest to forensic science such as soils,[76] inks,[53] and glass,[77] providing excellent sensitivity and selectivity with minimum sample preparation and virtually no sample consumption. It is therefore expected that LA-ICP-MS would perform effectively for the analysis of packaging tapes.

Laser Induced Breakdown Spectroscopy is proposed, for the first time, as a fast, sensitive, and selective method for the analysis of packaging tapes. The instrumentation for LIBS is considerably less expensive than LA-ICP-MS systems, and most matrices can be analyzed without the need for a carrier gas such as helium and argon. Laser induced breakdown spectroscopy has been applied to many different solid samples such as automotive paint,[78] glass,[79] soils,[80] printing inks,[53] among others. The potential of LIBS for forensic analyses lies on the simplicity of its operation, speed, and the minimal destruction of the samples. In addition, multiple emission lines can be used for each element, therefore increasing its confirmatory value.

The present study aims to test the performance of LIBS for the characterization, association and discrimination of packaging tape samples originating from Asia (see Table 29 for the list of samples). Laser ablation inductively coupled plasma mass spectrometry

is compared to LIBS for the elemental analysis of eight packaging tape samples. The current work includes the method development and optimization for both techniques, as well and the element menu obtained for the sample set under study. Spectral overlay comparisons were used to determine any differences between the tapes as previously reported by our group.[53] Principal component analysis of the multivariate data was used to visualize the groupings obtained by both techniques for samples known to originate from different sources. Duplicate tape samples were analyzed on separate days to assess the capabilities of both methods to generate correct associations.

The lack of matrix-matched quantitative standards required a normalization strategy in order to compare the tape samples for the LIBS results. The normalization strategy consists of normalization of each spectrum to the entire emission intensity followed by the integration of the area under selected peaks of the elements of interest. The normalization strategy has been found useful for the analysis of inks and electrical tapes.[44, 53] A normalized spectrum produced an improvement in both between-replicate repeatability and inter-day reproducibility across the mass regions of interest for the mass spectrometry application.[53] Internal normalization (normalization to a single element line) remains the most popular method for the normalization for LIBS data, however the internal normalization method requires that the element of interest must be the same concentration in all the samples.[81] An alternative would be to have different concentrations of the internal standard element line where these different concentrations are known. In the case of this sample set, the concentrations of elements are not known and therefore signal intensity normalization was used instead.

5.1 Instrumentation and measurement parameters

The analysis by LA-ICP-MS was performed using a quadruple ELAN DRC II (Perkin Elmer LAS, Shelton CT USA) ICP-MS coupled to a ns-Nd:YAG laser (NW UP213, New Wave, California). Data was acquired in mass scan mode scanning from m/z ^{7}Li to m/z ^{238}U. The final element list was reduced to 18 elements that were found to be relevant for the characterization of the backing components. Spectral regions that were anticipated to have large contribution from Ar isotopes and other polyatomic interferences were excluded from the scanning method. The measurements parameters for LA-ICP-MS were adapted from previous work performed on the backing of electrical tapes,[44] with minor changes in the energy of the laser to prevent contamination from the adhesive layer due to excess penetration of the laser into the backing layer.

The analysis by laser induced breakdown spectroscopy was performed using a commercial LIBS system (J200, Applied Spectra, Freemont, CA) consisting of a ns-Nd:YAG 266 nm laser coupled to a CCD detector. The optimization for LIBS was performed to account for the best signal to noise ratio (SNR), smaller percent RSD, while adjusting the laser energy to prevent contamination from the adhesive layer. The statistics analysis software JMP was utilized to create the most efficient design of experiment prior to optimization. Design of experiment was used and an automated method to assess the impact of each parameter in the resulting output, as well as determining the combination of parameters that offers the best analytical results. A random series of experiments composed of different parameter values were conducted to determine the combination that accounted for maximizing the Signal to Noise Ratio (SNR) and minimizing the Relative

Standard Deviation (% RSD). Table 30 shows the optimum instrumental parameters for LA-ICP-MS and LIBS.

Table 29 – Packaging tapes sample set information.[43]

Sample No.	Sample Name	Manufacturer	Country	Barcode
1	No.141	Teraoka	Japan	4964833141506
2	No.1532	Teraoka	Indonesia	4964833153257
3	No.102N	Nichiban	Japan	4987167029418
4	No.123	Nichiban	Japan	4987167029906
5	No.600V	Sekisui	Japan	4901860184625
6	No.357	Rinrei	Japan	4951107030215
7	No.750	Nito	Japan	4562168980014
8	No.3375	Sliontec	Indonesia	4961068001094

Table 30 – Optimized parameters for LA-ICP-MS and LIBS for packaging tape analysis.[43]

LA-ICP-MS Mass Scan		LIBS	
Laser	ns–Nd:YAG (213 nm)	Laser	ns-Nd:YAG (266 nm)
Energy	80% (0.6 mJ)	Energy	80% (19 mJ)
Stage Speed	40 µm/s	Stage Speed	1 mm/s
Spot Size	190 µm	Spot Size	100 µm
Frequency	10 Hz	Frequency	10 Hz
Ablation Mode	Line	Ablation Mode	Line
Line Length	~4 mm	Line Length	~20 mm
Spectrum Range	m/z 7 to m/z 238	Spectrum Range	180 nm to 1045 nm
Sweeps/Reading	40	Gate Delay	0.5 µs
Readings/Replicate	1	Shots	204
Carrier Gas	Helium (0.9 L/min)	Medium/Gas	Air

5.2 Sample collection and sample preparation

The sample set consisted of eight packing tapes purchased in Japan on 2016, comprising two different countries of origin and six different manufacturers (Table 29).

The tape rolls were extended, and the first 20 cm of the rolls were discarded to avoid contamination. The tape samples were placed on transparency films (Apollo, Acco Brands) and stored inside plastic protectors. Prior to LA-ICP-MS and LIBS analyses, a piece of ~1 cm by 2 cm of tape was cut and placed directly in the ablation chamber.

In the case of LIBS, seven replicates were analyzed for each 1 cm by 2 cm piece of tape for both the sample and the duplicate. In the case of LA-ICP-MS, six replicates were analyzed for each 1 cm by 2 cm piece of tape, and three replicates were analyzed for the duplicate samples. The duplicate samples consisted of another 1 cm by 2 cm tape fragment taken from a different location of the tape roll.

5.3 Data reduction and data analysis

Data reduction and statistical analyses were performed using Excel 2011 (version 14.6.1, Microsoft Corporation), JMP (version 12.0.0, SAS Institute Inc., NC), Plot2 for Mac (version 2.0.8, Berlin, Germany), and the Aurora software for LIBS data integration and peak identification.

5.3.1 Data pre-processing

Data pre-processing for LA-ICP-MS included the removal of non-relevant mass-to-charge peaks originating from polyatomic and isobaric interferences[53] and normalization to the sum of the mass spectrum intensities to account for any laser shot-to-

shot variation and/or inter-day variations and as a mean to compensate for mass removal differences between replicates. In the absence of an internal standard, this normalization strategy accounts for small differences in the ablated mass between samples and improves both repeatability and reproducibility.[43] All of the emission lines selected for LIBS were confirmed by checking the presence, and abundance, of more two or more emission lines for each element. The emission lines selected were those with no known interferences, smaller percent RSD, and larger SNR.

5.4 Comparison methods

Comparisons between samples, and between techniques, were performed by spectral overlay, principal component analysis, and by applying three different comparison criteria. The three comparison criteria used consisted of range overlap, $K_{mean} \pm 4s$, and $K_{mean} \pm 5s$, where the K_{mean} represents the average of the sample in comparison and s is the standard deviation of the sample (n = 7).

5.4.1 Spectral overlay

Comparison between samples was performed by spectral overlay as previously reported by our group.[43-44, 53] Overlay comparisons were conducted using Plot2 (version 2.0.8). In order to prevent bias in spectral overlay match decisions, the spectra were analyzed as a blind set by a second analyst.

Relative natural abundance of different isotopes was used to confirm the identification of each element for the LA-ICP-MS data. The presence or absence, and the relative peak height of different emission lines were used to confirm the identification of each element for the LIBS data. The overlay comparisons accounts for variability within

replicate measurements, which include instrumental variations and compositional variations in the sampled locations.[44]

5.4.2 Principal components analysis

In addition to spectral overlay, principal component analysis (PCA) was performed on the integrated peak areas for both techniques for visualization of the grouping between samples. The two-components PCA graphs were constructed using the software JMP (version 12.0.0, SAS Institute Inc., NC). The PCA plots for LA-ICP-MS included the following isotopes: ^{27}Al, ^{53}Cr, ^{57}Fe, ^{178}Hf, ^{24}Mg, ^{93}Nb, ^{121}Sb, ^{64}Zn, and ^{90}Zr. The PCA graph for LIBS data included the following emission lines: Ca (422.7 nm), Cr (520.6 nm), K (766.5 nm), Li (670.8 nm), Na (589.0 nm), Ti (334.9 nm), and Zn (481.1 nm).

5.4.3 Comparison criteria

In an effort to numerically compare the elements in the sample set, different comparison criteria were considered. The three comparison criteria used consisted of range overlap, $K_{mean} \pm 4s$, and $K_{mean} \pm 5s$, where the K_{mean} represents the average of the sample in comparison and s is the standard deviation of the sample (n = 7). If the average of the sample in question falls within ±4s or 5s of the sample in comparison, the two samples are determined to be indistinguishable from each other.

Signal intensity normalization followed by the integration of the area under selected peaks of the elements of interest was applied to the data used for numerical comparison. Signal intensity normalization was selected based on the success of this method for the normalization of mass spectrometry data previously reported by our group.[53]

5.5 Results and discussion

The results were separated by the different techniques: LA-ICP-MS and LIBS. The samples for each technique were compared by spectral overlay and by the different match criteria.

5.5.1 LA-ICP-MS results

Spectral overlay comparisons were performed to LA-ICP-MS data to estimate the grouping and element menu for each tape sample. LA-ICP-MS improved sensitivity and selectivity allows for a more complete characterization that provides confirmatory value to LIBS results. Therefore, LA-ICP-MS was compared to LIBS in terms of correct association, discrimination, and characterization capabilities.

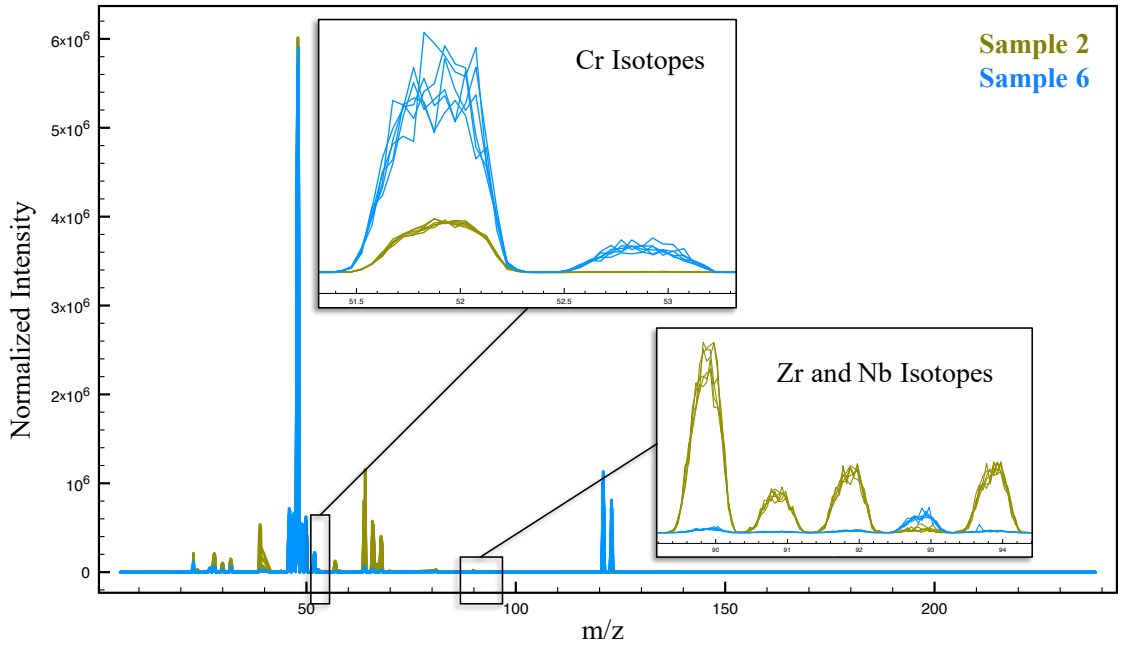

Figure 55 – Spectral overlay comparison by LA-ICP-MS for samples (Teraoka, Indonesia) and 6 (Rinrei, Japan) showing the differences in Cr and Zr.[43]

Analyses by LA-ICP-MS were performed using the parameters shown in Table 30. Six replicate measurements were taken for each sample. Figure 55 shows the spectral overlay comparison between samples 2 and 6. These samples were differentiated based on the significantly higher amounts of chromium in sample 6, and the higher amounts of zirconium in sample 2, as well as their differences in the zinc and antimony isotopes. Sample 2 corresponded to a Teraoka packaging tape manufactured in Indonesia, and sample 6 corresponded to a Rinrei packaging tape manufactured in Japan. Figure 56 shows the spectral overlay comparison between sample 5 (Sekisui, Japan) and sample 8 (Sliontec, Indonesia). Although these two tapes presented more similar elemental patterns, they were differentiated by LA-ICP-MS by the higher amounts of iron in sample 5 and the higher amounts of Niobium (Nb) in sample 8.

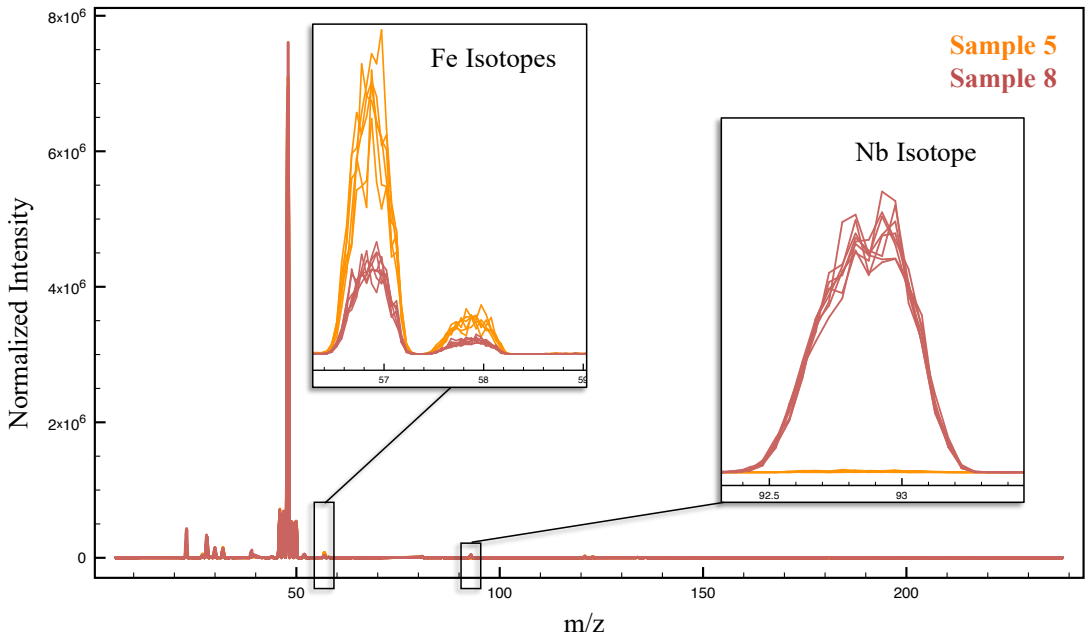

Figure 56 – Spectral overlay for LA-ICP-MS for the comparison of samples 5 (Sekisui, Japan) and 8 (Sliontec, Indonesia) showing the main differences in Fe and Nb.[43]

Figure 57 shows the spectral overlay comparison between samples 1 (Teraoka, Japan), 4 (Nichiban, Japan), and 7 (Nito, Japan). Sample 1 was distinguished from 4 and 7 based on the higher amounts of zinc present in sample 1 (Figure 57). Sample 7 was distinguished from 1 and 4 based on the higher amounts of zirconium in sample 7. These three samples presented a very similar elemental pattern by LA-ICP-MS; they were distinguished from each other by only one or two elements. Figure 57 also shows that lithium could not be detected by LA-ICP-MS (SNR<3).

The detection of eight distinctive groups from the eight samples was achieved by LA-ICP-MS.

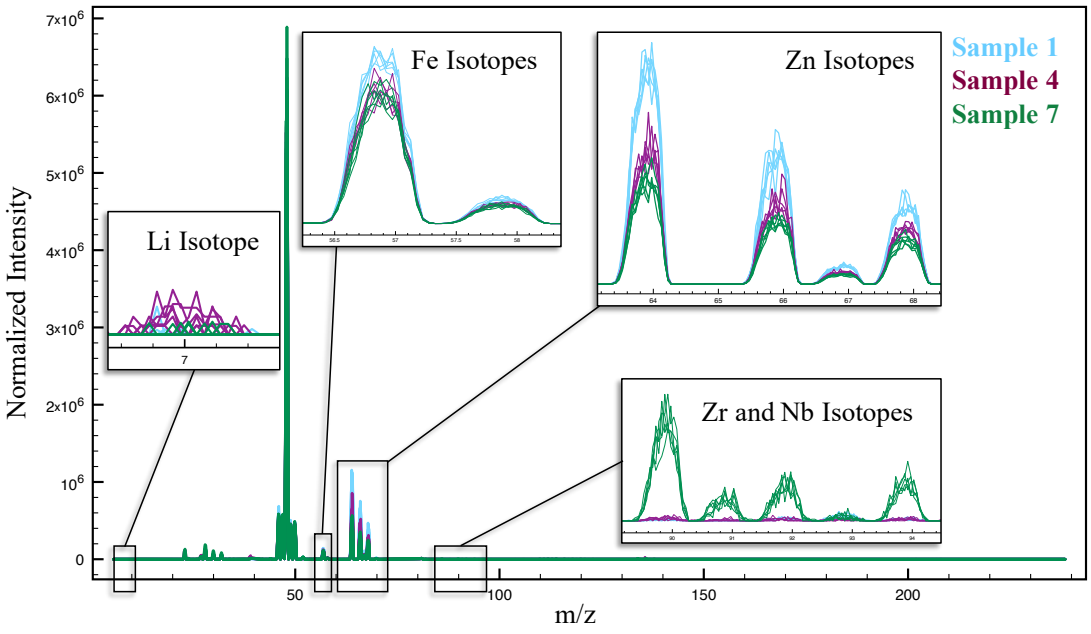

Figure 57 – Spectral overlay comparison by LA-ICP-MS for samples 1 (Teraoka), 4 (Nichiban) and 7 (Nito) manufactured in Japan showing the Li, Fe, Zn and Zr isotopes. Samples 1 and 4 were both distinguished from sample 7 based on zirconium. Lithium was not detected by LA-ICP-MS with a SNR>3 for any of the three samples.[43]

A set of duplicate samples was analyzed months apart to assess the association capabilities of LA-ICP-MS for the analysis of packaging tapes. All the eight samples

duplicates were indistinguishable from their originals analyzed on different months for all the monitored elements.

5.5.2 LIBS results

Spectral overlay comparisons were performed to LIBS results to estimate the grouping and element menu for each tape sample. The spectra were compared to each other, and to the respective duplicate, by examining the presence and abundance of the selected element lines and two or more lines for element. In addition, spectral overlay comparisons allowed to determine the element menu obtained by LIBS for the set of packaging tapes under study.

Analyses by LIBS were performed using the Aurora software for peak integration and peak identification. Seven replicate measurements were performed for each sample using the parameters shown in Table 30. Prior to spectral overlay comparisons, LIBS spectra were normalized to the entire emission intensity for each sample. Figure 58 shows the spectral overlay comparison for sample 3 and its duplicate analyzed days apart, before (left) and after (right) normalization. A normalized spectrum produced an improvement in both between-replicate repeatability and inter-day reproducibility.

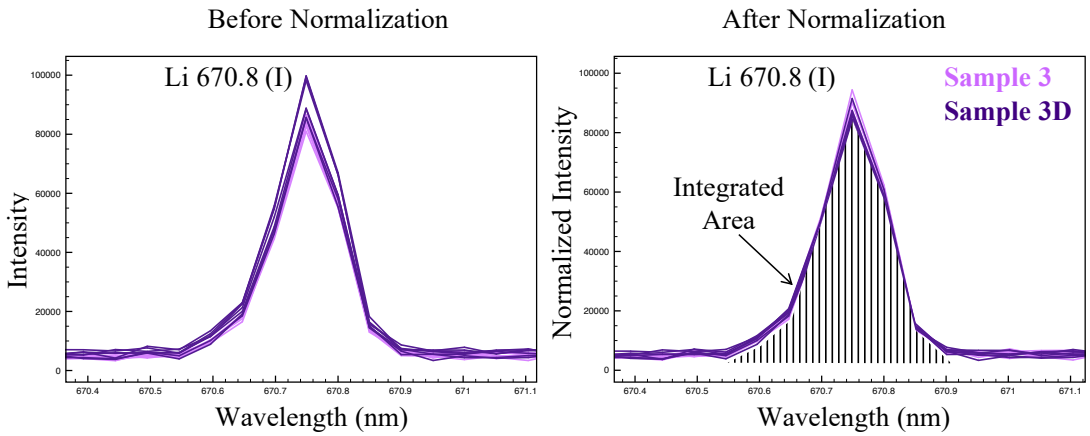

Figure 58 – Spectral overlay comparison for sample 3 and its duplicate before (left) and after (right) normalization.[43]

Figure 59 shows the spectral overlay of samples 2 (Teraoka, Indonesia) and sample 6 (Rinrei, Japan). The two samples were clearly distinguished from each other by their differences in chromium, lithium, iron, and zinc. These samples were distinguished by the same elements by LA-ICP-MS with the exception of lithium, which was not observed in the ICP-MS analyses.

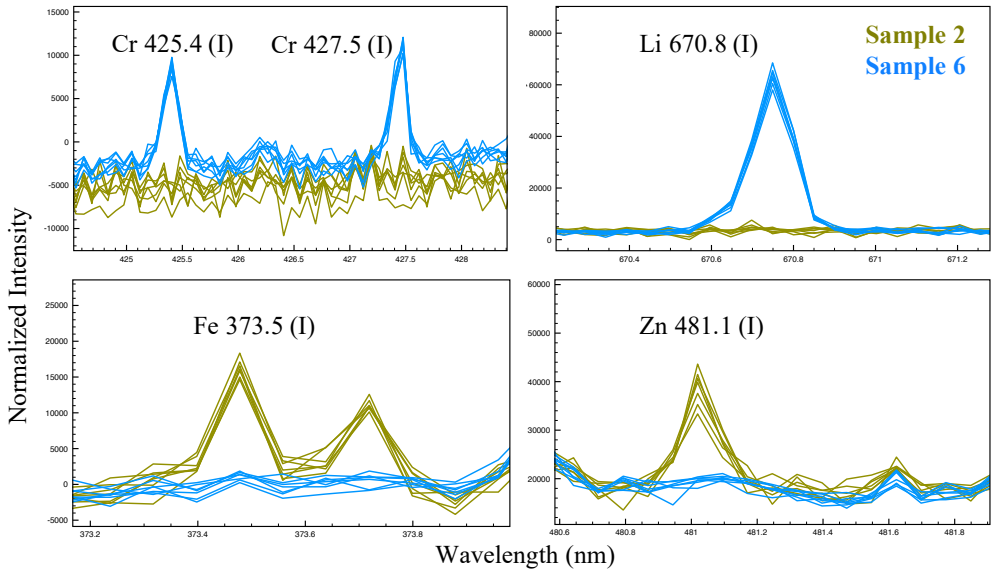

Figure 59 – Spectral overlay comparison by LIBS for samples 2 (Teraoka, Indonesia) and 6 (Rinrei, Japan) showing the main differences in the Cr, Li, Fe, and Zn.[43]

Figure 60 shows the spectral overlay of samples 1 (Teraoka, Japan), 4 (Nichiban, Japan), and 7 (Nito, Japan). Sample 4 was distinguished from samples 1 and 7 based on lithium. Samples 1 and 7 were discriminated from each other based on zinc. However, zinc is the only element that is different between samples 1 and 7, and the differences are small. Additional measurements from different sections of the tape roll would help to further evaluate the variation of the Zn content between and within the samples.

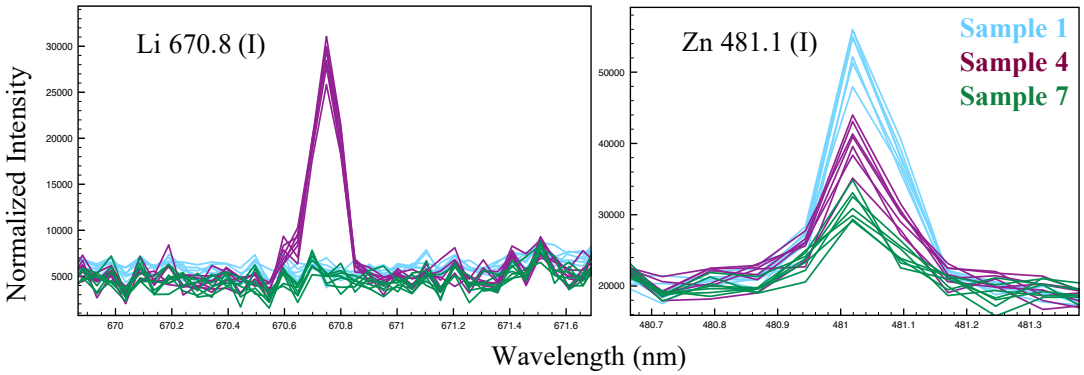

Figure 60 – Spectral overlay comparison by LIBS for samples 1 (Teraoka), 4 (Nichiban) and 7 (Nito) showing the differences in Li and Zn.[43]

Figure 61 shows the spectral overlay for samples 5 (Sekisui, Japan) and 8 (Sliontec, Indonesia). These tapes were not distinguished from each other by LIBS.

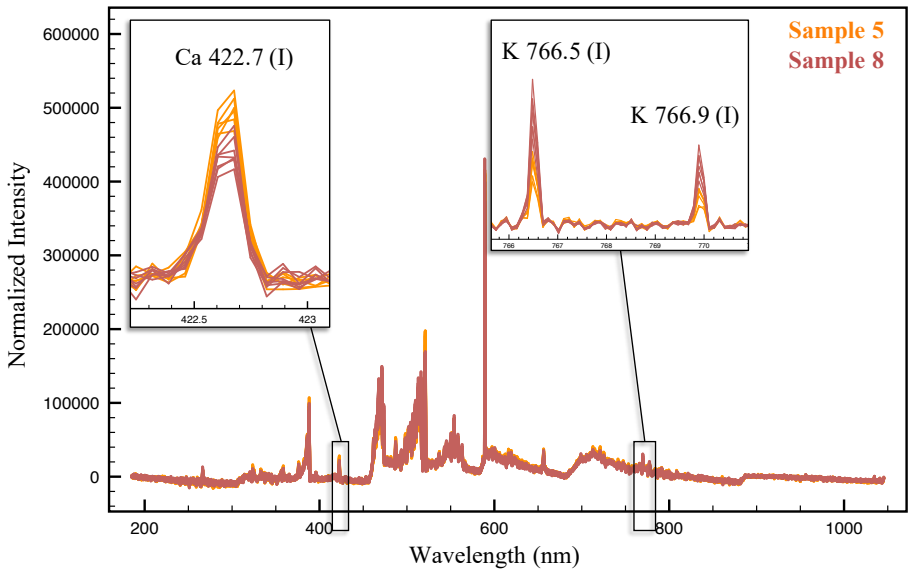

Figure 61 – Spectral overlay comparison by LIBS for samples and 8. These two samples were not distinguished from each other by LIBS.[43]

A set of duplicate samples was analyzed days apart to assess the association capabilities of LIBS for the analysis of packaging tapes. All the duplicates for the eight samples were indistinguishable when analyzed on different months for all the monitored elements.

From the eight samples in this sample set, seven distinctive groups were found by LIBS. Samples 5 and 8 constituted the only pair that was not discriminated.

5.5.2.1 Normalization strategy and numerical comparison criteria

Due to a lack of matrix-matched quantitative standards, a normalization strategy was used to compare the tape samples for the LIBS results. The normalization strategy consists of normalization of each spectrum to the entire emission intensity followed by the integration of the area under selected peaks of the elements of interest (7 elements, 1 integrated area per element) (Figure 58).

The resulting data obtained after the integration allowed applying different match criteria for the numerical comparison of each packaging tape sample. The match criteria under comparison included range overlap, $K_{mean} \pm 4s$ and $K_{mean} \pm 5s$, in addition to spectral overlay.

The duplicate samples where compared to the originals by the match criteria using the same normalization technique, and without any normalization. When the spectrum or peak areas were not normalized, samples 3 and its duplicates and 5 and its duplicates were distinguished from each other by 5s comparison criteria. When the spectrum is normalized all the duplicates were undistinguished from the original for all elements by 5s comparison criteria. When using range overlap, sample 5 was differentiated from its duplicate based on the potassium lines. Range overlap does no account for the variation within the samples, as opposed to 4s and 5s. In the presence of outliers, range overlap might incorrectly associate two samples that are otherwise different. For the analysis of tapes using LIBS, 5s was found to be more suitable as 4s was not appropriate for the reproducibility and repeatability of LIBS measurements.

In the same manner, each sample was compared to each other using the same comparison criteria before and after normalization. After normalization, the grouping corresponded to the one found by spectral overlay, where samples 5 and 8 were not distinguished from each other. All the other sample pairs were discriminated except from 5 and 8. Prior to normalizing the data, several samples pairs were not distinguished from each other by the match criteria under study. Examples of pairs that were not distinguished but that belong to different groups include samples 1 and 2, 1 and 7, 2 and 5, and 2 and 8.

These pairs of samples were distinguished from each other by spectral overlay, and in most cases by more than one element. As expected, normalization of the spectra reduced the variation between replicates, therefore decreasing the comparisons limits.

Table 31 – Distinguished elements using ±5s match criteria before and after normalization for LIBS, and spectral overlay comparison for both LIBS and LA-ICP-MS.[43]

	LIBS			LA-ICP-MS
Comparison Pairs	± 5s Comparison Criteria		Spectral Overlay	Spectral Overlay
	Before Normalization	After Normalization		
1 vs. 4	K, Li, Na, Zn	Li, Ti	Li	Zn
1 vs. 7	K, Na, Zn	Zn	Zn	Zn, Zr
2 vs. 6	Cr, K, Li	Ca, Cr, K, Li, Zn	Ca, Cr, K, Li, Zn	Cr, Fe, Hf, K, Nb, Sb, Ti, Zn, Zr
5 vs. 8	None	None	None	Nb, Fe, Zr

Table 31 shows the differentiated elements before and after normalization for the sample pairs 1 vs. 4, 1 vs. 7, 2 vs. 6, and 5 vs. 8. These samples were selected because they represent good examples of undistinguishable (5 vs. 8), similar (1 vs. 4 vs. 7), and dissimilar (2 vs. 6) tapes. Both, spectral overlay and the normalized comparisons for LIBS, agree in the grouping of samples 5 and 8 together.

5.5.3 LIBS and LA-ICP-MS comparison

Multivariate analysis was performed to visualize the complementarity between LA-ICP-MS and LIBS to group the eight packaging tape samples according to their elemental composition. PCA graphs were constructed for both techniques using two principal components and the selected element isotopes or emission lines.

The PCA plot of LA-ICP-MS data (Figure 62 left) shows two main groups of more than one sample: the first group consisting of samples 1, 4 and 7 and the second group consisting of samples 5 and 8. The rest of the samples were grouped individually. Samples

5 and 8 were discriminated based on niobium, iron and zirconium by spectral overlay (Figure 56). Samples 1, 4 and 7 were separated from each other by spectral overlay based on zinc and zirconium (Figure 57).

In the case of LIBS (Figure 62 right), samples 5 and 8 grouped together in the PCA plot and they were also not differentiated based on spectral overlay (or by any other comparison criteria). Samples 1, 4 and 7 grouped closer in the PCA plot as they present similar elemental patterns. However, the detection of lithium on sample 4 allowed separating this sample from samples 1 and 7. For both LA-ICP-MS and LIBS, samples 3 and 6 were completely separated from the rest of the groups.

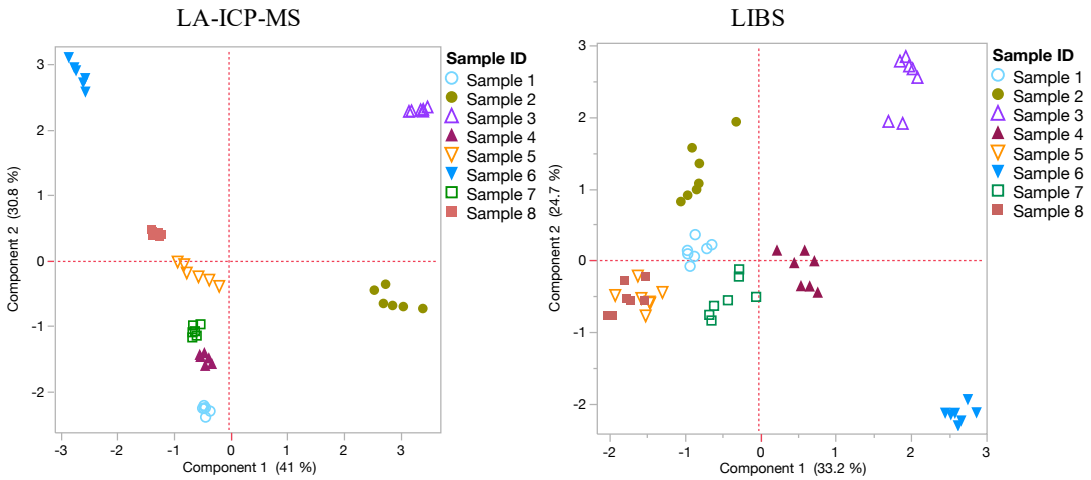

Figure 62 – Principal component analysis plot of LA-ICP-MS (left) and LIBS (right) showing the grouping by both techniques.[43]

Principal component analysis assisted in understanding the grouping by both techniques, and the complementarity of LIBS to LA-ICP-MS. The elements responsible for the highest variability included hafnium, niobium, and zirconium for the first principal component, and iron and zinc for the second principal component. It is interesting to notice the similarities of both techniques in grouping closer samples 5 and 8, and 1, 4 and 7.

However, because of the higher sensitivity of LA-ICP-MS samples such as 1 and 2, and 5 and 8 were more separated due to the detection of elements such as antimony, iron, niobium and zirconium by ICP-MS. These elements are not easily observed by LIBS. Likewise, because of the superiority of LIBS to detect good emitters such as lithium, sodium, and potassium, sample 4 could be separated from samples 1 and 7 based on lithium.

5.5.4 Discrimination potential and complementarity

The discrimination potential for both techniques was assessed using the spectral overlay comparison criterion. LA-ICP-MS allowed for the individual separation of the eight samples, while LIBS found seven distinctive groups. Samples 5 and 8 were not distinguished by LIBS due to the inability of LIBS to detect elements such as niobium, iron, and zirconium in this set of packaging tapes.

Table 32 shows the grouping found by LA-ICP-MS and LIBS using spectral overlay comparison and the element menu detected by each technique. LA-ICP-MS was able to detect up to 10 elements and LIBS was able to detect 7 elements, including lithium, potassium and sodium, which are problematic elements for LA-ICP-MS but very good emitters for LIBS. By combining both techniques, the element menu increased to 12 elements, with the addition of lithium and sodium. Potassium was additionally found in most samples by LIBS, and only detected in sample 6 by LA-ICP-MS. However, sodium and potassium must be carefully monitored in casework as they have shown to be present due to contamination from hand sweat.[53]

Table 32 – Grouping obtained for LIBS and LA-ICP-MS, and elements detected for each sample of packaging tape.[43]

LA-ICP-MS			LIBS		
Groups	Sample ID	Elements Detected	Groups	Sample ID	Elements Detected
I	1	Al, Fe, Ti, Zn	I	1	Ca, K, Na, Ti, Zn
II	2	Al, Fe, Hf, Ti, Zn, Zr	II	2	Ca, K, Na, Ti
III	3	Al, Fe, Hf, Ti, Zn, Zr	III	3	Ca, K, Li, Na, Ti
IV	4	Al, Fe, Ti, Zn	IV	4	Ca, Li, Na, Ti
V	5	Al, Fe, Ti	V	5, 8	Ca, K, Na, Ti
VI	6	Al, Cr, Fe, K, Nb, Sb, Ti, Zn			
VII	7	Al, Fe, Ti, Zn, Zr	VI	6	Ca, Cr, K, Li, Na, Ti
VIII	8	Al, Fe, Nb, Ti, Zr	VII	7	K, Na, Ti
Total Number of Elements		10 (Al, Cr, Fe, Hf, K, Nb, Sb, Ti, Zn, Zr)	Total Number of Elements		7 (Ca, Cr, K, Li, Na, Ti, Zn)

Relative standard deviation (RSD) percentages were calculated for both LIBS and LA-ICP-MS using either six or seven replicate measurements for each sample by both techniques. The percent RSD values were calculated using the integrated area under the element line (LIBS) or isotope (LA-ICP-MS) of interest. For both LA-ICP-MS and LIBS the percent RSD values were below 10%.

5.6 Conclusions for the analysis of packaging tapes by LA-ICP-MS and LIBS

The methods for LIBS and LA-ICP-MS were developed and optimized for the analysis of packaging tapes. The use of LIBS is reported for the first time for the analysis of packaging tape backings tapes. The sample set under study consisted of eight packaging tapes originating from Asia comprising six different manufacturers and two countries of origin. The results by LA-ICP-MS were used to compare to LIBS results, for the same set of samples. The analysis by LA-ICP-MS allowed separation of all the samples from each other. The analysis by LIBS was not able to distinguish between samples 5 and 8, which

were separated by LA-ICP-MS based on niobium, iron and zirconium. A total of 10 elements with a SNR>3 was detected by LA-ICP-MS. The element menu obtained by LIBS consisted of up to 7 elements, including lithium, potassium and sodium, which were not easily detected by LA-ICP-MS.

Signal intensity normalization was applied to the LIBS data to account for the variability between the measurements due to instrumental sources. Signal intensity normalization provided the best reproducibility and repeatability for this sample set.

The use of ±5s comparison criteria allowed to numerically compare the tape samples without the potential subjectivity of the spectral overlay method. The comparison criterion of ±5s produced the lowest error rates for the comparison of packaging tapes for the selected elements.

The results show the potential of LIBS for the analysis and comparison of adhesive tapes, and possibly other types of polymer materials. Laser induced breakdown spectroscopy represents an attractive alternative to the well-established LA-ICP-MS due to its operation simplicity, less expensive instrumentation, and its ability to analyze problematic elements to ICP-MS such as lithium and potassium.

The present work was used as a proof of concept for the utility of LIBS for the analysis of tapes, as well as a preliminary study of the complementary of LIBS and LA-ICP-MS for this type of samples. A more extensive sample set would be needed to fully validate LIBS for its use in tape analysis.

6 OVERALL CONCLUSIONS

A novel LA-ICP-MS method was developed, optimized and evaluated for the chemical characterization and comparison of electrical tape backings. The results showed the ability of LA-ICP-MS to improve the comparison capabilities for the analysis of electrical tapes. The homogeneity studies in the tapes showed that the intra-roll elemental variation was smaller than the inter-roll variation. The optimization of the penetration depth accounted for the ablation of representative material without contamination from the adhesive layer. The backings of 90 black electrical tapes were analyzed using LA-ICP-MS and the ability of the method to distinguish samples from different origin was evaluated by calculating the percentage of discrimination. The discrimination for the LA-ICP-MS analysis of the 90 samples was found to be 93.9%, which was greater than the discrimination power found using SEM-EDS (87.3%). Moreover, 100% correct association resulted for the 129 duplicate control samples evaluated in the present study.

The greater sensitivity of LA-ICP-MS provided improved discrimination over SEM-EDS and offered enhanced characterization of the tapes by detecting over 25 elements, most of which could not be detected by SEM-EDS. The discrimination between tapes originating from different sources is improved through LA-ICP-MS, and this method could be used to complement to organic methods for a full characterization of the tape samples.

The fast analysis capabilities and minimal sample destruction of this laser-based technique makes it attractive for the analysis of tape evidence. The increased sensitivity and selectivity of the LA-ICP-MS method provided enhanced discrimination and a more

complete characterization of the backing of electrical tape samples, making the method amenable to the development of a classification scheme of tape groups (possibly by country or by manufacturer) to support investigations.

Two quantitative methods were developed for the analysis of tapes and other polymers. In order to test the performance of the quantitative methods, polyethylene films made of certified reference materials were created. The first method consisted of an external calibration curve using poly-vinyl acetate (PVA) solutions at different concentrations ranging from 0 ppm to 300 ppm. Five calibration points were created; the linearity of the curves, percent bias, and percent RSD were used to test the performance of this method. Due to lack of internal standard in the tape and PVA samples, gold was used as a normalization standard by coating all the samples using a sputtering system. Carbon (^{13}C) was additionally evaluated as an internal standard for this method.

The second procedure to determine the concentrations of the elements present in tapes and plastics consisted of the quantitative method without matrix-matched standards. In the quantitative method without matrix-matched standards, the concentrations in an unknown solid can be found by using a known or standard solid to calculate a response factor specific to each isotope.

The accuracy of the method was tested using the different solid glass and plastic standards. The percent bias for the NIST 610 glass standard was found to be below 10% for most of the elements under study; the bias for the BCR-680 polyethylene plastic using ERM®-EC681m polyethylene plastic resulted in less than 10% for most elements under study.

Tape concentrations were measured using ERM®-EC681m polyethylene as a known standard and were found to be: 4 ± 1 ppm for As, 2104 ± 318 ppm for Cd, 39 ± 6 ppm for Cr, 5 ± 1 ppm for Pb, 37 ± 5 ppm for Sb, and 1796 ± 270 ppm for Zn.

These quantitative methods can help in creating and populating databases which can lead to the use of likelihood ratios and the development of standard methods of analysis and interpretation for tape evidence. These methods also have the potential to be used for different types of solids without the need to conduct acid digestions.

The method of analysis for LIBS was developed for electrical tape backings. Design of experiment was used for the optimization of the LIBS instrumentation for the analysis of tapes. Different factors were using for the experimental design: energy, gate delay, stage speed, and frequency.

The best parameters were those that provided a good compromise between maximizing the SNR, minimizing the percent RSD, and preventing the laser beam penetration into the adhesive layer of the tapes. The optimized parameters accounted for a penetration of about 50% into the backing of the thinnest tape in the collection (~83 μm).

A set of 90 electrical tapes previously examined by LA-ICP-MS was analyzed by LIBS using the optimized parameters. Fifty (50) groups were found by LIBS analysis, which was the same number of distinctive groups found by LA-ICP-MS. Additionally, LIBS allowed to separate some pairs of tapes that were not previously distinguished by LA-ICP-MS by detecting differences in lithium, calcium, and potassium. These elements are problematic in ICP-MS analysis, but typically really good emitters in optical spectroscopic techniques such as LIBS. Although the element menu for LIBS was found

to be smaller than of LA-ICP-MS, elements such as lithium, sodium and potassium were added to the characterization of specific samples when combining both techniques.

The tandem analysis of LIBS and LA-ICP-MS provides excellent characterization of the samples in a matter of seconds. The tandem analysis would greatly benefit the forensic community by reducing the analysis time and destruction of the samples, while obtaining improved characterization of the samples by detecting up to 14 elements by LIBS, and up to 29 elements by LA-ICP-MS.

Two interlaboratory exercises were designed to study the performance of different analytical methods for the forensic analysis of electrical tapes. The exercises simulated forensic case scenarios where known (K) samples are compared to question (Q) samples following the laboratory's analytical scheme.

Two of the laboratories performing SEM-EDS for the first interlaboratory test incorrectly associated two pairs of tapes belonging to different rolls, therefore resulting in a 16.7% false positives rate. One of the laboratories performing SEM-EDS for interlaboratory test #2 incorrectly associated two pairs of tapes belonging to different rolls, resulting in a 12.5% false positive rate. These false inclusions were the result of the lower selectivity of the method which prevented from detecting differences in calcium and antimony for selected samples, as well as the lower sensitivity of the technique which prevented the detection of elements present in tapes below SEM-EDS detection limits. Up to 7 and 8 elements were detected by SEM-EDS for interlaboratory test #1 and #2, respectively.

Elemental analysis of electrical tape backings provided valuable information about the inorganic components added to the formulation of tapes. The increased sensitivity and selectivity of LIBS and LA-ICP-MS methods allowed to always distinguish the pairs of tapes originating from different sources, to correctly associate the tapes belonging to the same rolls, and to increase the characterization of the samples by detecting up to 14 elements by LIBS and 27 elements by LA-ICP-MS for interlaboratory test #1, and 17 elements by LIBS and 32 elements by LA-ICP-MS for interlaboratory test #2.

Elemental analysis alone seems to have informative capability similar to combined organic analytical tools (i.e., IR and Py-GC-MS) with the advantage that analyses are less destructive and faster than Py-GC-MS, therefore it may be used as a fast screening step early in the analytical protocol to reduce backlog.

A match criterion of ±5s allowed to objectively compare LIBS ratios and LA-ICP-MS signal areas. This method proved useful is providing an automated way to show the elements/ratios responsible for the distinction of tapes originating from different sources.

Standardized methods currently exist for SEM-EDS, IR and Py-GC-MS. The present study is a first effort towards standardization of the LA-ICP-MS and LIBS analytical and comparison methods. The results show there is good analytical agreement among the participating laboratories. Further developments in the standardization of methods for comparison of spectrochemical data will improve the overall forensic utility of the methods described.

The methods for LIBS and LA-ICP-MS were developed and optimized for the analysis of packaging tapes. The use of LIBS is reported for the first time for the analysis

of packaging tape backings. The sample set under study consisted of eight packaging tapes originating from Asia comprising six different manufacturers and two countries of origin. LA-ICP-MS results were used to compare to LIBS results, for the same set of samples. The analysis by LA-ICP-MS allowed separation of all the samples from each other. The analysis by LIBS was not able to distinguish between two samples, which were separated by LA-ICP-MS based on niobium, iron and zirconium. By using LA-ICP-MS, 10 elements were detected with a SNR>3. The element menu obtained by LIBS consisted of up to 7 elements, including lithium, potassium and sodium, which were not easily detected by LA-ICP-MS. The use of ±5s comparison criteria allowed to numerically compare the tape samples without the potential subjectivity of the spectral overlay method.

The present work has shown that trace elemental analysis of tapes by LIBS and LA-ICP-MS can provide an improvement over traditional methods given the higher sensitivity and selectivity of these techniques. However, further work is needed to develop rugged quantitative analysis so that databases can be populated and probed to better estimate the statistical significance of tape comparisons. Nonetheless, the qualitative data obtained from LA-ICP-MS for tape analysis in the form of integrated intensity vs. m/z was successfully used for the application of a likelihood ratios approach using principal component analysis. The results for the likelihood ratios research by Gupta A. et al.[82] on the LA-ICP-MS data for the 90 electrical tapes analyzed at FIU suggests the potential of the PCA likelihood ratios estimation method to overcome the highly-dimensional data for the comparisons of tape samples by a large number of elements. In addition, low error rates and the absence of strongly misleading evidence for both, within- and between-source, comparisons were reported.

LIST OF REFERENCES

1. Smith, J. M., Forensic Examination of Pressure Sensitive Tape. In *Forensic Analysis on the Cutting Edge: New Methods for Trace Evidence Analysis*, Blackledge, R. D., Ed. 2007; pp 291-332.

2. Goodpaster, J. V.; Sturdevant, A. B.; Andrews, K. L.; Briley, E. M.; Brun‐Conti, L., Identification and Comparison of Electrical Tapes Using Instrumental and Statistical Techniques: II. Organic Composition of the Tape Backing and Adhesive. *Journal of Forensic Sciences* **2009,** *54* (2), 328-338.

3. Mehltretter, A. H.; Bradley, M. J.; Wright, D. M., Analysis and Discrimination of Electrical Tapes: Part I. Adhesives. *Journal of Forensic Sciences* **2011,** *56* (1), 82-94.

4. Mehltretter, A. H.; Bradley, M. J.; Wright, D. M., Analysis and Discrimination of Electrical Tapes: Part II. Backings. *Journal of Forensic Sciences* **2011,** *56* (6), 1493-1504.

5. Goodpaster, J. V.; Sturdevant, A. B.; Andrews, K. L.; Brun‐Conti, L., Identification and Comparison of Electrical Tapes Using Instrumental and Statistical Techniques: I. Microscopic Surface Texture and Elemental Composition. *Journal of Forensic Sciences* **2007,** *52* (3), 610-629.

6. Johnston, J.; Council, P. S. T., *Pressure Sensitive Adhesive Tapes: A Guide to Their Function, Design, Manufacture, and Use*. Pressure Sensitive Tape Council: 2000.

7. Shecut, W. H.; Day, H. H. U.S. Patent No. 3965. Improvement Is Adhesive Plasters. 1845.

8. Richards, A. U.S. Patent No. 111,682. Improvement in Medicated Plasters. 1871.

9. Oace, R. J.; Burns, S. R.; Eastwold, E. E. U.S. 2559990a. Insulating Tape. 1946.

10. Hofmann, C. F.; Vondracek, C. H.; Westervelt, D. C. U.S. 3082133a. High Temperature Electrical Insulating Tape. 1957.

11. Barton, D. M. Us3162722 Electric Tape Insulation. 1964.

12. Miller, J. A. Pressure Sensitive Adhesive Composition. 1970.

13. Blance, R. B.; Gardner, D. M. Us3632412 Electrical Tape. 1972.

14. Garcia-Ramirez, R.; Mahoney, D. V.; Ward, S. O. W.O. 2002018507a1. Solventless Plasticizer-Resistant Vinyl Electrical Tape. 2002.

15. Benson, J. D. In *Forensic Examination of Duct Tape*, Proceedings of the International Symposium on the Analysis and Identification of Polymers, 1984; pp 291-331.

16. Kee, T. G. In *The Characterization of Pvc Adhesive Tape*, Proceedings of the International Symposium on the Analysis and Identification of Polymers, 1984; pp 77-85.

17. Keto, R. O. In *Forensic Characterization of Black Polyvinyl Chloride Electrical Tape*, Proceedings of the International Symposium on the Analysis and Identification of Polymers, 1984; pp 77-85.

18. Blackledge, R., Tapes with Adhesive Backings: Their Characterization in the Forensic Science Laboratory. Carl Hanser Verlag, Munich: 1987; pp 413-421.

19. Snodgrass, H. In *Duct Tape Analysis as Trace Evidence*, Proceedings of the International Symposium on the Forensic Aspects of Trace Evidence, 1991; pp 69-73.

20. Smith, J. M., The Forensic Value of Duct Tape Comparisons. *Midwestern Association of Forensic Scientists Newsletter* **1998,** *27* (1), 28-33.

21. Maynard, P.; Gates, K.; Roux, C.; Lennard, C., Adhesive Tape Analysis: Establishing the Evidential Value of Specific Techniques. *Journal of Forensic Sciences* **2001,** *46* (2), 280-287.

22. Teetsov, A. S.; Stellmack, M. L., Hand-Sectioning and Identification of Pressure-Sensitive Tapes. *Modern Microscopy Journal* **2004**.

23. Bradley, M. J.; Keagy, R. L.; Lowe, P. C.; Rickenbach, M. P.; Wright, D. M.; LeBeau, M. A., A Validation Study for Duct Tape End Matches. *Journal of Forensic Sciences* **2006,** *51* (3), 504-508.

24. Bradley, M. J.; Gauntt, J. M.; Mehltretter, A. H.; Lowe, P. C.; Wright, D. M., A Validation Study for Vinyl Electrical Tape End Matches. *Journal of Forensic Sciences* **2011,** *56* (3), 606-611.

25. Mehltretter, A. H.; Bradley, M. J., Forensic Analysis and Discrimination of Duct Tapes. *Journal of the American Society of Trace Evidence Examiners* **2012,** *3* (1), 21-40.

26. Mehltretter, A. H.; Wright, D. M.; Dettman, J. R.; Smith, M. A., Intra-Roll and Intra-Jumbo Roll Variation of Duct Tapes. *Journal of the American Society of Trace Evidence Examiners* **2015,** *6* (1), 21-41.

27. Guideline for Forensic Examination of Pressure Sensitive Tapes: Scientific Working Group on Materials Analysis (Swgmat). *Journal of the American Society of Trace Evidence Examiners* **2011,** *2* (1), 88-97.

28. Guideline for Assessing Physical Characteristics in Forensic Tape Examinations: Scientific Working Group on Materials Analysis (Swgmat). *Journal of the American Society of Trace Evidence Examiners* **2014,** *5* (1), 22-33.

29. Guideline for Using Light Microscopy in Forensic Examinations of Tape Components: Scientific Working Group on Materials Analysis (Swgmat). *Journal of the American Society of Trace Evidence Examiners* **2011,** *2* (1), 106-111.

30. Merrill, R. A.; Edward G. Bartick, Analysis of Pressure Sensitive Adhesive Tape: I. Evaluation of Infrared Atr Accessory Advances. *Journal of Forensic Sciences* **2000,** *45* (1), 93-98.

31. Dobney, A. M.; Wiarda, W.; de Joode, P.; van der Peijl, G. J., Sector Field ICP-MS Applied to the Forensic Analysis of Commercially Available Adhesive Packaging Tapes. *Journal of Analytical Atomic Spectrometry* **2002,** *17* (5), 478-484.

32. Sakayanagi, M.; Konda, Y.; Watanabe, K.; Harigaya, Y., Identification of Pressure-Sensitive Adhesive Polypropylene Tape. *Journal of Forensic Sciences* **2003,** *48* (1), 68-76.

33. Kumooka, Y., Analysis of Deteriorated Rubber-Based Pressure Sensitive Adhesive by Pyrolysis-Gas Chromatography/Mass Spectrometry and Attenuated Total Reflectance Fourier Transform Infrared Spectrometry. *Forensic science international* **2006,** *163* (1), 132-137.

34. Zieba-Palus, J.; Augustynek, A., Effective Differentiation of Adhesive Tapes by the Use of Infrared Spectroscopy and Pyrolytic-Gas Chromatography for Criminalistic Purposes. *Problems of Forensic Sciences* **2011,** *86*, 103-113.

35. Wright, D. M.; Mehltretter, A. H., Duct Tape Sourcing Examinations: Developing Investigative Leads Using Multiple Resources. *Journal of the American Society of Trace Evidence Examiners* **2013,** *4* (1), 13-28.

36. Guideline for Using Fourier Transform Infrared Spectroscopy in Forensic Tape Examinations: Scientific Working Group on Materials Analysis (Swgmat). *Journal of the American Society of Trace Evidence Examiners* **2011,** *2* (1), 112-121.

37. Williams, E. R.; Munson, T. O., The Comparison of Black Polyvinylchloride (Pvc) Tapes by Pyrolysis Gas Chromatography. *Journal of Forensic Sciences* **1988,** *33* (5), 1163-1170.

38. Standard Guide for Using Pyrolysis Gas Chromatography and Pyrolysis Gas Chromatography/Mass Spectrometry in Forensic Tape Examinations: Scientific Working Group on Materials Analysis (Swgmat). *Journal of the American Society of Trace Evidence Examiners* **2014,** *5* (1), 42-50.

39. Jenkins Jr, T. L. In *Elemental Examination of Silver Duct Tape Using Energy Dispersive X-Ray Spectrometry*, Proceedings of the International Symposium on the Analysis and Identification of Polymers, 1984; pp 147-149.

40. Dobney, A. M.; Wiarda, W.; de Joode, P.; van der Peijl, G. J. In *Elemental Analysis Comparison of Packaging Tapes Using HR ICP/Ms*, Proceedings of the Second European Academy of Forensic Science Meeting, Cracow, Poland, 2000; pp 12-16.

41. Dobney, A. M.; Wiarda, W.; de Joode, P.; van der Pejil, G. J. Q., Elemental Comparison of Packaging Tapes Using HR-ICP-MS. *Problems of Forensic Sciences* **2001,** *47*, 275-287.

42. Guideline for Using Scanning Electron Microscopy/Energy Dispersive X-Ray Spectroscopy in Forensic Tape Examinations: Scientific Working Group on Materials Analysis (Swgmat). *Journal of the American Society of Trace Evidence Examiners* **2011,** *2* (1), 122-132.

43. Martinez-Lopez, C.; Sakayanagi, M.; Almirall, J. R., Elemental Analysis of Packaging Tapes by LA-ICP-MS and LIBS. *Forensic Chemistry* **2018,** *8*, 40-48.

44. Martinez-Lopez, C.; Trejos, T.; Mehltretter, A. H.; Almirall, J. R., Elemental Analysis and Characterization of Electrical Tape Backings by LA-ICP-MS. *Forensic Chemistry* **2017**, 96-107.

45. Taylor, H. E., *Inductively Coupled Plasma-Mass Spectrometry: Practices and Techniques*. Academic Press: 2000.

46. Russo, R. E.; Mao, X.; Liu, H.; Gonzalez, J.; Mao, S. S., Laser Ablation in Analytical Chemistry—a Review. *Talanta* **2002,** *57* (3), 425-451.

47. Russo, R. E.; Mao, X.; Gonzalez, J. J.; Zorba, V.; Yoo, J., Laser Ablation in Analytical Chemistry. *Journal of Analytical Chemistry* **2013,** *85* (13), 6162-77.

48. Longerich, H., Laser Ablation–Inductively Coupled Plasma–Mass Spectrometry (LA-ICP-MS): An Introduction. In *Laser Ablation ICP-MS in the Earth Sciences: Current Practices and Outstanding Issues*, Sylvester, P., Ed. Canada, 2008; pp 1-18.

49. Singh, J. P.; Thakur, S. N., *Laser-Induced Breakdown Spectroscopy*. Elsevier: 2007.

50. Cremers, D. A.; Yueh, F. Y.; Singh, J. P.; Zhang, H., *Laser‐Induced Breakdown Spectroscopy, Elemental Analysis*. Wiley Online Library: 2006.

51. Noll, R., *Laser-Induced Breakdown Spectroscopy*. Springer: 2012; p 7-15.

52. Royal Society of Chemistry. Charge-Coupled-Device Detector. http://www.rsc.org/publishing/journals/prospect/ontology.asp?id=CMO:0002245&MSID=b917348j (Accessed Sep, 2018).

53. Trejos, T.; Corzo, R.; Subedi, K.; Almirall, J., Characterization of Toners and Inkjets by Laser Ablation Spectrochemical Methods and Scanning Electron Microscopy-Energy Dispersive X-Ray Spectroscopy. *Spectrochimica Acta Part B: Atomic Spectroscopy* **2014,** *92*, 9-22.

54. Miller, J. N.; Miller, J. C., *Statistics and Chemometrics for Analytical Chemistry*. Pearson/Prentice Hall: 2005.

55. Kataria, A.; Singh, M., A Review of Data Classification Using K-Nearest Neighbour Algorithm. *International Journal of Emerging Technology and Advanced Engineering* **2013,** *3* (6), 354-360.

56. Trejos, T.; Torrione, P.; Corzo, R.; Raeva, A.; Subedi, K.; Williamson, R.; Yoo, J.; Almirall, J., A Novel Forensic Tool for the Characterization and Comparison of Printing Ink Evidence: Development and Evaluation of a Searchable Database Using Data Fusion of Spectrochemical Methods. *Journal of Forensic Sciences* **2016,** *61* (3), 715-24.

57. Pakiela, M.; Wojciechowski, M.; Wagner, B.; Bulska, E., A Novel Procedure of Powdered Samples Immobilization and Multi-Point Calibration of LA-ICP-MS. *Journal of Analytical Atomic Spectrometry* **2011,** *26* (7), 1539-1543.

58. Günther, D.; Quadt, A. v.; Wirz, R.; Cousin, H.; Dietrich, V., Elemental Analyses Using Laser Ablation-Inductively Coupled Plasma-Mass Spectrometry (LA-ICP-MS) of Geological Samples Fused with Li 2 B 4 O 7 and Calibrated without Matrix-Matched Standards. *Microchimica Acta* **2001,** *136* (3-4), 101-107.

59. O'Connor, C.; Landon, M. R.; Sharp, B. L., Absorption Coefficient Modified Pressed Powders for Calibration of Laser Ablation Inductively Coupled Plasma Mass Spectrometry. *Journal of Analytical Atomic Spectrometry* **2007,** *22* (3), 273-282.

60. Cizdziel, J.; Bu, K.; Nowinski, P., Determination of Elements in Situ in Green Leaves by Laser Ablation ICP-MS Using Pressed Reference Materials for Calibration. *Journal of Analytical Methods* **2012,** *4* (2), 564-569.

61. Do, T.-M.; Hsieh, H.-F.; Chang, W.-C.; Chang, E.-E.; Wang, C.-F., Analysis of Liquid Samples Using Dried-Droplet Laser Ablation Inductively Coupled Plasma Mass Spectrometry. *Spectrochimica Acta Part B: Atomic Spectroscopy* **2011,** *66* (8), 610-618.

62. Aeschliman, D. B.; Bajic, S. J.; Baldwin, D. P.; Houk, R., Spatially-Resolved Analysis of Solids by Laser Ablation-Inductively Coupled Plasma-Mass Spectrometry:

Trace Elemental Quantification without Matrix-Matched Solid Standards. *Journal of Analytical Atomic Spectrometry* **2003,** *18* (8), 872-877.

63. May, T. W.; Wiedmeyer, R. H., A Table of Polyatomic Interferences in ICP-MS. *Atomic Spectroscopy* **1998,** *19* (5), 150-155.

64. Nischkauer, W.; Vanhaecke, F.; Bernacchi, S.; Herwig, C.; Limbeck, A., Radial Line-Scans as Representative Sampling Strategy in Dried-Droplet Laser Ablation of Liquid Samples Deposited on Pre-Cut Filter Paper Disks. *Spectrochimica Acta Part B: Atomic Spectroscopy* **2014,** *101*, 123-129.

65. Voss, M.; Nunes, M. A.; Corazza, G.; Flores, E. M.; Müller, E. I.; Dressler, V. L., A New Approach to Calibration and Determination of Selected Trace Elements in Food Contact Polymers by LA-ICP-MS. *Talanta* **2017,** *170*, 488-495.

66. Frick, D. A.; Günther, D., Fundamental Studies on the Ablation Behaviour of Carbon in LA-ICP-MS with Respect to the Suitability as Internal Standard. *Journal of Analytical Atomic Spectrometry* **2012,** *27* (8), 1294-1303.

67. Umpierrez, S. Elemental Analysis of Glass by Laser Ablation - Inductively Ccoupled Plasma - Mass Spectrometry (LA-ICP-MS) without Matrix- Matched Standards. Florida International University, Miami, Florida, 2006.

68. Pontes, M. J. C.; Cortez, J.; Galvão, R. K. H.; Pasquini, C.; Araújo, M. C. U.; Coelho, R. M.; Chiba, M. K.; de Abreu, M. F.; Madari, B. E., Classification of Brazilian Soils by Using LIBS and Variable Selection in the Wavelet Domain. *Journal of Analytica Chimica Acta* **2009,** *642* (1-2), 12-18.

69. Syvilay, D.; Wilkie-Chancellier, N.; Trichereau, B.; Texier, A.; Martinez, L.; Serfaty, S.; Detalle, V., Evaluation of the Standard Normal Variate Method for Laser-Induced Breakdown Spectroscopy Data Treatment Applied to the Discrimination of Painting Layers. *Spectrochimica Acta Part B: Atomic Spectroscopy* **2015,** *114*, 38-45.

70. Ismaël, A.; Bousquet, B.; Michel-Le Pierres, K.; Travaillé, G.; Canioni, L.; Roy, S., In Situ Semi-Quantitative Analysis of Polluted Soils by Laser-Induced Breakdown Spectroscopy (LIBS). *Journal of Applied Spectroscopy* **2011,** *65* (5), 467-473.

71. Borba, F. d. S. L.; Cortez, J.; Asfora, V. K.; Pasquini, C.; Pimentel, M. F.; Pessis, A.-M.; Khoury, H. J., Multivariate Treatment of LIBS Data of Prehistoric Paintings. *Journal of the Brazilian Chemical Society* **2012,** *23* (5), 958-965.

72. Noble, W.; Wheals, B.; Whitehouse, M., The Characterisation of Adhesives by Pyrolysis Gas Chromatography and Infrared Spectroscopy. *Journal of Forensic Sciences* **1974,** *3*, 163-174.

73. Zieba-Palus, J.; Zadora, G.; Milczarek, J. M.; Koscielniak, P., Pyrolysis-Gas Chromatography/Mass Spectrometry Analysis as a Useful Tool in Forensic Examination of Automotive Paint Traces. *Journal of Chromatography A* **2008,** *1179* (1), 41-46.

74. Ernst, T.; Berman, T.; Buscaglia, J.; Eckert‐Lumsdon, T.; Hanlon, C.; Olsson, K.; Palenik, C.; Ryland, S.; Trejos, T.; Valadez, M., Signal‐to‐Noise Ratios in Forensic Glass Analysis by Micro X‐Ray Fluorescence Spectrometry. *X‐Ray Spectrometry* **2014,** *43* (1), 13-21.

75. Sun, Z.; Quan, Y.; Sun, Y., Elemental Analysis of White Electrical Tapes by Wavelength Dispersive X-Ray Fluorescence Spectrometry. *Forensic science international* **2013,** *232* (1-3), 169-72.

76. Arroyo, L.; Trejos, T.; Hosick, T.; Machemer, S.; Almirall, J. R.; Gardinali, P. R., Analysis of Soils and Sediments by Laser Ablation Inductively Coupled Plasma Mass Spectrometry (LA-ICP-MS): An Innovative Tool for Environmental Forensics. *Environmental forensics* **2010,** *11* (4), 315-327.

77. Trejos, T.; Montero, S.; Almirall, J. R., Analysis and Comparison of Glass Fragments by Laser Ablation Inductively Coupled Plasma Mass Spectrometry (LA-ICP-MS) and ICP-MS. *Journal of Analytical and Bioanalytical Chemistry* **2003,** *376* (8), 1255-1264.

78. Hobbs, A. L.; Almirall, J. R., Trace Elemental Analysis of Automotive Paints by Laser Ablation–Inductively Coupled Plasma–Mass Spectrometry (La–ICP–Ms). *Journal of Analytical and Bioanalytical Chemistry* **2003,** *376* (8), 1265-1271.

79. Rodriguez-Celis, E.; Gornushkin, I.; Heitmann, U.; Almirall, J.; Smith, B.; Winefordner, J.; Omenetto, N., Laser Induced Breakdown Spectroscopy as a Tool for Discrimination of Glass for Forensic Applications. *Journal of Analytical and Bioanalytical Chemistry* **2008,** *391* (5), 1961.

80. Jantzi, S. C.; Almirall, J. R., Characterization and Forensic Analysis of Soil Samples Using Laser-Induced Breakdown Spectroscopy (LIBS). *Journal of Analytical and Bioanalytical Chemistry* **2011,** *400* (10), 3341-3351.

81. Karki, V.; Sarkar, A.; Singh, M.; Maurya, G. S.; Kumar, R.; Rai, A. K.; Aggarwal, S. K., Comparison of Spectrum Normalization Techniques for Univariate Analysis of Stainless Steel by Laser-Induced Breakdown Spectroscopy. *Pramana* **2016,** *86* (6), 1313-1327.

82. Gupta, A.; Martinez-Lopez, C.; Curran, J. M.; Almirall, J. R., Multi-Element Comparisons of Tapes Evidence Using Dimensionality Reduction for Calculating Likelihood Ratios. *Forensic Science International (Submitted)* **2018**.

VITA

CLAUDIA MARTINEZ LOPEZ

Born, Havana, Cuba

2014	B.S., Chemistry Florida International University Miami, Florida
2015-2016	NSF Bridge to Doctorate Fellowship Florida International University Miami, Florida
2017	M.S., Chemistry Florida International University Miami, Florida
2017 -2018	Doctoral Candidate Florida International University Miami, Florida
	Dissertation Year Fellowship Florida International University Miami, Florida

PUBLICATIONS AND PRESENTATIONS

C. Martinez-Lopez, J. Almirall. Characterization of Electrical Tapes by Laser Ablation Inductively Coupled Plasma Mass Spectrometry and Scanning Electron Microscopy Energy Dispersive Spectroscopy (SEM-EDS). Presented at American Academy of Forensic Scientists 67th Annual Meeting, Orlando, Florida, USA, February 2015.

C. Martinez-Lopez, J. Almirall. Elemental Profiling of Electrical Tapes by Laser Ablation Inductively Coupled Plasma Mass Spectrometry (LA-ICP-MS). Presented at American Society for Mass Spectrometry Sanibel Conference, Clearwater Beach, Florida, USA, January 2015.

C. Martinez-Lopez, J. Almirall. Elemental Profiling of Electrical Tapes by Laser Ablation Inductively Coupled Plasma Mass Spectrometry. Presented at Graduate Student Appreciation Week, Miami, Florida, USA, April 2015.

C. Martinez-Lopez, J. Almirall. Validation of an analytical method for the identification of SmartWater CSI Forensic Marking Technology. Presented at International Forensic Research Institute 4th Annual Symposium, Miami, Florida, USA, May 2015.

C. Martinez-Lopez, J. Almirall. Elemental Analysis of Electrical Tapes by LA-ICP-MS. Presented at Southern Association of Forensic Scientists 50th Anniversary Meeting, Sarasota, Florida, USA, September 2016.

C. Martinez-Lopez, J. Almirall. Tape Analysis and Interpretation: Interlaboratory Test 1. Presented at Tape Working Group Meeting, Miami, Florida, USA, December 2016.

C. Martinez-Lopez, J. Almirall. Elemental analysis of packaging tapes by LA-ICP-MS and LIBS. Presented at Six Conference, Reno, Nevada, USA, October 2017.

C. Martinez-Lopez, J. Almirall. LA-ICP-MS analysis and characterization of adhesive tapes as forensic evidence. Presented at SciX Conference, Reno, Nevada, USA, October 2017.

C. Martinez-Lopez; T. Trejos; A. H. Mehltretter; J. R. Almirall, Elemental Analysis and Characterization of Electrical Tape Backings by LA-ICP-MS. *Forensic Chemistry* 2017, 96-107.

C. Martinez-Lopez; M. Sakayanagi; J. R. Almirall, Elemental Analysis of Packaging Tapes by LA-ICP-MS and LIBS. *Forensic Chemistry* 2018, *8*, 40-48.

C. Martinez-Lopez, J. Almirall. Elemental Analysis of Adhesive Tapes as Forensic Evidence by LA-ICP-MS and LIBS. Presented at Impression Pattern and Trace Evidence Symposium, Arlington, Virginia, USA, January 2018.

F. Liu; V. Kozlovskaya; O. Zavgorodnya; C. Martinez-Lopez; S. Catledgebc; E. Kharlampieva, Encapsulation of Anticancer Drug by Hydrogen-Bonded Multilayers of Tannic Acid. *Soft Matter* 2014, *10*, 9237-9247.